

Melanoma Inhibitory Activity (MIA) Protein – Molecular Relevance and Functional Characterization

Dissertation

zur Erlangung des Doktorgrades der Naturwissenschaften

(Dr. rer. nat.)

an der Fakultät für Chemie und Pharmazie

der Universität Regensburg



vorgelegt von

Jennifer Schmidt

aus Holzminden

2010

The experimental part of this work was conducted between March 2007 and February 2010 at the Institute of Molecular Pathology, University Hospital Regensburg, Germany and the Institute for Organic Chemistry, University of Regensburg, Germany under supervision of Prof. Dr. Anja Katrin Bosserhoff and Prof. Dr. Burkhard König.

Submission of PhD-thesis: 18. March 2010

Colloquium: 26. April 2010

Board of examiners:

Chairman: Prof. Dr. Arno Pfitzner

1st Referee: Prof. Dr. Burkhard König

2nd Referee: Prof. Dr. Anja Katrin Bosserhoff

3rd Referee: Prof. Dr. Joachim Wegener

Declaration

The work submitted in this dissertation is the result of my own investigation, unless stated otherwise.

Jennifer Schmidt, 18. March 2010

**Dedicated to Flo
and my wonderful family**

Acknowledgement

The accomplishment of this dissertation has been the most significant academic challenges I have ever had to face. Without the support, patience and guidance of the following people, this study would not have been completed. I owe my deepest gratitude to all those people who have made this dissertation possible.

First and foremost I would like to thank my advisor Prof. Dr. Anja Katrin Bosserhoff for providing this interesting project and for excellent supervision. I have been amazingly fortunate that she allowed me great latitude to manage my research project - always open minded for new methods and ideas. Her insightful comments and constructive criticisms at different stages of my research were thought-provoking and they helped me to focus my ideas.

I am also grateful to my supervisor Prof. Dr. Burkhard König for his encouragement and support throughout this work. He has been always there to listen and give advice. I would like to thank him for constructive discussions that inspired me and helped me to improve my knowledge in the field of medicinal chemistry.

I am also indebted to my research partners Prof. Dr. Roland Schönherr and Kristin Friebe from the University of Jena, with whom I have successfully collaborated during the course of my graduate studies. Thank you for performing electro physical recordings and for critically reading the manuscript.

Thanks are extended to Prof. Dr. Peter Oefner and the Center of Excellence for Fluorescent Bioanalytics for providing access to the Polarstar microplate reader, Dr. Jörg Plümpe (Active Motif Chromeon) for the generous gift of the Ru(bpy)₃-isothiocyanate dye, and the analytical departments of the University of Regensburg for prompt and accurate measurement of my samples. Special thanks to Dr. Rudolf Vasold and Simone Strauss for help with analytical and preparative HPLC purification.

This is a great opportunity to thank my workgroup, in particular laboratory 3, for creating a positive, constructive as well as relaxed working atmosphere.

I would like to acknowledge Dr. Ann-Kathrin Wenke for introducing me theoretically as well as practically to the field of molecular biology, Dr. Thomas Amann for help with the

animal experiments, Daniel Müller and Stephanie Arndt for constructive discussions in terms of cloning and Simone Kaufmann and Martina Weber for technical assistance.

Particularly, I would like to thank Robert Lechner for always being so creative and relaxed in every circumstance, Ulrike Mägdefrau and Simone Braig for incredible amusing women's evenings, Jacqueline Schlegel for funny hikes in deep snow with mid-height footwear, for "Hölle"- insider tips and for her genial straightforwardness, and Sibylla Lodermeier for descrying excellent hiding-places for treasure map filled 50 ml Falcon tubes on a volcanic island in the Atlantic ocean, that could easily be relocated by 60 years old people.

I am heartily thankful to my dear lab colleagues Johanna Schmidt and Susanne Wallner, whose pure presence felt like a personal gain in the laboratory workaday to me. I am grateful for them to make sure that the days in the laboratory were never tedious. We had elaborate discussions as well as half-witted talks often resulting in great laughs. Johanna and Susanne have helped me stay sane through these years. Their support and care helped me overcome setbacks and stay focused on my graduate study.

Very special thanks go to Alexander Riechers for a great and successful cooperation. Without this collaboration I could not have established such relevant data during this time span. Thanks for many constructive discussions, for inspiration and apparently never ending optimism. The humour that we share enables me to better bear setbacks (he may ask now: "what setbacks?"). Thank you for always creating a relaxed work atmosphere, countless funny moments and great laughs.

I am heartily thankful to my best friend Patrick Kleemann. He always supported me and gave me encouragement in terms of my professional career as well as in private issues. I greatly value his friendship.

Most importantly, none of this would have been possible without the love and patience of my family. My family, to whom this dissertation is dedicated to, has been a constant source of love and support all these years, encouraging me throughout this time.

My most special thanks go to my wonderful husband Florian. He showed me that life is full of marvelous things and that it offers much more than work and research. With

seemingly never ending patience he gave me encouragement, emotional support and love. I deeply value his belief in me.

Finally, I appreciate the financial support from DFG (Deutsche Forschungsgemeinschaft) that funded parts of the research discussed in this dissertation.

**The most exciting phrase to hear in science,
the one that heralds the most discoveries,
is not "Eureka!" but rather "That's weird..."**

Isaac Asimov, 1920 – 1992
American author and professor of biochemistry

Table of Content

1	MIA - a New Target Protein for Malignant Melanoma Therapy	1
1.1	Malignant Melanoma – incidence and risk factors	2
1.2	Facilitation of tumor cell detachment from the pericellular matrix promotes invasion and formation of metastases	2
1.3	Clinical relevance of MIA protein	3
1.4	Cellular processing of MIA protein during migration	4
1.5	Functional inhibition of MIA protein	5
1.6	Antimetastatic agents as a new therapy strategy	6
1.7	References	7
2	Directed, Migration-associated Secretion of Melanoma Inhibitory Activity (MIA) at the Cell Rear is supported by KCNN4 Potassium Channels	11
2.1	Introduction	12
2.2	Results	13
2.2.1	<i>Targeted MIA protein transport to the rear of migrating cells</i>	13
2.2.2	<i>Intracellular transport of MIA protein follows the conventional secretory pathway</i>	15
2.2.3	<i>MIA protein secretion is a Ca^{2+}-regulated process</i>	18
2.3	Discussion	23
2.4	Materials and Methods	26
2.5	Acknowledgements	30
2.6	References	31
3	Processing of MIA protein during melanoma cell migration	38
3.1	Introduction	39
3.2	Results	40
3.2.1	<i>Unidirectional internalization of MIA protein</i>	40
3.2.2	<i>Internalization of MIA-integrin complexes at the rear of migrating cells</i>	42
3.2.3	<i>Intracellular dissociation of MIA-integrin complexes and degradation of MIA protein</i>	45

3.3	Discussion	48
3.4	Materials and Methods	50
3.5	Acknowledgements	53
3.6	References	53
3.7	Supplementary information	57
4	Heterogeneous Transition Metal-based Fluorescence Polarization (HTFP) Assay for Probing Protein Interactions	60
4.1	Introduction	61
4.2	Results	62
4.2.1	<i>Heterogeneous Transition metal based Fluorescence Polarization (HTFP) assay development</i>	62
4.2.2	<i>Functional activity of Ru(bpy)₃-labeled MIA protein</i>	64
4.2.3	<i>Heterogeneous Transition metal based Fluorescence Polarization (HTFP) assay results</i>	64
4.2.3.1	<i>Binding of MIA-Ru(bpy)₃ to AR54, 30 kDa and 70 kDa fibronectin fragments</i>	64
4.2.3.2	<i>Buffer additives and detergent controls</i>	66
4.2.3.3	<i>Multimerization studies</i>	66
4.3	Discussion	68
4.4	Materials and Methods	69
4.5	Acknowledgements	72
4.6	References	72
5	Dissociation of Functionally Active MIA Protein Dimers by Dodecapeptide AR71 Strongly Reduces Formation of Metastases in Malignant Melanoma	75
5.1	Introduction	76
5.2	Results	77
5.2.1	<i>MIA protein is functionally active as a dimer</i>	77
5.2.2	<i>Peptide AR71 prevents MIA protein dimerization</i>	79
5.2.3	<i>MIA interacts with AR71</i>	81
5.2.4	<i>Effect of MIA inhibitory peptide AR71 on formation of metastases in vivo</i>	82
5.3	Discussion	85

5.4	Materials and Methods	87
5.5	Acknowledgements	93
5.6	References	93
6	Summary	97
7	Zusammenfassung	99
8	Abbreviations	101
9	Appendix	103

1 MIA - a New Target Protein for Malignant Melanoma Therapy

Abstract

Malignant melanoma, a malignancy of pigment-producing cells, causes the greatest number of skin cancer-related deaths worldwide. The tumor is characterized by its aggressive phenotype and can grow deep into the skin at very early stages of the disease. After invasion into healthy tissue, melanoma cells can reach the blood and lymphatic vessels and spread through the whole body, causing a life-threatening condition. Since metastatic lesions are usually characterized by an intrinsic resistance to standard chemotherapy, the prognosis of this tumor remains very poor in advanced cases.

Melanoma inhibitory activity (MIA), an 11 kDa protein expressed and secreted by cells after malignant transformation, is known to play a key role in melanoma development, progression and tumor cell invasion. After its secretion, which is restricted to the rear pole of migrating cells, MIA protein directly interacts with cell adhesion receptors and extracellular matrix molecules. By this mechanism, MIA protein actively facilitates focal cell detachment from surrounding structures at the cell rear and strongly promotes tumor cell invasion and formation of metastases. Analysis at molecular level revealed that MIA protein reaches functional activity by self assembly. Functional inactivation of MIA protein by dodecapeptides that directly bind to the dimerization interface, leads to a strongly reduced tumor cell invasion in an *in vivo* mouse melanoma model. The molecular understanding of the contribution of MIA protein to formation of metastases provides an excellent starting point for the development of a new strategy in malignant melanoma therapy.

Manuscript in preparation for submission:

Schmidt J., Bosserhoff A. K.; MIA – a New Target Protein for Malignant Melanoma Therapy, **2010**;

This introduction will be submitted as a review article once all other chapters of this thesis have been accepted for publication

1.1 Malignant melanoma – incidence and risk factors

Malignant melanoma is the most aggressive type of cutaneous cancer originating from pigment producing cells in the skin, the melanocytes. This highly invasive tumor is known for its uncontrollable growth and for its ability to give rise to metastases into several tissues in early stages of the disease. The incidence of malignant melanoma is rising dramatically in caucasian populations, with the highest recorded incidence occurring in Australia, where the annual rates are 10 and over 20 times the rates in Europe for women and men, respectively. High, intermittent exposure to solar UV appears to be a significant risk factor for the development of malignant melanoma.

From an initial phase of radial growth, the tumor may evolve into the more dangerous vertical growth phase. In advanced cases, tumor cells acquire a strong potential to disseminate. Metastatic lesions are usually characterized by an intrinsic resistance to standard chemotherapy representing one of the major causes of the very poor prognosis of the tumor.

The subsequent promotion of detachment of radial and vertical growth phase melanomas from basement membrane or matrix proteins serves as a unique progression mechanism for melanoma. This exceptionally high migratory potential is probably inherent in these cells, since it is also observed during or shortly after neurulation, an embryological event marked by neural tube closure. In this process, neural crest cells, including pigment producing cells, quickly migrate in succession of migratory stimuli by inhibitory or attractive signals to their destination and proliferate there. Nowadays, it has been described that many of the genes expressed in melanoma cell lines and melanocytic tumors are required specifically during melanoma development, and similar categories of genes are expressed in metastatic melanoma and in migratory neural crest cells.¹⁻³ At present, it is discussed whether melanoma cells reactivate their strong migratory ability during cancer development.

However, the molecular mechanisms that are involved in melanoma growth and progression are still poorly understood. All previous attempts of targeted therapies, although the targets chosen were relevant, did not lead to any success in the treatment of melanoma patients. New target molecules in melanoma therapy are strongly needed.

1.2 Facilitation of tumor cell detachment from the pericellular matrix promotes invasion and formation of metastases

To build up metastases in healthy tissues and organs distant from their origin cancer cells, released from the primary tumor, spread through blood vessels, lymphatic ducts, or cavities

to form colonies. It is a highly dynamic process that essentially depends on the ability of cancer cells to detach from the pericellular matrix, migrate, invade intact tissue structures, and finally to overcome physiological barriers such as basement membranes upon intra- and extravasation.

Cell migration, physiologically exhibited during wound healing, angiogenesis, embryonic development, and immune function, is initiated by migratory stimuli triggered by attractants like chemokines and ECM gradients.⁴ Generally, cells respond by local activation and amplification of signaling events facilitating localized actin polymerization leading to morphological polarity and establishment of a dominant-leading pseudopodium and rear cell body compartment.^{4,5} Integrin cell adhesion receptors tether the extending membrane to the substratum by formation of new focal complexes at the leading front of the extending membrane. This adhesion process provides necessary signals to fine-tune and maintain directional growth, while retraction mechanisms are suppressed. Cell movement then commences as the cell undergoes repeated cycles of membrane extension and integrin ligation at the front to provide traction points, and cell body retraction at the rear.^{4, 6} Changes in cell shape occurring during migratory processes are further supported by ion channels and aquaporins regulating cell volume by fluctuations.⁶ Intracellular Ca^{2+} plays a crucial role in almost all cellular processes including regulation of membrane-fusion as well as cell migration.⁷⁻¹⁰ By modulating turnover of actin filaments, involvement of calpain and recycling of integrins, Ca^{2+} coordinates different components of the cellular migration machinery.¹¹⁻¹²

1.3 Clinical relevance and structural analysis of MIA protein

MIA (melanoma inhibitory activity) protein has been described to play a key role in melanoma development and progression.¹³ In order to identify autocrine growth-regulatory factors secreted by melanoma cells, MIA, an 11 kDa protein, strongly expressed and secreted by melanocytic tumor cells, was purified from tissue culture supernatant of the human melanoma cell line HTZ-19.¹³⁻¹⁴ In normal skin MIA protein is not detectable. Physiologically, it is produced by cartilage and plays a role in chondrocyte differentiation.¹⁵ Interestingly, MIA expression is induced by UV irradiation, which resembles a link between the role of UV in melanoma induction and MIA expression.¹⁶ MIA protein strongly contributes to the invasive and migratory potential of melanoma cells and promotes the formation of tumor metastases.^{13, 17-18} Increased MIA protein plasma levels directly correlate with progressive malignancy and a more advanced state of

melanocytic tumors.^{17, 19} Thus, MIA protein serves as a reliable clinical tumor marker to detect and monitor metastatic diseases in patients suffering from malignant melanoma.²⁰⁻²¹ In 2001, the three-dimensional structure of the protein was solved by multidimensional nuclear magnetic resonance (NMR) and X-ray crystallography techniques.²²⁻²³ Structural analysis revealed that MIA protein comprises an SH3 domain like fold in solution, a structure with two perpendicular, antiparallel, three- and five-stranded beta-sheets.²⁴⁻²⁵ MIA represents a novel class of secreted proteins comprising an SH3 domain.²⁶ The MIA protein family consists of MIA and the homologous proteins OTOR, MIA-2 and TANGO (MIA-3).

1.4 Cellular processing of MIA protein during migration

The MIA protein transport was found to take the conventional secretion pathway, including COPI and COPII mediated vesicle sorting in the endoplasmic reticulum and Golgi apparatus, to exit the cell.²⁷ By N-terminal labeling of MIA protein using a HisTag and cloning of an N-terminal secretion sequence, the intracellular protein transport was followed. Interestingly, the transport along the microtubule system to the cell periphery is restricted to the rear of migrating cells (*Figure 1*).

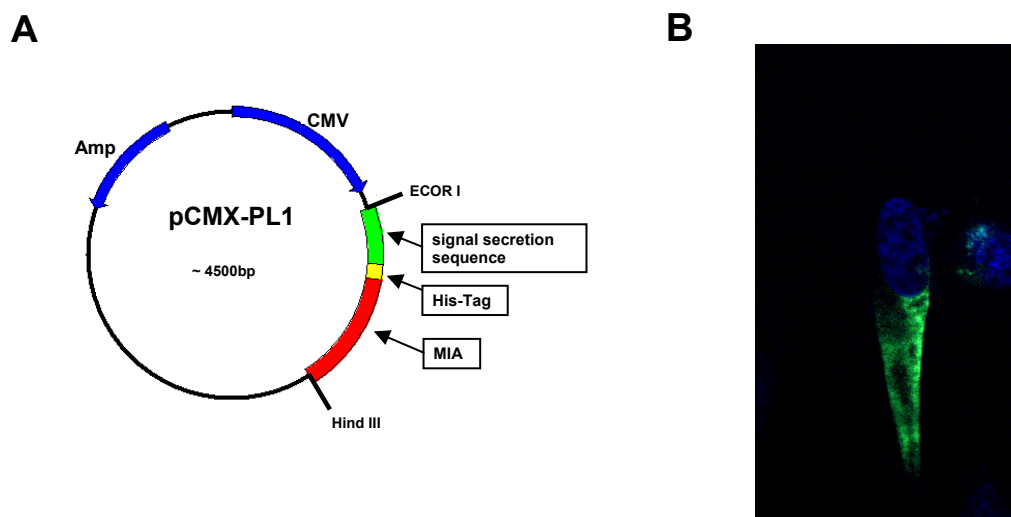
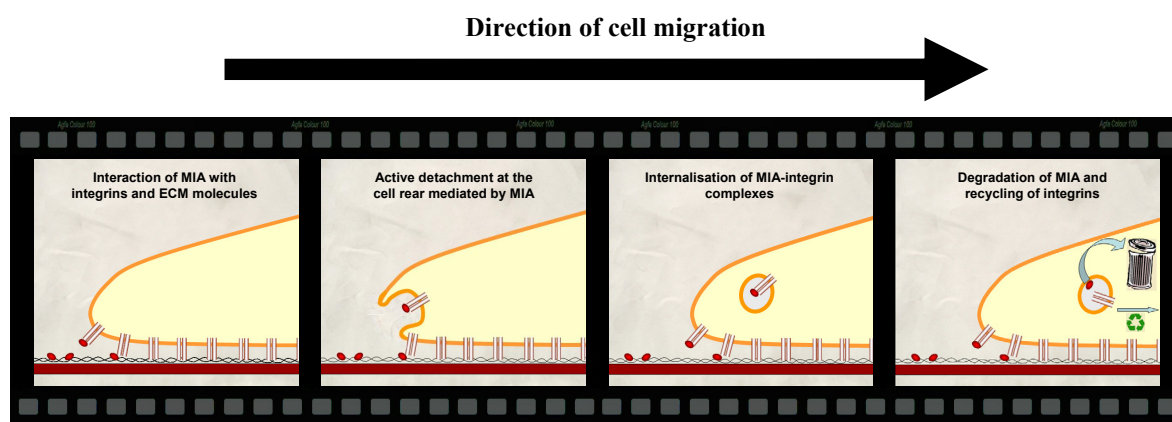


Figure 1: *MIA protein transport is restricted to the cell rear of migrating cells*

(A) Cloning strategy (B) After cleavage of the N-terminal secretion sequence, His-tagged MIA protein is transported along the microtubule system to the rear of migrating cells.

The final release of MIA protein is a triggered event that depends on an increase in intracellular Ca^{2+} concentration. It was further shown that secretion of MIA protein is significantly augmented by KCNN4 potassium channel activity. This channel type was

found to be aberrantly expressed in various tumor types and implicated in the promotion of cell migration and cell proliferation.²⁸⁻³¹ In migrating cells, KCNN4 channel activity was detected predominantly at the rear cell pole, which may be due to the intracellular Ca^{2+} gradient in polarized, migrating cells.³² As illustrated in *Scheme 1*, MIA protein strongly contributes to the invasive and migratory potential of melanoma cells by inhibiting attachment to extracellular matrix structures including fibronectin, laminin and tenascin *in vivo*.^{25, 33-34} Following localized protein secretion, a direct interaction of MIA protein with cell adhesion receptors integrin $\alpha_4\beta_1$ and $\alpha_5\beta_1$ results in locally reduced cell adhesion contacts. Formed MIA-integrin-complexes are subsequently internalized into the cell at the rear.³⁵ This localized uptake of MIA protein results in focal cell detachment at the cell rear and allows a directed cellular movement. Inside the cell these complexes are dissociated and MIA protein is degraded in lysosomes, while integrins are recycled and transported to the cell front in order to form new adhesion contacts. Changes in metastatic behavior in correlation with the expression level of MIA provide evidence that upregulation of MIA during malignant transformation of melanocytic cells is causally involved in acquisition of the malignant cancer cell phenotype.



Scheme 1: Processing of MIA protein during cellular migration

MIA protein promotes localized cell detachment at the rear cell pole by modulating integrin activity. By directly binding to these cell adhesion receptors and extracellular matrix structures it thus strongly contributes to the invasive and migratory potential of melanoma cells. Formed MIA-integrin-complexes are subsequently internalized into the cell at the rear pole. This focal cell detachment allows a directed cell movement. Inside the cell MIA-integrin complexes are dissociated, MIA protein is degraded in acidic vesicles while integrins are recycled and transported to the cell front in order to form new adhesion contacts.

1.5 Functional inhibition of MIA protein

NMR spectroscopy and Western blot analysis revealed that MIA protein has a tendency to build homomeric assemblies with head-to-tail linkages. By functionally analyzing MIA protein mutant forms *in vitro* it was demonstrated that MIA protein achieves activity by

self assembly.³⁶ Monomeric species are completely inactive, suggesting that the binding site for integrins, probably generated by protein assembly, could be located at the surface involving both MIA subunits. Inactivation of MIA protein by peptidic dimerization inhibitors provides an excellent starting point for the development of a new inhibitory strategy to reduce tumor cell invasion and formation of metastases. To selectively screen for substances that directly bind to the MIA protein dimerization domain and thus generate inactive monomers, a transition metal based fluorescence polarization assay was established.³⁷ AR71, a dodecapeptide identified in this screening assay, was analyzed for its MIA inhibitory potential *in vitro* and *in vivo* studies. Binding to the dimerization domain was confirmed by NMR-spectroscopy. Interestingly, inhibition of MIA protein function in the *in vivo* mouse melanoma model led to strongly reduced numbers of metastases in mice being treated with daily *iv* injections of peptide AR71 as shown in *Figure 2*.³⁶ Based on these data, the rational design and development of a novel pharmacophore which inhibits MIA protein dimerization may provide a key element in malignant melanoma therapy.

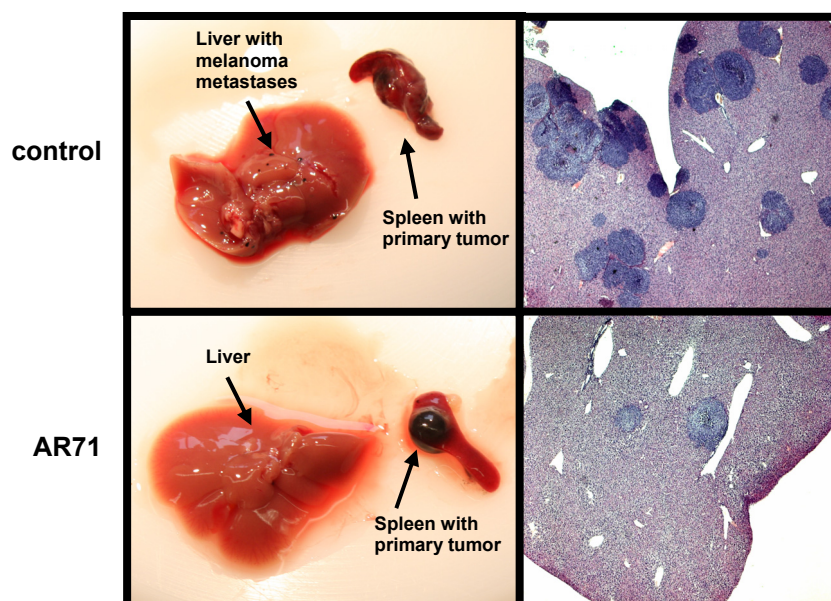


Figure 2: Dodecapeptide AR71 strongly reduces formation of melanoma metastasis *in vivo*

Wild type murine B16 melanoma cells were injected into the spleen of B1/6N mice with the mice being subsequently treated with *i.v.* injections of AR71. Histological analyses revealed a significant reduction of metastases in the liver of mice treated with AR71 compared to the liver of untreated control mice.

1.6 Antimetastatic agents as a new therapy strategy

Conventional chemotherapy treatments target all fast dividing cells and thus indiscriminately kill cancer cells as well as hair follicle cells and cells in the mucous membranes in the gastrointestinal tract. By targeting MIA protein, which is only expressed

in malignant melanoma and in early-phase differentiating chondrocytes, the expected side effects of treatment with MIA inhibitory compounds should be minimal. Side effects on cartilage are not expected as MIA-deficient mice show no phenotype.³⁸ Next to cytotoxic compounds and angiogenesis inhibitors, a MIA inhibitor will present a novel antimetastatic therapeutic strategy of cancer treatment. Only in rare cases the primary tumor is fatal for patients suffering from malignant melanoma. Mostly, the cause of death is the failure of vital organs due to the formation of metastases. Development of antimetastatic agents could be of great importance and a milestone in the treatment of malignant melanoma.

1.7 References

1. Gammill, L. S.; Bronner-Fraser, M., Genomic analysis of neural crest induction. *Development* **2002**, 129, (24), 5731-41.
2. Segal, N. H.; Pavlidis, P.; Noble, W. S.; Antonescu, C. R.; Viale, A.; Wesley, U. V.; Busam, K.; Gallardo, H.; DeSantis, D.; Brennan, M. F.; Cordon-Cardo, C.; Wolchok, J. D.; Houghton, A. N., Classification of clear-cell sarcoma as a subtype of melanoma by genomic profiling. *J Clin Oncol* **2003**, 21, (9), 1775-81.
3. Clark, E. A.; Golub, T. R.; Lander, E. S.; Hynes, R. O., Genomic analysis of metastasis reveals an essential role for RhoC. *Nature* **2000**, 406, (6795), 532-5.
4. Lauffenburger, D. A.; Horwitz, A. F., Cell migration: a physically integrated molecular process. *Cell* **1996**, 84, (3), 359-69.
5. Parent, C. A.; Devreotes, P. N., A cell's sense of direction. *Science* **1999**, 284, (5415), 765-70.
6. Schwab, A.; Nechyporuk-Zloy, V.; Fabian, A.; Stock, C., Cells move when ions and water flow. *Pflugers Arch* **2007**, 453, (4), 421-32.
7. Brundage, R. A.; Fogarty, K. E.; Tuft, R. A.; Fay, F. S., Calcium gradients underlying polarization and chemotaxis of eosinophils. *Science* **1991**, 254, (5032), 703-6.
8. Hahn, K.; DeBiasio, R.; Taylor, D. L., Patterns of elevated free calcium and calmodulin activation in living cells. *Nature* **1992**, 359, (6397), 736-8.
9. Komuro, H.; Kumada, T., Ca(2+) transients control CNS neuronal migration. *Cell Calcium* **2005**, 37, (5), 387-93.
10. Schwab, A.; Wojnowski, L.; Gabriel, K.; Oberleithner, H., Oscillating activity of a Ca(2+)-sensitive K(+) channel. A prerequisite for migration of transformed Madin-Darby canine kidney focus cells. *J Clin Invest* **1994**, 93, (4), 1631-6.

11. Franco, S. J.; Huttenlocher, A., Regulating cell migration: calpains make the cut. *J Cell Sci* **2005**, 118, (Pt 17), 3829-38.
12. Pettit, E. J.; Fay, F. S., Cytosolic free calcium and the cytoskeleton in the control of leukocyte chemotaxis. *Physiol Rev* **1998**, 78, (4), 949-67.
13. Bosserhoff, A. K.; Kaufmann, M.; Kaluza, B.; Bartke, I.; Zirngibl, H.; Hein, R.; Stolz, W.; Buettner, R., Melanoma-inhibiting activity, a novel serum marker for progression of malignant melanoma. *Cancer Res* **1997**, 57, (15), 3149-53.
14. Blesch, A.; Bosserhoff, A. K.; Apfel, R.; Behl, C.; Hessdoerfer, B.; Schmitt, A.; Jachimczak, P.; Lottspeich, F.; Buettner, R.; Bogdahn, U., Cloning of a novel malignant melanoma-derived growth-regulatory protein, MIA. *Cancer Res* **1994**, 54, (21), 5695-701.
15. Bosserhoff, A. K.; Buettner, R., Establishing the protein MIA (melanoma inhibitory activity) as a marker for chondrocyte differentiation. *Biomaterials* **2003**, 24, (19), 3229-34.
16. Marr, D. G.; Poser, I.; Shellman, Y. G.; Bosserhoff, A. K.; Norris, D. A., Ultraviolet radiation induces release of MIA: a new mechanism for UVR-induced progression of melanoma. *Int J Oncol* **2004**, 25, (1), 105-11.
17. Bosserhoff, A. K.; Echtenacher, B.; Hein, R.; Buettner, R., Functional role of melanoma inhibitory activity in regulating invasion and metastasis of malignant melanoma cells in vivo. *Melanoma Res* **2001**, 11, (4), 417-21.
18. Bosserhoff, A. K.; Stoll, R.; Sleeman, J. P.; Bataille, F.; Buettner, R.; Holak, T. A., Active detachment involves inhibition of cell-matrix contacts of malignant melanoma cells by secretion of melanoma inhibitory activity. *Lab Invest* **2003**, 83, (11), 1583-94.
19. Guba, M.; Bosserhoff, A. K.; Steinbauer, M.; Abels, C.; Anthuber, M.; Buettner, R.; Jauch, K. W., Overexpression of melanoma inhibitory activity (MIA) enhances extravasation and metastasis of A-mel 3 melanoma cells in vivo. *Br J Cancer* **2000**, 83, (9), 1216-22.
20. Dreau, D.; Bosserhoff, A. K.; White, R. L.; Buettner, R.; Holder, W. D., Melanoma-inhibitory activity protein concentrations in blood of melanoma patients treated with immunotherapy. *Oncol Res* **1999**, 11, (1), 55-61.
21. Stahlecker, J.; Gauger, A.; Bosserhoff, A.; Buettner, R.; Ring, J.; Hein, R., MIA as a reliable tumor marker in the serum of patients with malignant melanoma. *Anticancer Res* **2000**, 20, (6D), 5041-4.

22. Loughheed, J. C.; Holton, J. M.; Alber, T.; Bazan, J. F.; Handel, T. M., Structure of melanoma inhibitory activity protein, a member of a recently identified family of secreted proteins. *Proc Natl Acad Sci U S A* **2001**, 98, (10), 5515-20.
23. Stoll, R.; Renner, C.; Ambrosius, D.; Golob, M.; Voelter, W.; Buettner, R.; Bosserhoff, A. K.; Holak, T. A., Sequence-specific ^1H , ^{13}C , and ^{15}N assignment of the human melanoma inhibitory activity (MIA) protein. *J Biomol NMR* **2000**, 17, (1), 87-8.
24. Stoll, R.; Renner, C.; Buettner, R.; Voelter, W.; Bosserhoff, A. K.; Holak, T. A., Backbone dynamics of the human MIA protein studied by ^{15}N NMR relaxation: implications for extended interactions of SH3 domains. *Protein Sci* **2003**, 12, (3), 510-9.
25. Stoll, R.; Renner, C.; Zweckstetter, M.; Bruggert, M.; Ambrosius, D.; Palme, S.; Engh, R. A.; Golob, M.; Breibach, I.; Buettner, R.; Voelter, W.; Holak, T. A.; Bosserhoff, A. K., The extracellular human melanoma inhibitory activity (MIA) protein adopts an SH3 domain-like fold. *EMBO J* **2001**, 20, (3), 340-9.
26. Stoll, R.; Bosserhoff, A., Extracellular SH3 domain containing proteins - features of a new protein family. *Curr Protein Pept Sci* **2008**, 9, (3), 221-6.
27. Schmidt, J.; Friebel, K.; Schönherr, R.; Coppolino, M. G.; Bosserhoff, A. K., Directed, Migration-associated Secretion of Melanoma Inhibitory Activity (MIA) at the Cell Rear is supported by KCNN4 Potassium Channels. *Cell Res* **2010**, (submitted).
28. Jager, H.; Dreker, T.; Buck, A.; Giehl, K.; Gress, T.; Grissmer, S., Blockage of intermediate-conductance $\text{Ca}(2+)\text{-activated K}(+)$ channels inhibit human pancreatic cancer cell growth in vitro. *Mol Pharmacol* **2004**, 65, (3), 630-8.
29. Lallet-Daher, H.; Roudbaraki, M.; Bavencoffe, A.; Mariot, P.; Gackiere, F.; Bidaux, G.; Urbain, R.; Gosset, P.; Delcourt, P.; Fleurisse, L.; Slomianny, C.; Dewailly, E.; Mauroy, B.; Bonnal, J. L.; Skryma, R.; Prevarskaya, N., Intermediate-conductance $\text{Ca}(2+)\text{-activated K}(+)$ channels (IKCa1) regulate human prostate cancer cell proliferation through a close control of calcium entry. *Oncogene* **2009**, 28, (15), 1792-806.
30. Tajima, N.; Schonherr, K.; Niedling, S.; Kaatz, M.; Kanno, H.; Schonherr, R.; Heinemann, S. H., $\text{Ca}(2+)\text{-activated K}(+)$ channels in human melanoma cells are up-regulated by hypoxia involving hypoxia-inducible factor-1alpha and the von Hippel-Lindau protein. *J Physiol* **2006**, 571, (Pt 2), 349-59.

31. Wang, J.; Xu, Y. Q.; Liang, Y. Y.; Gongora, R.; Warnock, D. G.; Ma, H. P., An intermediate-conductance $\text{Ca}(2+)$ -activated $\text{K}(+)$ channel mediates B lymphoma cell cycle progression induced by serum. *Pflugers Arch* **2007**, 454, (6), 945-56.
32. Schwab, A.; Gabriel, K.; Finsterwalder, F.; Folprecht, G.; Greger, R.; Kramer, A.; Oberleithner, H., Polarized ion transport during migration of transformed Madin-Darby canine kidney cells. *Pflugers Arch* **1995**, 430, (5), 802-7.
33. Bauer, R.; Humphries, M.; Fassler, R.; Winklmeier, A.; Craig, S. E.; Bosserhoff, A. K., Regulation of integrin activity by MIA. *J Biol Chem* **2006**, 281, (17), 11669-77.
34. Bosserhoff, A. K.; Golob, M.; Buettner, R.; Landthaler, M.; Hein, R., MIA ("melanoma inhibitory activity"). Biological functions and clinical relevance in malignant melanoma. *Hautarzt* **1998**, 49, (10), 762-9.
35. Schmidt, J.; Bosserhoff, A. K., Processing of MIA protein during melanoma cell migration. *Int J Cancer* **2009**, 125, (7), 1587-94.
36. Schmidt, J.; Riechers, A.; Stoll, R.; Amann, T.; Fink, F.; Hellerbrand, C.; Gronwald, W.; König, B.; Bosserhoff, A., Dissociation of functionally active MIA dimers by dodecapeptide AR71 strongly reduces formation of metastases in malignant melanoma. *Nat Med* **2010**, submitted.
37. Riechers, A.; Schmidt, J.; König, B.; Bosserhoff, A. K., Heterogeneous transition metal-based fluorescence polarization (HTFP) assay for probing protein interactions. *Biotechniques* **2009**, 47, (4), 837-44.
38. Moser, M.; Bosserhoff, A. K.; Hunziker, E. B.; Sandell, L.; Fassler, R.; Buettner, R., Ultrastructural cartilage abnormalities in MIA/CD-RAP-deficient mice. *Mol Cell Biol* **2002**, 22, (5), 1438-45.

2 Directed, Migration-associated Secretion of Melanoma Inhibitory Activity (MIA) at the Cell Rear is supported by KCNN4 Potassium Channels

Abstract

Malignant melanoma, characterized by invasive local growth and early formation of metastases, is the most aggressive type of skin cancer. Melanoma Inhibitory Activity (MIA), secreted by malignant melanoma cells, interacts with the cell adhesion receptors integrin $\alpha_4\beta_1$ and $\alpha_5\beta_1$, facilitating cell detachment and promoting formation of metastases. In the present study, we demonstrate that MIA secretion is confined to the rear end of migrating cells, while in non-migrating cells MIA accumulates in the actin-cortex. MIA protein takes a conventional secretory pathway including COPI- and COPII-dependent protein transport to the cell periphery, where its final release depends on intracellular Ca^{2+} ions. Interestingly, the Ca^{2+} -activated potassium channel KCNN4, known to be active at the rear end of migrating cells, was found to support MIA secretion. Secretion was diminished by the specific KCNN4 channel inhibitor TRAM-34 and by expression of dominant-negative mutants of the channel. In summary, we have elucidated the directed, migration-associated transport of MIA protein to the cell rear and disclosed a new mechanism by which KCNN4 potassium channels promote cell migration.

The results of this chapter have been submitted for publication:

Schmidt J., Friebe K., Schönherr R., Coppolino M. G., Bosserhoff A. K.; Directed, Migration-associated Secretion of Melanoma Inhibitory Activity (MIA) at the Cell Rear is supported by KCNN4 Potassium Channels. *Cell Res* **2009**; (submitted)

Author Contributions:

I focused on all cell culture experiments, ELISA measurements, immunofluorescence studies and cloning. K. Friebe has performed electrophysiological recordings. M. G. Coppolino has helped to analyze vesicular transport and secretion processes. R. Schönherr and A. K. Bosserhoff have been supervising this project.

2.1 Introduction

Previously, melanoma inhibitory activity (MIA) has been identified as an 11 kDa protein physiologically produced by cartilage and strongly expressed and secreted by malignant melanoma cells.¹⁻² MIA protein is known to play a key role in melanoma development, progression and formation of metastasis.²⁻³ Increased MIA protein plasma levels directly correlate with progressive malignancy and a more advanced state of melanocytic tumors.^{1, 4} Thus, MIA protein serves as a reliable clinical tumor marker to detect and monitor metastatic disease in patients suffering from malignant melanoma.^{1, 5-6} MIA protein strongly contributes to the invasive and migratory potential of melanoma cells and promotes the formation of tumor metastases; however, the mechanistic link between MIA protein and cell motility remains unclear.² Recent data describe a direct interaction of MIA protein with cell adhesion receptors integrin $\alpha_4\beta_1$ and integrin $\alpha_5\beta_1$ followed by facilitation of cell detachment.⁷ Cell migration requires adhesion to the extracellular matrix to provide traction points and to stabilize protrusions at the cell front. Conversely, retraction of the rear cell end demands the release of adhesion contacts. In line with this assumption, external addition of MIA protein does not support migration but results in unpolarized cell detachment and reduced invasiveness in Boyden chamber assays.² To account for the promigratory effect of endogenously expressed and secreted MIA protein, we proposed that MIA secretion is directed to the rear end of a migrating cell where it can bind to integrins and thereby promote cell retraction.⁷ MIA-integrin complexes are subsequently internalized at the rear of the cell.⁸

The MIA secretion pathway has not yet been analyzed in detail, but the protein comprises a typical N-terminal ER-signal peptide that is processed during synthesis.⁹ In the conventional secretory pathway, protein synthesis at the ER is followed by its translocation to the Golgi apparatus via COPII-coated vesicles. Further protein sorting in the Golgi depends on the formation of COPI-coated vesicular intermediates, which mediate retrograde movement of components in the Golgi and back to the ER as well as anterograde movements to the cell membrane.¹⁰ Following vesicle tethering, docking and membrane fusion, the cargo proteins are released into the extracellular space. The final release can either be a constitutive process or a triggered event that depends on an increase in intracellular Ca^{2+} concentration. Both scenarios involve N-ethylmaleimide-sensitive factor attachment protein receptor (SNARE) protein complexes to mediate vesicle docking and fusion.¹¹

Intracellular Ca^{2+} plays a crucial role in almost all cellular processes; including regulation of membrane-fusion as well as cell migration.¹²⁻¹³ By modulating turnover of actin filaments, activation of calpain mediating release of cell-matrix contacts and recycling of integrins, Ca^{2+} coordinates different components of the cellular migration machinery.¹⁴⁻¹⁷ Another player linking intracellular Ca^{2+} ions and cell migration is the calcium-activated potassium channel KCNN4. This channel type was found to be aberrantly expressed in various tumor types and implicated in the promotion of cell migration and cell proliferation.¹⁸⁻²¹ In migrating cells, KCNN4 channel activity was detected predominantly at the rear cell pole, which may be due to the intracellular Ca^{2+} gradient in polarized, migrating cells.²² While it was shown that specific inhibition of KCNN4 channels reduces cell migration, the underlying mechanisms are still largely elusive.²³⁻²⁵

Here, we used a HisTag-labeled MIA protein construct to monitor MIA secretion in melanoma cells. We show that in migrating cells, MIA secretion is restricted to the rear of the cell. This could be crucial for the mechanism through which MIA contributes to migration. Experiments using specific inhibitors and dominant negative mutants revealed that MIA follows a conventional secretion pathway, involving COPI- and COPII-dependent protein transport to the cell periphery, where the final release depends on intracellular Ca^{2+} ions. Further, we show that secretion of MIA protein is significantly augmented by KCNN4 potassium channel activity. In summary, we provide experimental evidence for our model, first hypothesized in 2006, of facilitated retraction at the rear of migrating cells controlled in part by directed secretion of MIA protein.⁷

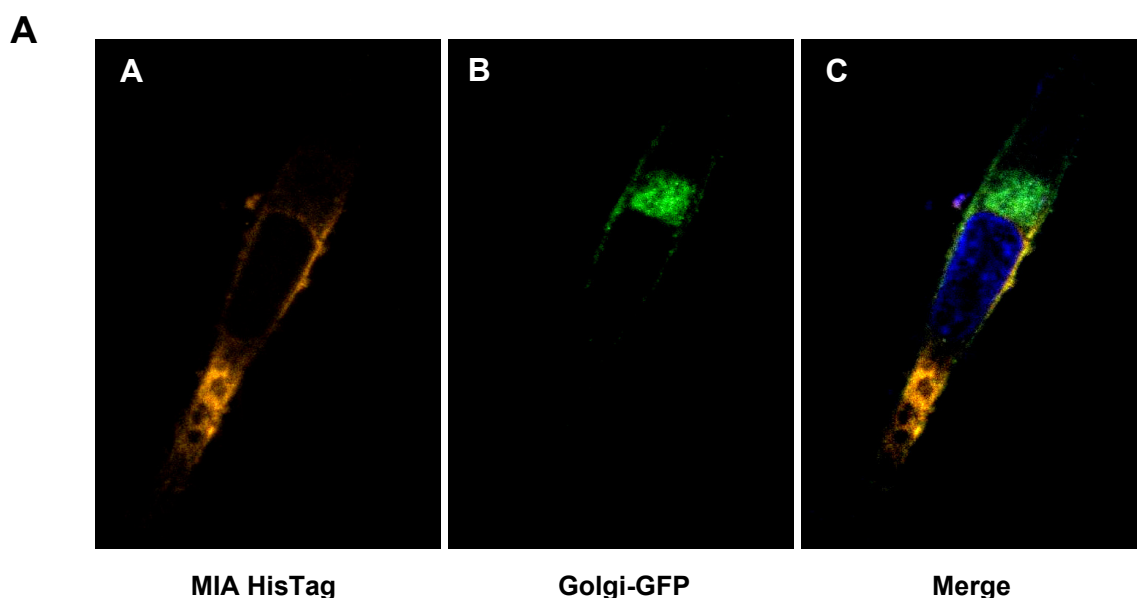
2.2 Results

2.2.1 Targeted MIA protein transport to the rear of migrating cells

We aimed to elucidate the MIA protein secretion pathway to further understand the contribution of MIA protein to the enhanced migratory ability of melanoma cells. To follow MIA protein transport and distribution in migrating and non-migrating cells we visualized MIA protein by transiently transfecting Mel Im cells with a His-tagged MIA protein-containing expression plasmid. The MIA-HisTag conjugate was visualized in immunofluorescence studies using primary anti-HisTag and fluorescently labeled secondary antibodies. To verify the direction of migration, we co-stained the Golgi apparatus, since it is generally known that in migrating cells reorientation of the MTOC repositions the Golgi apparatus toward the leading edge of the cell and contributes to directional cell migration.²⁶ Figure 1A presents Mel Im cells that were co-transfected with

pCMX-PL1-hMIA-HisTag and Golgi-GFP (endomannosidase) plasmids to monitor intracellular MIA protein distribution. In polarized migrating cells MIA protein is asymmetrically distributed at one cell pole as shown in *Figure 1A,(A)*. Deduced from the localization of the Golgi on the side of the nucleus towards the leading edge in migrating cells *Figure 1A,(B)*, we conclude that MIA protein is transported to the rear cell pole (*Figure 1A,(C)*). Compared to migrating cells, non-polarized, non-migrating cells show a homogeneous distribution of MIA protein in the cytoplasm, as illustrated in *Figure 1B*. Interestingly, MIA protein appears to accumulate at the actin cortex, possibly in a vesicle pool as shown in *Figure 1B,(A)* and *(D)* using the two melanoma cell lines Mel Im and Mel Ju.

To further analyze the involvement of the actin cytoskeleton in secretion of MIA protein, we tested the effect of Jasplakinolide, which induces actin-polymerization. Exposure of cells to 5 nM and 50 nM Jasplakinolide results in a decrease of about 20% to 30% in the amount of secreted MIA protein, respectively, compared to the corresponding DMSO control (data not shown). These observations indicate involvement of the actin network in MIA protein transport towards the cell rear.



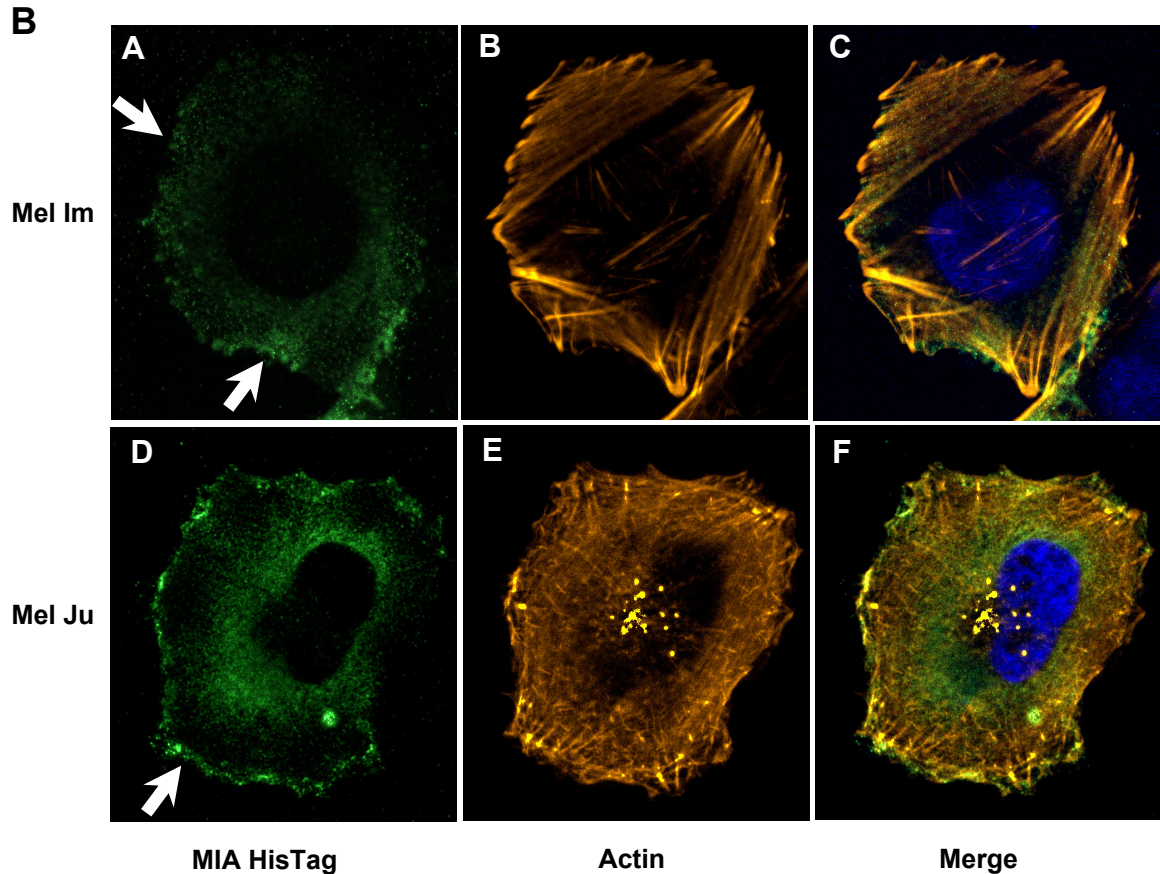


Figure 1: Targeted MIA protein transport to the cell rear in migrating cells

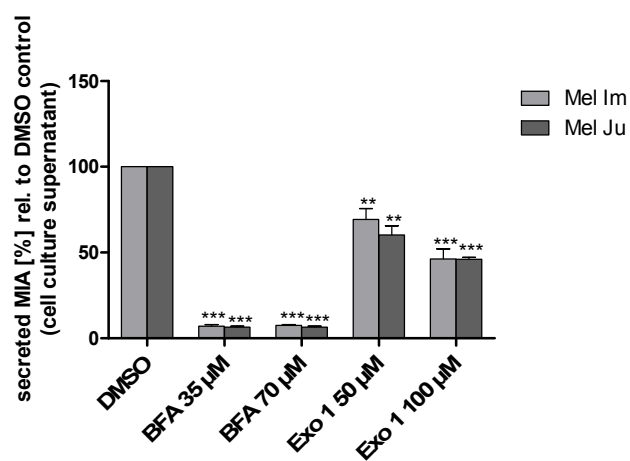
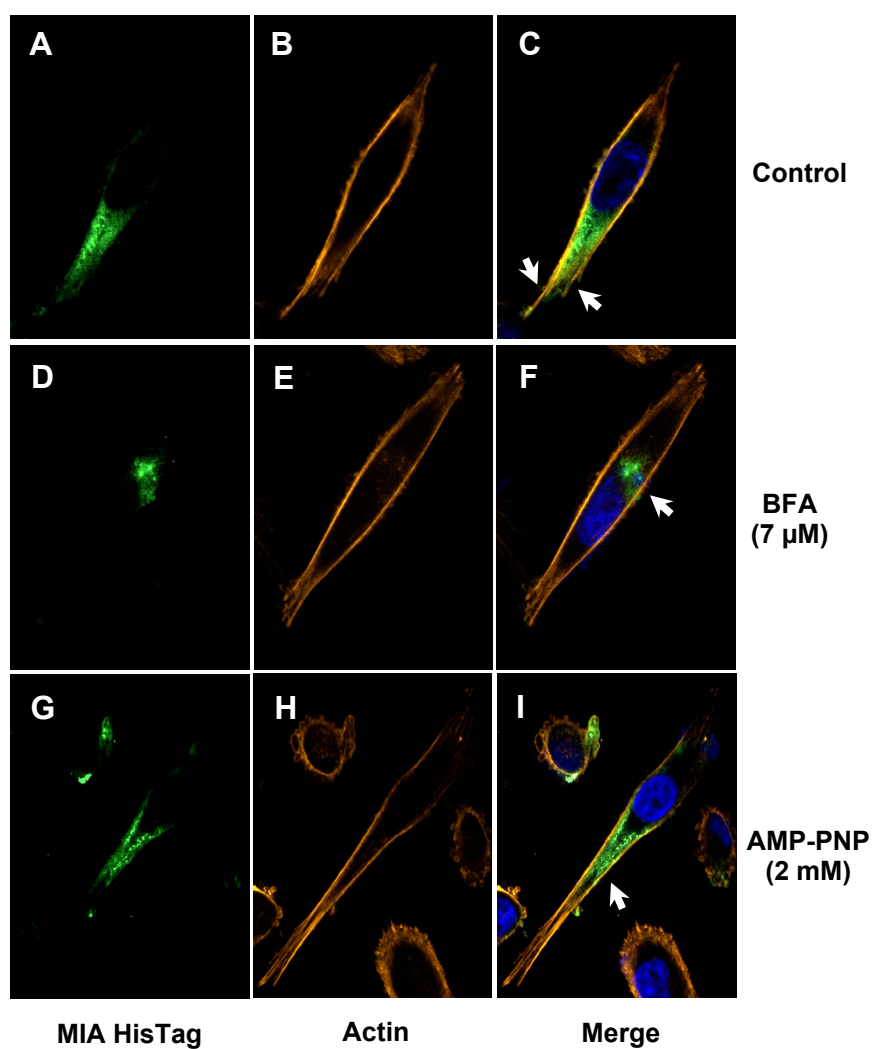
(A) Mel Im cells were co-transfected with pCMX-PL1-hMIA-HisTag and Golgi-GFP (endomannosidase) plasmids to detect intracellular MIA protein distribution and define direction of movement. In polarized migrating cells MIA protein is asymmetrically distributed at one cell pole, indicated by the white arrow (A). The Golgi apparatus is reoriented toward the leading edge of the cell during migration (B). (C) In migrating cells MIA protein is transported to the cell rear. (B) Adhered, non-polarized and non-migrating cells transiently transfected with pCMX-PL1-hMIA-HisTag construct show a homogeneous distribution of MIA protein in the cytoplasm. At the actin cortex MIA protein accumulates in a vesicle pool as indicated by white arrows in (A) for Mel Im cells and in (D) for Mel Ju cells. All experiments were performed at least in triplicates.

2.2.2 Intracellular transport of MIA protein follows the conventional secretory pathway

To characterize the MIA protein secretion pathway more closely, we analyzed whether MIA protein is transported through the conventional secretory pathway or if it takes an unconventional route to the cell surface in a Golgi-independent manner. Cells were treated with the fungal metabolite Brefeldin A, which blocks the recruitment of the ADP-ribosylation factor ARF1 to the Golgi, impairing the formation of COP I-coated vesicles and ultimately inhibiting ER-to-Golgi transport.²⁷ Cells were also exposed to Exo-1, which inhibits traffic emanating from the ER by inducing rapid collapse of the Golgi into the ER. After cell treatment with these compounds, the MIA protein concentration in cell culture supernatant was determined by MIA-ELISA. The DMSO or H₂O control, respectively,

was set to 100%. BFA at concentrations of 3.5 μ M and 7.0 μ M almost completely inhibits MIA protein secretion in both Mel Im and Mel Ju cells (*Figure 2A*). Treatment of cells with Exo1 at a concentration of 50 μ M and 100 μ M significantly reduced MIA protein secretion. *Figure 2B* presents the corresponding immunofluorescence analysis of the MIA protein. It demonstrates that migrating Mel Im cells, transiently transfected with a pCMX-PL1-hMIA-HisTag vector and treated with 7 μ M BFA, showed an altered distribution of MIA protein. To delineate cell boundaries, the actin cytoskeleton was stained with rhodamine-phalloidin. The control cells show MIA protein distribution at the cell rear (*Figure 2B,(A)*). In the overlay of MIA protein and actin filament staining in *Figure 2B,(C)* it is clearly visible that the MIA protein is delivered into the tip of the rear cell edge. After treatment of Mel Im cells with BFA, MIA protein accumulates proximal to the nucleus (*Figure 2B,(F)*). Cells were also transiently transfected with a dominant negative Sar1p (H79G) construct or mock transfected as controls. Sar1p is a small ER-associated GTPase, necessary for COPII-dependent vesicle formation at the ER.²⁸⁻³¹ As shown in *Figure 2C*, overexpression of the dominant-negative Sar1p mutant (H79G) leads to a reduction of MIA protein secretion relative to mock control, indicating that ER exit of MIA protein is mediated by COP II-coated vesicles.

We further confirmed microtubule based transport of MIA protein by treatment of melanoma cells with 25 μ M and 50 μ M Nocodazole, which leads to depolymerization of microtubules, and 1 mM and 2 mM AMP-PNP, a non-hydrolysable analogue of adenosine 5'-triphosphate which blocks the ATP-dependent microtubule motor protein kinesin.³² Both compounds reduce MIA protein exocytosis in a dose dependent manner (*Figure 2D*). Immunofluorescence analysis of Mel Im cells treated with the kinesin family inhibitor AMP-PNP at a concentration of 2 mM revealed a perturbed distribution of MIA protein: it is delivered to the cell rear, but it is not visible at the rear tip of the cell, suggesting that the peripheral microtubule based MIA protein transport has been interrupted (*Figure 2B,(I)*).

A**B**

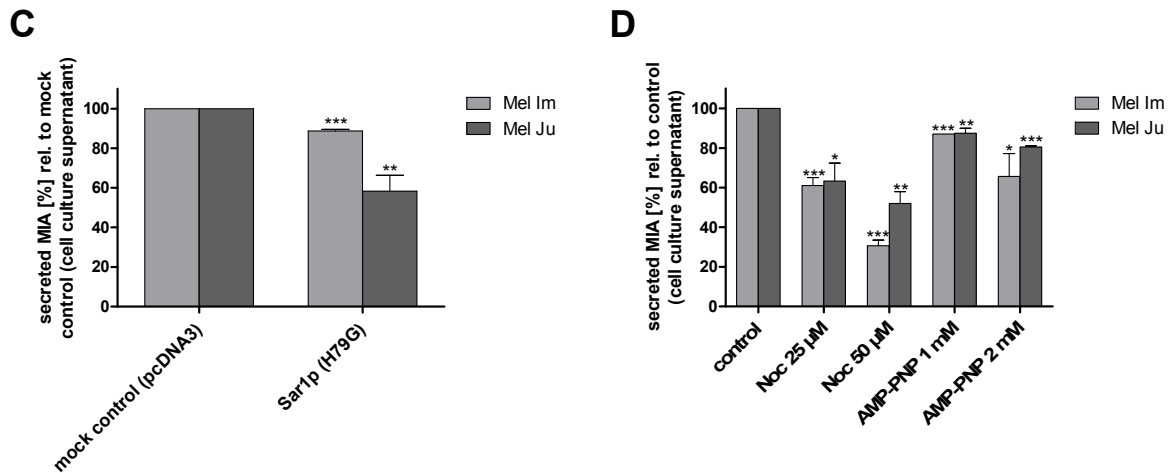


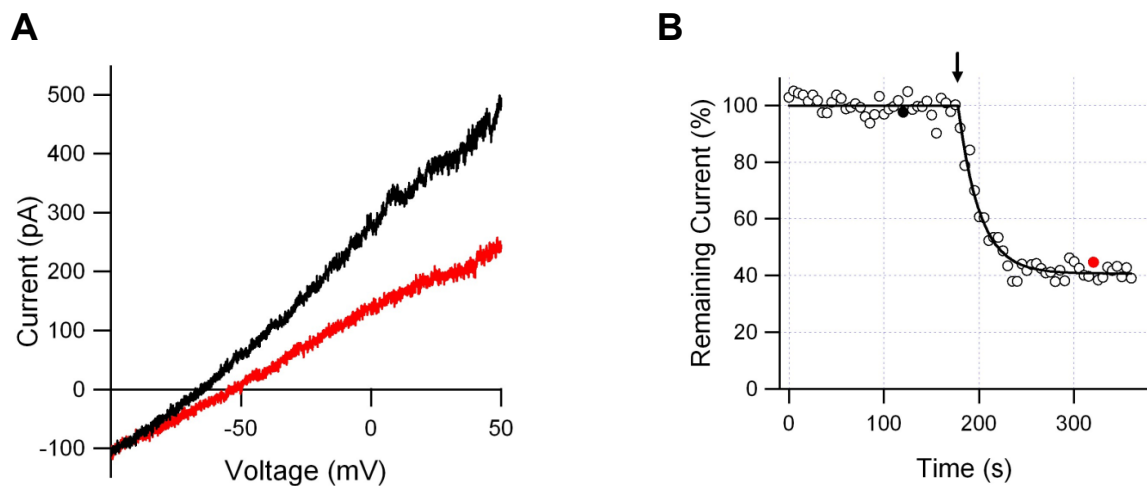
Figure 2: ER and Golgi-dependent MIA protein sorting and microtubule-based transport to the rear cell pole (A) Mel Im cells and Mel Ju cells were treated with BFA and with Exo1, both inhibiting the ER-Golgi transport. BFA at a concentration of 3.5 μ M and 7.0 μ M almost completely inhibits MIA protein secretion in both cell lines. Treatment of cells with Exo1 at a concentration of 50 μ M and 100 μ M significantly reduces MIA protein exocytosis compared to the respective H₂O or DMSO control. **(B)** Immunofluorescence analysis of Mel Im cells that were transiently transfected with a pCMX-PL1-hMIA-HisTag plasmid and stained for MIA protein using a mouse anti-HisTag antibody and a FITC-labeled anti mouse secondary antibody, were treated with 7 μ M BFA and AMP-PNP at a concentration of 2 mM. For a better illustration of cell borders an actin staining was performed in addition. Inhibition of ER-to-Golgi-transport by BFA treatment results in an accumulation of MIA protein in close proximity to the nucleus (F). Exposure to AMP-PNP, the vesicle transporter protein inhibitor, leads to a characteristic distribution of MIA protein, which is delivered to the cell rear, but it is not visible at the rear tip of the cell since the peripheral microtubule based MIA protein transport is interrupted (I). In contrast, in the untreated control cells MIA protein is delivered into the rear cell tip (C), as indicated by the white arrows. **(C)** Cells that were transiently transfected with a dominant negative Sar1p (H79G) construct show a reduction of MIA protein secretion relative to mock control. **(D)** To investigate microtubule involvement in MIA protein secretion, melanoma cells were treated with 25 μ M and 50 μ M Nocodazole, and 1 mM and 2 mM AMP-PNP. Both compounds reduce MIA protein exocytosis in a dose dependent manner. All experiments were performed at least in triplicates.

2.2.3 MIA protein secretion is a Ca^{2+} -regulated process

It is generally accepted that migrating cells are polarized along their axis of movement and establish an intracellular Ca^{2+} gradient with a lower Ca^{2+} concentration at the cell front.^{14-15, 17} By mediating salt efflux or influx, followed by osmotic water flow, ion channels and transporters play a pivotal role in regulating cell volume during migration. These considerations apply in particular to the KCNN4 channel, which is activated in migrating cells by increased Ca^{2+} , especially at the cell rear.^{17, 22, 33} Since KCNN4 channel expression was observed in malignant melanoma cells we decided to test for KCNN4-mediated potassium currents in Mel Im cells and to investigate whether there is a direct association of channel activity and MIA-protein secretion.²⁰ Figure 3A shows a typical current response of Mel Im cells to a voltage ramp ranging from -100 mV to +50 mV in the whole-cell patch clamp configuration. Bath application of the KCNN4-specific channel blocker TRAM-34 resulted in a rapid decrease of the current amplitude (Figure 3A,B),

indicating that this channel is in fact in an active state.³⁴ The residual current is most likely due to other ion channels present in this cell line. At least in part, this remaining current is not carried by potassium-selective channels, as indicated by right-shifted reversal potentials in the presence of TRAM-34.

The above results prompted us to analyze whether inhibition of the KCNN4 channel by TRAM-34 impacts MIA protein distribution. In the cytoplasm of Mel Im cells that were transiently transfected with His-tagged MIA protein, treatment of migrating cells with TRAM-34 did not prevent transport of MIA protein to the cell rear. In these treated cells, however, the MIA protein accumulated at the plasma membrane as shown by white arrows in *Figure 3C,(F)*.



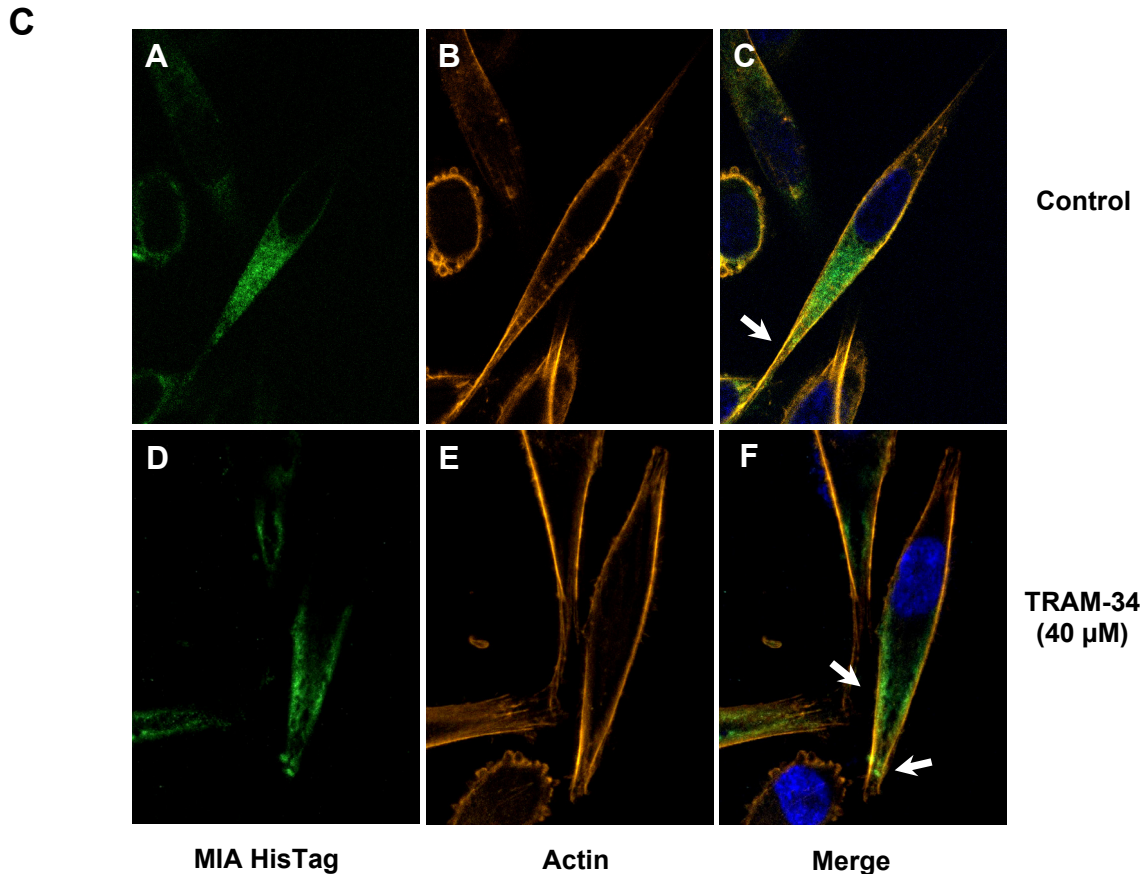


Figure 3: *MIA* protein secretion is a Ca^{2+} -regulated process

(A) Verification of active KCNN4 channels in Mel Im cells. Representative current traces in response to voltage ramps from -100 mV to +50 mV, recorded before (black) and after (red) application of 200 nM TRAM-34. (B) Time course of KCNN4 inhibition by TRAM-34. The percentage of remaining current is plotted as a function of time. The start of TRAM-34 application is indicated by the arrow. The continuous line describes the time course of channel block according to a single exponential function. Data points with filled circles correspond to current traces shown in panel B. (C) The corresponding immunofluorescence of Mel Im cells transiently transfected with pCMX-PL1-hMIA-HisTag and treated with 40 μ M TRAM-34 revealed an accumulation of MIA protein at the cell membrane, as indicated by the white arrow (F). In the corresponding control cells (C), MIA protein, transported to the rear cell tip, is homogeneously distributed in the cytoplasm, (shown by white arrows). Experiments were performed at least in triplicates.

To address the functional impact of KCNN4 channel activity on MIA protein secretion, we investigated the effects of treatment with activators and inhibitors as well as dominant-negative constructs of the KCNN4 channel. As shown in *Figure 4A*, activation of the KCNN4 channel by 100 μ M and 200 μ M 1-EBIO leads to a small increase of MIA protein secretion, suggesting that these channels are already in the active state. Mel Ju cells, which display a weaker tendency to migrate compared to Mel Im cells, showed a larger increase in MIA protein secretion after KCNN4 channel activation. Inhibition of the KCNN4 channel either by treatment with TRAM-34 at concentrations of 20 μ M and 40 μ M or after transfection with two different dominant-negative mutant forms of the KCNN4 channel, dnKCNN4 Y253L and dnKCNN4 AAA, significantly decreased MIA protein secretion

(Figure 4B).³⁵ The dominant-negative KCNN4 constructs encode channel subunits with mutations in the potassium selectivity filter. Upon tetrameric coassembly with wild-type subunits they generate nonfunctional channels. To confirm the dominant negative activity of the mutant KCNN4 constructs, HEK293 cells were transfected with the wild-type expression construct alone, or in combination with increasing amounts of dominant negative KCNN4 constructs (Figure 4C,D). Both dnKCNN4 constructs decreased the mean potassium currents at least 70-fold upon transfection in 4:1 ratio to wild-type KCNN4. Mock-transfected HEK293 cells did not exhibit any calcium-activated potassium currents (not shown).

To further assess the direct association between MIA protein secretion and expression of the KCNN4 channel, we transiently co-transfected HEK293 cells (which normally express neither MIA protein nor KCNN4 channels) with a MIA protein-containing plasmid, pCMX-PL1-hMIA, a KCNN4 channel-containing plasmid, and with the dominant-negative KCNN4 construct (dnKCNN4 AAA), using a range of amounts of the different vectors (Figure 4E). Co-transfection of MIA protein and KCNN4 channel containing vectors increased MIA protein secretion approximately 40% relative to cells that were transfected with a MIA protein-containing vector alone. This effect could be reduced in a dose dependent manner to the level of the control by co-transfection of cells with dnKCNN4 AAA, the mutant form of the KCNN4 channel. This observation clearly represents a direct association of MIA protein secretion and KCNN4 channel activity.

Since the KCNN4 channel activity is increased by an elevation in the intracellular Ca^{2+} concentration, we also examined the influence of Ca^{2+} on MIA protein secretion. This is of particular interest, since the Ca^{2+} concentration is elevated at the rear of migrating cells, where MIA protein is also secreted. Treatment of cells with 1 μM and 5 μM BAPTA-AM, a membrane permeable, selective chelator of intracellular Ca^{2+} , leads to a significant decrease in MIA protein secretion in a dose dependent manner (Figure 4F).³⁶ Additionally, we incubated Mel Im and Mel Ju cells with 1 nM and 10 nM Calcimycin (A23187), an ionophore that is highly selective for Ca^{2+} ions leading to an elevation of the intracellular Ca^{2+} concentration.³⁷ Interestingly, the amount of MIA protein secreted into the cell culture supernatant increased by 20% compared to DMSO-treated control cells. All these results strongly argue for a KCNN4 channel associated regulated MIA protein secretion.

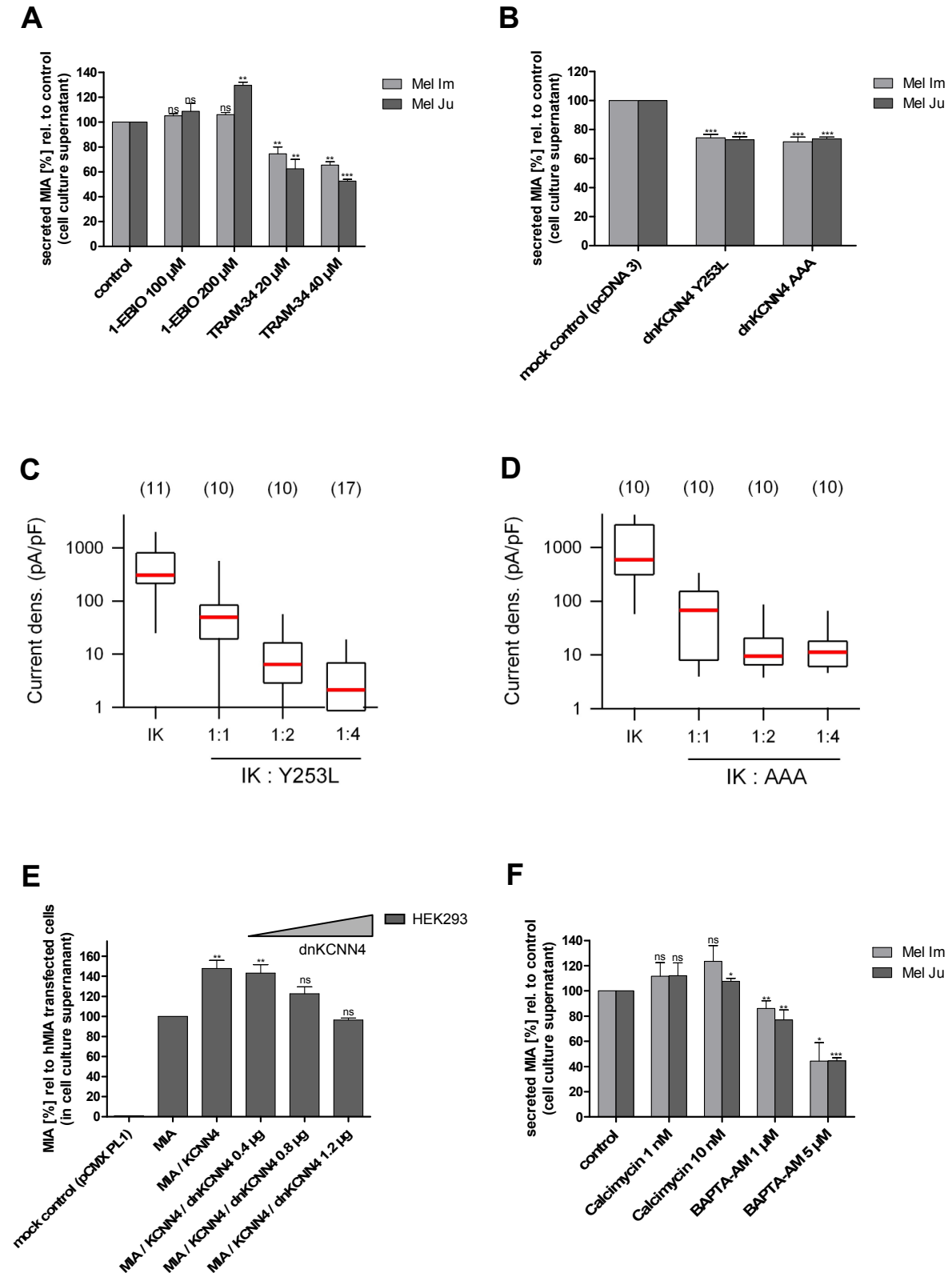


Figure 4: MIA protein secretion is associated to KCNN4 channel activity

(A) Mel Im and Mel Ju cells were treated with 100 μ M and 200 μ M 1-EBIO, a KCNN4 channel activator, and with 20 μ M and 40 μ M TRAM-34, a specific inhibitor of the KCNN4 channel. Activation of the KCNN4 channel by 1-EBIO results in a small increase of MIA protein secretion, suggesting that the KCNN4 channel is already in an active state. Inhibition of the KCNN4 channel by TRAM-34 leads to a significant reduction in MIA protein secretion. (B) Mel Im and Mel Ju cells were transiently transfected with two different dominant negative mutant forms of the KCNN4 channel, dnKCNN4 Y253L and dnKCNN4 AAA. Compared

to the mock control, these treated cells show a significant reduction in MIA protein secretion in both cases. **(C, D)** Verification of dominant-negative activity of dnKCNN4 Y253L (C) and dnKCNN4 AAA (D). HEK293 cells were transfected with the wild-type KCNN4 expression construct alone (IK), or in combination with increasing amounts of dominant negative constructs. Current densities are presented as box and whisker plots. Medians are indicated in red. Boxes range from 25-75% of all data points. Whiskers indicate the lowest and highest current densities. The numbers of individual experiments are indicated in parenthesis. **(E)** To better demonstrate the direct association of MIA protein secretion and the expression of the KCNN4 channel, HEK293 cells, which normally neither express MIA protein nor KCNN4 channels, were transiently co-transfected with pCMX-PL1-hMIA, a KCNN4 channel containing plasmid and with the dominant negative construct of the KCNN4 channel dnKCNN4 AAA with varying vector amounts. Co-transfection of MIA protein and KCNN4 channel containing vectors leads to an increase of MIA protein secretion of about 40% relative to MIA protein exocytosis of cells, which were transfected with a MIA protein containing vector pCMX-PL1-hMIA alone. This effect can be reduced to the level of the control by co-transfection of cells with the dnKCNN4 AAA mutant form of the KCNN4 channel, in a dose dependent manner. **(F)** The influence of intracellular Ca^{2+} concentration on MIA protein secretion was investigated by exposure of Mel Im and Mel Ju cells to 1 nM and 10 nM Calcimycin (A23187) and 1 μM and 5 μM BAPTA-AM. Relative to cell culture supernatant from DMSO treated control cells, the secreted MIA protein amount increases up to 120% after Calcimycin treatment, while exposure to BABTA-AM results in a significant decrease in MIA protein secretion. Experiments were performed in triplicates.

2.3 Discussion

In the present study we elucidated the secretory pathway of MIA protein, which was previously identified to play a key role in the formation of metastases in malignant melanoma. MIA protein was described to directly interact with cell adhesion receptors integrin $\alpha_4\beta_1$ and integrin $\alpha_5\beta_1$ as well as with extracellular matrix molecules including fibronectin, tenascin and laminin.^{2, 7} As a result, matrix structures surrounding the cell and integrin adhesion molecules are masked by MIA protein, which consequently impacts melanoma cell attachment. Thus, we proposed that the contribution of MIA protein to the enhanced invasive capacity of malignant melanoma cells can be ascribed to a mechanism requiring targeted MIA protein transport and secretion. To enable a tumor cell to migrate in a defined direction, localized cell detachment is a prerequisite and could be achieved by directed MIA protein transport to the cell rear followed by localized MIA protein exocytosis. Based on this proposal, we have now investigated the secretion pathway of MIA protein and for the first time describe a targeted, migration-associated transport of a secretory protein to the rear cell pole.

Induction of cell migration triggers directed MIA protein delivery to the rear cell pole

Non-polarized and non-migrating cells show a homogeneous distribution of MIA protein in the cytoplasm. After external stimuli the initial response of a cell is to polarize, meaning that molecular processes at the cell front differ from that at the cell rear. The cell starts to extend protrusions at the leading edge which are stabilized by adhesion to the extracellular matrix. These adhesion contacts serve as traction points for migration and initiate signals

that regulate adhesion dynamics and trailing edge retraction. Dynamic responses that drive migration are dependent on a highly organized cytoskeleton function.

In polarized control cells, we clearly defined the direction of migration by staining both the MIA protein and the Golgi apparatus, which, together with the MTOC, is reoriented toward the leading edge. Thus, we were able to follow MIA protein delivery to the rear cell pole. Generally, migration is initiated in response to extracellular stimuli. Required cell polarity is mediated by a set of interlinked positive feedback loops. Following the increased activity of Rho-family GTPases, integrins form focal adhesions, and subsequently phosphoinositide 3-kinases, microtubules, vesicular transport and other factors are involved.³⁸ The fine regulation of the actin cytoskeleton presupposes complex control mechanisms to ensure coordinated migration, which can be turned on and off by the cell on the requirements of a given situation.³⁹ At this time, the molecular details of the initiation of migration are not completely understood. Upon examining immunofluorescence staining of migrating cells, we deduced that regulation of directed MIA protein transport is critical to the intricate process of initiating migration. The characteristic unidirectional MIA protein distribution is clearly visible, even if the MIA protein transport is perturbed by treatment with AMP-PNP or TRAM-34, respectively. This observation of specifically targeted MIA protein secretion agrees well with data established in previous studies that demonstrate an uptake of MIA protein-integrin complexes at the cell rear of migrating cells and thus strongly supports our hypothesis.⁸

Our findings suggest that exocytic vesicles containing MIA protein take the conventional secretory pathway to the cell exterior. MIA contains an amino-terminal signal peptide that directs its translation into the ER. Afterwards, it is transported through the ER-Golgi pathway of protein export involving COP II and COP I coated vesicles. Mediated by the motor protein kinesin, MIA protein-containing secretory vesicles are transported along the microtubule system. After transport through the dense meshwork of actin filaments, MIA protein reaches the plasma membrane at the cell rear where it is finally exocytosed.

MIA protein secretion is a Ca^{2+} regulated process and is directly associated with KCNN4 channel activity

We determined that MIA protein secretion is a Ca^{2+} -regulated process, similar to the previously described secretion of many other specialized exocytic vesicles such as azurophilic granules in neutrophils, specific granules in mast cells and lytic granules in cytotoxic T-lymphocytes.⁴⁰⁻⁴³ The most thoroughly characterized Ca^{2+} -triggered exocytosis

is the release of neurotransmitters into the synaptic space.⁴⁴ Elevation of intracellular Ca^{2+} levels induces vesicle docking and fusion events at the plasma membrane mediated by SNARE proteins. In addition to these fusion events, several other factors involved at different stages of the secretory pathway are reported to be potential Ca^{2+} targets during the regulation of neurotransmitter release; for example, protein kinases as well as other Ca^{2+} -regulated proteins like rabphilin; α -actinin and β -adductin, which are involved in regulation of actin filament organization.⁴⁵⁻⁴⁷ Here, we show that in the meshwork of actin filaments a pool of MIA protein-containing secretory vesicles is stored and is only visible in adherent, non-migrating melanoma cells. Interestingly, intracellular Ca^{2+} has also been found to be responsible for the recovery of the storage pool following neurotransmitter release.⁴⁸

Intracellular Ca^{2+} plays a fundamental role in regulating cellular events and signaling. Cell migration is a process that strongly depends on intracellular Ca^{2+} , including the influences that Ca^{2+} has on volume-regulating mechanisms. Cell volume, which is subjected to fluctuations that are related to permanent cell shape changes, increases during protrusion of the lamellopodium at the cell front and decreases during retraction of the rear cell body.⁴⁹⁻⁵⁰ In addition to setting the cell volume, intracellular Ca^{2+} modulates the turnover of actin filaments; an elevation of Ca^{2+} promotes actin depolymerisation, whereas a low Ca^{2+} concentration favors actin polymerization. The regulation of the cytoskeletal migration machinery is supported by the intracellular gradient of Ca^{2+} with the higher concentration at the cell rear.^{14-15, 17} Another relevant factor for the motility of cells is the Ca^{2+} -controlled function of calpains in the release of cell-extracellular matrix contacts at the cell rear.¹⁶ Subsequently, this release is then followed by the recycling of integrins.⁵¹ Further, the contraction of the rear cell body by Ca^{2+} -regulated phosphorylation of myosin light chain is an important step during migration.⁵² The close relationship between intracellular Ca^{2+} ion concentration and cell migration-promoting processes strongly suggests a crucial role for ion channel activity. Since Ca^{2+} -activated K^+ channels are expressed in most (if not all) cells possessing the ability to migrate, including leukocytes and many tumor cells, their role in cell migration warrants close examination.^{18, 53-59} In previous studies, it was described that the KCNN4 channel is highly expressed in malignant melanoma cells.²⁰ Ion fluctuations mediated by the KCNN4 channel are known to play a fundamental role in cell migration, since specific inhibition or activation of this ion channel results in impaired cell mobility.^{25, 60-63} Interestingly, it was also reported that

the KCNN4 channels are only active at the rear cell pole of migrating cells due to the intracellular Ca^{2+} gradient. At the cell front KCNN4 channels appear to be inactive.^{22, 63}

The results described here are consistent with the observation of Ca^{2+} -regulated secretion of MIA protein at the cell rear and support a model that underlines the pivotal function of MIA protein in promoting directed migration. A migratory stimulus leads to elevation in intracellular Ca^{2+} concentration, which activates the KCNN4 channel and functions as a signal amplifier causing hyperpolarization of the cell membrane, thus leading to an enhanced electrochemical driving force for Ca^{2+} influx.^{19, 64} Since these ion channels are mainly active at the cell rear, the increase in intracellular Ca^{2+} promotes cell migration by several mechanisms mentioned above and simultaneously induces fusion of MIA protein containing secretory vesicles with the plasma membrane at the rear cell pole. While KCNN4 activity clearly facilitates MIA secretion, it is not an indispensable prerequisite for the secretion process, neither in melanoma cells nor in transfected HEK293 cells. It is important to mention that our experimental strategies, used to eliminate KCNN4 function, do not remove the channel complexes, but rather interfere with the pore function. For the voltage-gated potassium channel Kv2.1 (KCNB1) it was recently shown that it facilitates exocytosis in PC12 chromaffin cells by direct interaction with the SNARE protein syntaxin, independently of the functional pore.⁶⁵ While a direct interaction of KCNN4 with the export machinery may not be excluded at this time, its function in MIA exocytosis does require potassium efflux through the channel pore.

Once MIA is exocytosed at the cell rear, it is able to mask extracellular matrix structures and facilitate cell detachment through a direct interaction with cell adhesion receptors integrin $\alpha_4\beta_1$ and integrin $\alpha_5\beta_1$. While at the rear pole cell-extracellular matrix contacts are detached followed by internalization of MIA protein-integrin-complexes, at the cell front recycled integrins are exocytosed at the surface allowing new cell-ECM contacts to form. Thus, migration-associated MIA protein secretion at the cell rear strongly supports directed cell movement and helps to explain the aggressive migratory behavior and metastatic potential of malignant melanoma cells.

2.4 Materials and Methods

Cell lines and cell culture conditions

The melanoma cell line Mel Im, established from a human metastatic bioptic sample (generous gift from Dr. Johnson, University of Munich, Germany), was used in almost all

experiments. Additionally, main experiments were also conducted using the human cell line Mel Ju, which was derived from metastases of malignant melanoma. HEK293 cells were obtained from the German Collection of Microorganisms and Cell Cultures (DSMZ, Braunschweig, Germany). All cells were maintained in DMEM (PAA Laboratories GmbH, Austria) supplemented with penicillin (400 U/mL), streptomycin (50 µg/mL), l-glutamine (300 µg/mL) and 10% fetal calf serum (Pan Biotech GmbH, Germany) and split in 1:5 ratio every 3 days.

MIA secretion assay

2.5 x 10⁵ cells per mL were seeded in 6-well plates (Corning Omnilab, Germany) and cultured in 2 mL of Dulbecco's modified Eagle's medium (PAA, Germany) with 10% fetal calf serum (Pan, Germany). Cells were treated with various inhibitory compounds (all purchased from Sigma Aldrich, Germany) in different final concentrations: 3-(4-fluorobenzoylamino)-benzoic acid methyl ester (Exo1) was used at a final concentration of 50 µM and 100 µM, Brefeldin A (BFA) at 3.5 µM and 7 µM, Nocodazole at 25 µM and 50 µM, Jasplakinolide was used at 5 nM and 50 nM, adenosine 5'-(β,γ-imido)triphosphate tetralithium salt hydrate (AMP-PNP) at 1 mM and 2 mM, 1,2-bis(2-aminophenoxy)ethane-N,N,N',N'-tetraacetic acid tetrakis(acetoxymethyl ester) (BAPTA-AM) at 1 µM and 5 µM, Calcimycin (A23187) at 1 nM and 10 nM, 1-ethyl-2-benzimidazolinone (1-EBIO) at 100 µM and 200 µM and 1-[(chlorophenyl)diphenylmethyl]1-H-pyrazole (TRAM-34) was used at a final concentration of 20 µM and 40 µM. Except AMP-PNP, which was dissolved in H₂O, all compounds mentioned above were dissolved in DMSO, which was also used in the corresponding control experiment. After treatment cells were incubated for 8 h at 37°C and 8% CO₂. Afterwards, the cell culture supernatant was collected for quantification of secreted MIA protein using an ELISA system (Roche Applied Science, Germany). Monoclonal antibodies conjugated with biotin or peroxidase, respectively, were used to quantify MIA protein in a 96-well plate coated with streptavidin. 2,2'-azino-di[3-ethylbenzthiazoline sulfonate] (ABTS) was used as substrate and measured at 405 nm using a fluorescence microplate reader (E_{max} precision microplate reader, Molecular Devices).

MIA-HisTag and dnKCNN4 plasmid construction

MIA HisTag expression plasmid was created by PCR amplification of human melanoma cDNA using the MJ Research PTC-200 Peltier Thermo Cycler (BioRad). The cDNA was

generated from RNA isolated from the melanoma cell line Mel Im using the total RNA Kit (Omega Biotech, USA) followed by reverse transcription using superscript (Invitrogen, Germany). The HisTag sequence was inserted between the hydrophobic signal-peptide sequence responsible for transport into the endoplasmatic reticulum and the MIA sequence according to the site-directed mutagenesis by overlap extension (SOE)-method using the primers 5'- GAC GAA TTC ATG GCC CGG TCC CTG GTG - 3' and 5'- CAT AGG ACC ACC GTG ATG GTG ATG GTG ATG GTG ATG CCT GAC ACC AGG -3' for the signal-peptide-HisTag fragment and 5'- CCT GGT GTC AGG CAT CAC CAT CAC CAT CAC CAT CAC GGT GGT CCT ATG -3' and 5'- GAC AAG CTT TCA CTG GCA GTA GAA ATC CCA -3' for amplification of HisTag-MIA fragment.⁶⁶ After fusion of these two fragments and digestion of the resulting PCR product with EcoRI and HindIII (NEB, Germany) this insert was purified by gel extraction (Qiagen, Germany) and cloned into the EcoRI and HindIII sites of the eukaryotic expression vector pCMX-PL1 which was previously purified and prepared for ligation using T4-Ligase (NEB, Germany).⁶⁷ After transformation in DH10 β cells (NEB, Germany) according to the manufacturer's instructions the plasmids were isolated using the MIDI Kit (Qiagen, Germany) and quantified by a gene quant II RNA/DNA Calculator (Pharmacia Biotech). The dnKCNN4 constructs with amino acid replacements in the selectivity filter of the potassium channel were generated with the QuikChange Mutagenesis kit (Stratagene, Germany). The introduced amino acids are Leu253 (replacing Tyr; dnKCNN4 Y253L) and Ala252-Ala253-Ala254 (replacing Gly-Tyr-Gly; dnKCNN4 AAA). The sequences of the PCR-generated clones were confirmed by DNA sequencing.

Transient Transfection

For transient transfection, 2×10^5 cells per mL were seeded in 6-well plates (Corning Omnilab, Germany) and cultured in 2 mL of Dulbecco's modified Eagle's medium (PAA, Germany) with 10% fetal calf serum (Pan, Germany). Cells were transiently transfected with 1 μ g of the respective plasmid using the LipofectaminPlus (Invitrogen, Germany) method according to the manufacturer's instructions. The transfection efficiency was approximately 45%. To investigate the MIA protein secretion pathway Mel Im cells and Mel Ju cells were transfected with Sar1p (H79G) mutant (generous gift from Ben Distel, University of Amsterdam, NL) and the respective mock control plasmid pcDNA3. To demonstrate involvement of the KCNN4 channel in regulation of MIA protein secretion cells were transiently transfected with the expression plasmids KCNN4 (generous gift from

Albrecht Schwab, University of Münster, Germany), pCMX-PL1 hMIA, the dominant negative form dnKCNN4 AAA or dnKCNN4 Y253L and the respective mock control pCMX-PL1 and pcDNA3.⁶⁷ 48 h after transfection the cell culture supernatant was collected for quantification of secreted MIA protein by using an ELISA system (Roche Applied Science, Germany) as described above.

For immunofluorescence staining experiments 10⁵ Mel Im cells and Mel Ju cells, respectively, were grown on a four well chamber slide (Falcon, BD Bioscience, Germany). Transient transfection and co-transfection of these cells with MIA HisTag and Golgi-GFP (endomannosidase) plasmids (kindly provided by Christof Voelker, University of Bonn, Germany) and the respective mock control, respectively, were also performed using the LipofectaminPlus (Invitrogen, Germany) method according to the manufacturer's instructions. First, cells were transfected with the Golgi-GFP plasmid and incubated for 24 h before further treatment. During this time span the reorientation of the microtubule organizing center (MTOC), a comparatively slow process that can take several hours after migratory stimuli, is ensured. Afterwards, cells were co-transfected with the MIA HisTag plasmid and the respective mock control pCMX-PL1. After another 24 h cells were treated with various inhibitory compounds in different final concentrations, fixed and prepared for immunofluorescence microscopy.

Immunofluorescence assays

5 x 10⁵ melanoma cells Mel Im and Mel Ju and human epithelial kidney cell line HEK293 cells, respectively, were grown in a 4-well chamber slide (Falcon, BD Bioscience, Germany). After transient transfection and co-transfection with MIA HisTag and Golgi-GFP plasmids and the respective mock control, cells were treated with BFA at final concentrations of 3.5 μ M and 7 μ M, AMP-PNP at final concentrations of 1 mM and 2 mM, TRAM-34 at final concentrations of 20 μ M and 40 μ M and the respective DMSO control. After incubation for 1.5 h at 37°C and 8% CO₂, cells were washed and fixed using 4% paraformaldehyde in 0.1 M phosphate-buffered saline (PBS) for 15 min. After permeabilization of cells, blocking of non-specific binding sites with blocking solution (1% BSA/PBS) for 1 h at 4°C was performed followed by incubation with primary antibody mouse anti-HisTag antibody (BD Bioscience, Pharmingen, Germany) at a concentration of 1 μ g/mL at 4°C for 2 h. After rinsing with PBS for 5 times, cells were covered with a 1:30 dilution of the secondary antibody (FITC-conjugated polyclonal rabbit anti mouse immunoglobulin, DakoCytomation, USA) in PBS at 4°C for 1 h. For a better

illustration of the cell border cells were simultaneously stained for actin with phalloidin rhodamine dye (Biotium, USA) according to the manufactures instructions. Afterwards, cells were washed with PBS and coverslips were mounted on slides using Hard Set Mounting Medium with DAPI (Vectashield, H-1500, Linearis, Germany) and imaged using an Axio Imager Zeiss Z1 fluorescence microscope (Axiovision Rel. 4.6.3) equipped with an Axio Cam MR camera. Images were taken using 63x oil immersion lenses.

Electrophysiological recordings

Potassium currents were recorded at room temperature in the whole-cell configuration, using an EPC9 patch clamp amplifier (HEKA Elektronik, Germany) controlled with PatchMaster software (HEKA Elektronik). In all experiments, the holding potential was -80 mV. Series-resistance errors were compensated in the range of 70–90%. Patch pipettes were fabricated from Kimax-51 glass (Kimble Glass, USA) with resistance values in the range of 0.8-1.5 MΩ. Off-line analysis of data was performed using IgorPro (WaveMetrics, USA) and FitMaster (HEKA Elektronik). The internal solution contained (mM): KCl 130, MgCl₂ 2, EGTA 10, Hepes 10 and CaCl₂ 9.3 to yield 1 μM free Ca²⁺; pH was adjusted to 7.4 with KOH. The standard bath solution contained (mM): KCl 5, NaCl 155, CaCl₂ 2 and Hepes 10; pH was adjusted to 7.4 with NaOH. Currents were elicited by 500-ms voltage ramps, ranging from -100 mV to +50 mV. In block experiments with TRAM-34 the same ramp protocol was applied every 5 seconds. Mean current densities were determined between -40 mV and -25 mV. Current recordings on transfected HEK293 cells were performed 1-3 days after transfection.

Statistical analysis

In the bar graphs, results are expressed as mean ± s.d. (range) or percent. Comparison between groups was made using the Student's unpaired t-test. A p-value <0.05 was considered as statistically significant (ns: not significant, *: p<0.05, **: p<0.01, ***: p<0.001). All calculations were made using the GraphPad Prism Software (GraphPad Software, Inc., San Diego, USA).

2.5 Acknowledgements

We are indebted to Dr. J. Johnson (University of Munich, Germany) for providing the melanoma cell lines Mel Im and Mel Ju and to Dr. B. Distel (University of Amsterdam, Netherlands) for providing the Sar1p (H79G) vector. We also thank A. Schwab (University

of Muenster, Germany) for the generous donation of the expression vector of the KCNN4 channel and Dr. C. Voelker (University of Bonn, Germany) for the Golgi-GFP (endomannosidase) plasmid. This work was supported by grants from the DFG and the German Cancer Aid (Melanoma Research Network).

2.6 References

1. Bosserhoff, A. K.; Kaufmann, M.; Kaluza, B.; Bartke, I.; Zirngibl, H.; Hein, R.; Stolz, W.; Buettner, R., Melanoma-inhibiting activity, a novel serum marker for progression of malignant melanoma. *Cancer Res* **1997**, *57*, (15), 3149-53.
2. Bosserhoff, A. K.; Stoll, R.; Sleeman, J. P.; Bataille, F.; Buettner, R.; Holak, T. A., Active detachment involves inhibition of cell-matrix contacts of malignant melanoma cells by secretion of melanoma inhibitory activity. *Lab Invest* **2003**, *83*, (11), 1583-94.
3. Poser, I.; Tatzel, J.; Kuphal, S.; Bosserhoff, A. K., Functional role of MIA in melanocytes and early development of melanoma. *Oncogene* **2004**, *23*, (36), 6115-24.
4. Bosserhoff, A. K.; Lederer, M.; Kaufmann, M.; Hein, R.; Stolz, W.; Apfel, R.; Bogdahn, U.; Buettner, R., MIA, a novel serum marker for progression of malignant melanoma. *Anticancer Res* **1999**, *19*, (4A), 2691-3.
5. Dreau, D.; Bosserhoff, A. K.; White, R. L.; Buettner, R.; Holder, W. D., Melanoma-inhibitory activity protein concentrations in blood of melanoma patients treated with immunotherapy. *Oncol Res* **1999**, *11*, (1), 55-61.
6. Stahlecker, J.; Gauger, A.; Bosserhoff, A.; Buettner, R.; Ring, J.; Hein, R., MIA as a reliable tumor marker in the serum of patients with malignant melanoma. *Anticancer Res* **2000**, *20*, (6D), 5041-4.
7. Bauer, R.; Humphries, M.; Fassler, R.; Winklmeier, A.; Craig, S. E.; Bosserhoff, A. K., Regulation of integrin activity by MIA. *J Biol Chem* **2006**, *281*, (17), 11669-77.
8. Schmidt, J.; Bosserhoff, A. K., Processing of MIA protein during melanoma cell migration. *Int J Cancer* **2009**, *125*, (7), 1587-94.
9. Blesch, A.; Bosserhoff, A. K.; Apfel, R.; Behl, C.; Hessdoerfer, B.; Schmitt, A.; Jachimczak, P.; Lottspeich, F.; Buettner, R.; Bogdahn, U., Cloning of a novel malignant melanoma-derived growth-regulatory protein, MIA. *Cancer Res* **1994**, *54*, (21), 5695-701.

10. Rabouille, C.; Klumperman, J., Opinion: The maturing role of COPI vesicles in intra-Golgi transport. *Nat Rev Mol Cell Biol* **2005**, 6, (10), 812-7.
11. Jena, B. P., Membrane fusion: role of SNAREs and calcium. *Protein Pept Lett* **2009**, 16, (7), 712-7.
12. Komuro, H.; Kumada, T., Ca(2+) transients control CNS neuronal migration. *Cell Calcium* **2005**, 37, (5), 387-93.
13. Pettit, E. J.; Fay, F. S., Cytosolic free calcium and the cytoskeleton in the control of leukocyte chemotaxis. *Physiol Rev* **1998**, 78, (4), 949-67.
14. Brundage, R. A.; Fogarty, K. E.; Tuft, R. A.; Fay, F. S., Calcium gradients underlying polarization and chemotaxis of eosinophils. *Science* **1991**, 254, (5032), 703-6.
15. Hahn, K.; DeBiasio, R.; Taylor, D. L., Patterns of elevated free calcium and calmodulin activation in living cells. *Nature* **1992**, 359, (6397), 736-8.
16. Franco, S. J.; Huttenlocher, A., Regulating cell migration: calpains make the cut. *J Cell Sci* **2005**, 118, (Pt 17), 3829-38.
17. Schwab, A.; Wojnowski, L.; Gabriel, K.; Oberleithner, H., Oscillating activity of a Ca(2+)-sensitive K(+) channel. A prerequisite for migration of transformed Madin-Darby canine kidney focus cells. *J Clin Invest* **1994**, 93, (4), 1631-6.
18. Jager, H.; Dreker, T.; Buck, A.; Giehl, K.; Gress, T.; Grissmer, S., Blockage of intermediate-conductance Ca(2+)-activated K(+) channels inhibit human pancreatic cancer cell growth in vitro. *Mol Pharmacol* **2004**, 65, (3), 630-8.
19. Lallet-Daher, H.; Roudbaraki, M.; Bavencoffe, A.; Mariot, P.; Gackiere, F.; Bidaux, G.; Urbain, R.; Gosset, P.; Delcourt, P.; Fleurisse, L.; Slomianny, C.; Dewailly, E.; Mauroy, B.; Bonnal, J. L.; Skryma, R.; Prevarskaya, N., Intermediate-conductance Ca(2+)-activated K(+) channels (IKCa1) regulate human prostate cancer cell proliferation through a close control of calcium entry. *Oncogene* **2009**, 28, (15), 1792-806.
20. Tajima, N.; Schonherr, K.; Niedling, S.; Kaatz, M.; Kanno, H.; Schonherr, R.; Heinemann, S. H., Ca(2+)-activated K(+) channels in human melanoma cells are up-regulated by hypoxia involving hypoxia-inducible factor-1alpha and the von Hippel-Lindau protein. *J Physiol* **2006**, 571, (Pt 2), 349-59.
21. Wang, J.; Xu, Y. Q.; Liang, Y. Y.; Gongora, R.; Warnock, D. G.; Ma, H. P., An intermediate-conductance Ca(2+)-activated K(+) channel mediates B lymphoma cell cycle progression induced by serum. *Pflugers Arch* **2007**, 454, (6), 945-56.

22. Schwab, A.; Gabriel, K.; Finsterwalder, F.; Folprecht, G.; Greger, R.; Kramer, A.; Oberleithner, H., Polarized ion transport during migration of transformed Madin-Darby canine kidney cells. *Pflugers Arch* **1995**, 430, (5), 802-7.
23. Cruse, G.; Duffy, S. M.; Brightling, C. E.; Bradding, P., Functional KCa3.1 K(+) channels are required for human lung mast cell migration. *Thorax* **2006**, 61, (10), 880-5.
24. Kessler, W.; Budde, T.; Gekle, M.; Fabian, A.; Schwab, A., Activation of cell migration with fibroblast growth factor-2 requires calcium-sensitive potassium channels. *Pflugers Arch* **2008**, 456, (5), 813-23.
25. Schwab, A.; Reinhardt, J.; Schneider, S. W.; Gassner, B.; Schuricht, B., K(+) channel-dependent migration of fibroblasts and human melanoma cells. *Cell Physiol Biochem* **1999**, 9, (3), 126-32.
26. Palazzo, A. F.; Joseph, H. L.; Chen, Y. J.; Dujardin, D. L.; Alberts, A. S.; Pfister, K. K.; Vallee, R. B.; Gundersen, G. G., Cdc42, dynein, and dynactin regulate MTOC reorientation independent of Rho-regulated microtubule stabilization. *Curr Biol* **2001**, 11, (19), 1536-41.
27. Nebenfuhr, A.; Ritzenthaler, C.; Robinson, D. G., Brefeldin A: deciphering an enigmatic inhibitor of secretion. *Plant Physiol* **2002**, 130, (3), 1102-8.
28. Aridor, M.; Bannykh, S. I.; Rowe, T.; Balch, W. E., Sequential Coupling between CopII and CopI Vesicle Coats in Endoplasmic-Reticulum to Golgi Transport. *Journal of Cell Biology* **1995**, 131, (4), 875-893.
29. Barlowe, C.; Orci, L.; Yeung, T.; Hosobuchi, M.; Hamamoto, S.; Salama, N.; Rexach, M. F.; Ravazzola, M.; Amherdt, M.; Schekman, R., COPII: a membrane coat formed by Sec proteins that drive vesicle budding from the endoplasmic reticulum. *Cell* **1994**, 77, (6), 895-907.
30. Kuge, O.; Kuge, S., COP-coated vesicles in intracellular protein transport. *Tanpakushitsu Kakusan Koso* **1995**, 40, (16), 2427-35.
31. Gaynor, E. C.; Graham, T. R.; Emr, S. D., COPI in ER/Golgi and intra-Golgi transport: do yeast COPI mutants point the way? *Biochim Biophys Acta* **1998**, 1404, (1-2), 33-51.
32. Hachiya, N. S.; Watanabe, K.; Yamada, M.; Sakasegawa, Y.; Kaneko, K., Anterograde and retrograde intracellular trafficking of fluorescent cellular prion protein. *Biochem Biophys Res Commun* **2004**, 315, (4), 802-7.

33. Schwab, A., Function and spatial distribution of ion channels and transporters in cell migration. *Am J Physiol Renal Physiol* **2001**, 280, (5), F739-47.
34. Ghanshani, S.; Wulff, H.; Miller, M. J.; Rohm, H.; Neben, A.; Gutman, G. A.; Cahalan, M. D.; Chandy, K. G., Up-regulation of the IKCa1 potassium channel during T-cell activation. Molecular mechanism and functional consequences. *J Biol Chem* **2000**, 275, (47), 37137-49.
35. Barfod, E. T.; Moore, A. L.; Roe, M. W.; Lidofsky, S. D., Ca(2+)-activated IK1 channels associate with lipid rafts upon cell swelling and mediate volume recovery. *J Biol Chem* **2007**, 282, (12), 8984-93.
36. Strayer, D. S.; Hoek, J. B.; Thomas, A. P.; White, M. K., Cellular activation by Ca(2+) release from stores in the endoplasmic reticulum but not by increased free Ca(2+) in the cytosol. *Biochem J* **1999**, 344 Pt 1, 39-46.
37. Kauffman, R. F.; Taylor, R. W.; Pfeiffer, D. R., Cation transport and specificity of ionomycin. Comparison with ionophore A23187 in rat liver mitochondria. *J Biol Chem* **1980**, 255, (7), 2735-9.
38. Ridley, A. J.; Schwartz, M. A.; Burridge, K.; Firtel, R. A.; Ginsberg, M. H.; Borisy, G.; Parsons, J. T.; Horwitz, A. R., Cell migration: integrating signals from front to back. *Science* **2003**, 302, (5651), 1704-9.
39. Vicente-Manzanares, M.; Webb, D. J.; Horwitz, A. R., Cell migration at a glance. *J Cell Sci* **2005**, 118, (Pt 21), 4917-9.
40. Burkhardt, J. K.; Hester, S.; Lapham, C. K.; Argon, Y., The lytic granules of natural killer cells are dual-function organelles combining secretory and pre-lysosomal compartments. *J Cell Biol* **1990**, 111, (6 Pt 1), 2327-40.
41. Peters, P. J.; Borst, J.; Oorschot, V.; Fukuda, M.; Krahenbuhl, O.; Tschopp, J.; Slot, J. W.; Geuze, H. J., Cytotoxic T lymphocyte granules are secretory lysosomes, containing both perforin and granzymes. *J Exp Med* **1991**, 173, (5), 1099-109.
42. Jamur, M. C.; Vugman, I.; Hand, A. R., Ultrastructural and cytochemical studies of acid phosphatase and trimetaphosphatase in rat peritoneal mast cells developing in vivo. *Cell Tissue Res* **1986**, 244, (3), 557-63.
43. Borregaard, N.; Lollike, K.; Kjeldsen, L.; Sengelov, H.; Bastholm, L.; Nielsen, M. H.; Bainton, D. F., Human neutrophil granules and secretory vesicles. *Eur J Haematol* **1993**, 51, (4), 187-98.
44. Bennett, M. K., Ca(2+) and the regulation of neurotransmitter secretion. *Curr Opin Neurobiol* **1997**, 7, (3), 316-22.

45. Greengard, P.; Valtorta, F.; Czernik, A. J.; Benfenati, F., Synaptic vesicle phosphoproteins and regulation of synaptic function. *Science* **1993**, 259, (5096), 780-5.
46. Kato, M.; Sasaki, T.; Ohya, T.; Nakanishi, H.; Nishioka, H.; Imamura, M.; Takai, Y., Physical and functional interaction of rabphilin-3A with alpha-actinin. *J Biol Chem* **1996**, 271, (50), 31775-8.
47. Miyazaki, M.; Shirataki, H.; Kohno, H.; Kaibuchi, K.; Tsugita, A.; Takai, Y., Identification as beta-adducin of a protein interacting with rabphilin-3A in the presence of Ca(2+) and phosphatidylserine. *Biochem Biophys Res Commun* **1994**, 205, (1), 460-6.
48. Weis, S.; Schneggenburger, R.; Neher, E., Properties of a model of Ca(2+)-dependent vesicle pool dynamics and short term synaptic depression. *Biophys J* **1999**, 77, (5), 2418-29.
49. Saadoun, S.; Papadopoulos, M. C.; Hara-Chikuma, M.; Verkman, A. S., Impairment of angiogenesis and cell migration by targeted aquaporin-1 gene disruption. *Nature* **2005**, 434, (7034), 786-92.
50. Stock, C.; Schwab, A., Role of the Na/H exchanger NHE1 in cell migration. *Acta Physiol (Oxf)* **2006**, 187, (1-2), 149-57.
51. Lawson, M. A.; Maxfield, F. R., Ca(2+)- and calcineurin-dependent recycling of an integrin to the front of migrating neutrophils. *Nature* **1995**, 377, (6544), 75-9.
52. Yang, S.; Huang, X. Y., Ca(2+) influx through L-type Ca(2+) channels controls the trailing tail contraction in growth factor-induced fibroblast cell migration. *J Biol Chem* **2005**, 280, (29), 27130-7.
53. Aiyar, J., Potassium channels in leukocytes and toxins that block them: Structure, function and therapeutic implications. *Perspect Drug Discov* **1999**, 16, 257-280.
54. Eder, C., Ion channels in microglia (brain macrophages). *Am J Physiol* **1998**, 275, (2 Pt 1), C327-42.
55. Kohler, R.; Wulff, H.; Eichler, I.; Kneifel, M.; Neumann, D.; Knorr, A.; Grgic, I.; Kampfe, D.; Si, H.; Wibawa, J.; Real, R.; Borner, K.; Brakemeier, S.; Orzechowski, H. D.; Reusch, H. P.; Paul, M.; Chandy, K. G.; Hoyer, J., Blockade of the intermediate-conductance calcium-activated potassium channel as a new therapeutic strategy for restenosis. *Circulation* **2003**, 108, (9), 1119-25.

56. Meyer, R.; Schonherr, R.; Gavrilova-Ruch, O.; Wohlrab, W.; Heinemann, S. H., Identification of ether a go-go and calcium-activated potassium channels in human melanoma cells. *J Membr Biol* **1999**, 171, (2), 107-15.
57. Ouadid-Ahidouch, H.; Roudbaraki, M.; Delcourt, P.; Ahidouch, A.; Joury, N.; Prevarskaya, N., Functional and molecular identification of intermediate-conductance Ca(2+)-activated K(+) channels in breast cancer cells: association with cell cycle progression. *Am J Physiol Cell Physiol* **2004**, 287, (1), C125-34.
58. Parihar, A. S.; Coghlan, M. J.; Gopalakrishnan, M.; Shieh, C. C., Effects of intermediate-conductance Ca(2+)-activated K(+) channel modulators on human prostate cancer cell proliferation. *Eur J Pharmacol* **2003**, 471, (3), 157-64.
59. Schwab, A.; Westphale, H. J.; Wojnowski, L.; Wunsch, S.; Oberleithner, H., Spontaneously oscillating K(+) channel activity in transformed Madin-Darby canine kidney cells. *J Clin Invest* **1993**, 92, (1), 218-23.
60. Jin, M.; Defoe, D. M.; Wondergem, R., Hepatocyte growth factor/scatter factor stimulates Ca(2+)-activated membrane K(+) current and migration of MDCK II cells. *J Membr Biol* **2003**, 191, (1), 77-86.
61. Schilling, T.; Stock, C.; Schwab, A.; Eder, C., Functional importance of Ca(2+)-activated K(+) channels for lysophosphatidic acid-induced microglial migration. *Eur J Neurosci* **2004**, 19, (6), 1469-74.
62. Schwab, A.; Schuricht, B.; Seeger, P.; Reinhardt, J.; Dartsch, P. C., Migration of transformed renal epithelial cells is regulated by K(+) channel modulation of actin cytoskeleton and cell volume. *Pflugers Arch* **1999**, 438, (3), 330-7.
63. Schwab, A.; Wulf, A.; Schulz, C.; Kessler, W.; Nechyporuk-Zloy, V.; Romer, M.; Reinhardt, J.; Weinhold, D.; Dieterich, P.; Stock, C.; Hebert, S. C., Subcellular distribution of calcium-sensitive potassium channels (IK1) in migrating cells. *J Cell Physiol* **2006**, 206, (1), 86-94.
64. Rao, J. N.; Platoshyn, O.; Li, L.; Guo, X.; Golovina, V. A.; Yuan, J. X.; Wang, J. Y., Activation of K(+) channels and increased migration of differentiated intestinal epithelial cells after wounding. *Am J Physiol Cell Physiol* **2002**, 282, (4), C885-98.
65. Feinshreiber, L.; Singer-Lahat, D.; Ashery, U.; Lotan, I., Voltage-gated potassium channel as a facilitator of exocytosis. *Ann N Y Acad Sci* **2009**, 1152, 87-92.
66. Ho, S. N.; Hunt, H. D.; Horton, R. M.; Pullen, J. K.; Pease, L. R., Site-directed mutagenesis by overlap extension using the polymerase chain reaction. *Gene* **1989**, 77, (1), 51-9.

67. Tatzel, J.; Poser, I.; Schroeder, J.; Bosserhoff, A. K., Inhibition of melanoma inhibitory activity (MIA) expression in melanoma cells leads to molecular and phenotypic changes. *Pigment Cell Res* **2005**, 18, (2), 92-101.

3 Processing of MIA Protein during Melanoma Cell Migration

Abstract

MIA (melanoma inhibitory activity) protein, identified as a small 11 kDa protein highly expressed and secreted by malignant melanoma cells, plays an important functional role in melanoma development, progression and tumor cell invasion. Recent data describe a direct interaction of MIA protein with cell adhesion receptors integrin $\alpha_4\beta_1$ and integrin $\alpha_5\beta_1$ and extracellular matrix molecules. By modulating integrin activity MIA protein mediates detachment of melanoma cells from surrounding structures resulting in enhanced invasive and migratory potential. However, until today a detailed understanding of the processes of MIA function is missing.

In the present study, we show that after binding of MIA protein to integrin $\alpha_5\beta_1$, MIA protein is internalized together with this cell adhesion receptor at the cell rear. This mechanism enables tumor cells to migrate in a defined direction as appropriate for invasion processes. Treatment of melanoma cells with PKC-inhibitors strongly reduced internalization of MIA protein. Endocytosis is followed by dissociation of MIA-integrin complexes. In acidic vesicles MIA protein is degraded while integrins are recycled. Treatment of melanoma cells with MIA inhibitory peptides almost completely blocked the MIA protein uptake into cells.

Since MIA protein has a major contribution to the aggressive characteristics of malignant melanoma in particular to formation of metastasis, it is important to elucidate the MIA functional mechanism in tumor cells to find novel therapeutic strategies in the fight against skin cancer.

The results of this chapter have been published:

Schmidt J., Bosserhoff A.K.; Processing of MIA protein during cell migration. *Int J Cancer* **2009**; 125(7):1587-94

3.1 Introduction

Malignant melanoma is characterized by aggressive local growth and early formation of metastasis, and accounts for 75 percent of deaths associated with skin cancer. Previously, melanoma inhibitory activity (MIA) has been identified as an 11 kDa protein strongly expressed and secreted by malignant melanoma cells but not expressed in melanocytes.¹ Subsequent *in vitro* and *in vivo* experiments revealed that MIA protein plays an important functional role in melanoma development and cell invasion, hence MIA expression levels parallel closely the capability of melanoma cells to form metastases in syngeneic animals.²⁻⁴ Increased MIA serum concentrations serve as a reliable clinical tumor marker to detect and monitor metastatic diseases in patients with malignant melanomas.^{1, 5-6}

The three-dimensional structure of the protein was solved by multidimensional nuclear magnetic resonance (NMR) and X-ray crystallography techniques.⁷⁻¹⁰ Corresponding data indicate that MIA defines a novel type of secreted protein: the MIA protein family, consisting of MIA and the homologous proteins OTOR, MIA-2 and TANGO (MIA-3). The MIA protein family is the first family of secreted proteins comprising an SH3 domain like fold in solution.¹¹ Furthermore, phage display experiments and NMR spectra revealed that MIA protein interacts with peptides matching to extracellular matrix proteins including human fibronectin type III repeats and laminin structures. In previous studies using far Western blotting and co-immunoprecipitation MIA protein was identified to bind to the cell surface proteins integrin $\alpha_4\beta_1$ and integrin $\alpha_5\beta_1$.¹² Thus, MIA protein modulates integrin activity and thereby mediates detachment of cells from extracellular matrix proteins, resulting in enhanced invasive and migratory potential of melanoma cells.

In cell migration processes integrins, mediating cell-cell and cell-extracellular matrix contacts, undergo endocytic-exocytic transport. Adhesion receptor recycling is described as a process where at the cell rear integrins are internalized and subsequently transported within recycling vesicles to the leading edge of the migrating cell. Here, they are re-exocytosed to build new adhesion contacts to extracellular matrix molecules.¹³⁻¹⁴ Now the question arises, how MIA protein contributes to migration and invasion after its secretion from tumor cells. This study elucidates the mechanism by which MIA protein promotes cell detachment and thus influences formation of cancer metastases. We found that extracellular MIA protein, directly binding to integrin $\alpha_5\beta_1$, is internalized together with this cell adhesion receptor at the cell rear. This located uptake of MIA protein results in focal cell detachment at the rear cell pole and allows a directed migration. We also demonstrate that after MIA-integrin endocytosis, these receptor-MIA complexes dissociate

and MIA protein is degraded in acidic vesicles. Treatment of melanoma cells with MIA-inhibitory peptides results in a dramatical decrease of MIA protein internalization in a dose dependant manner. Since MIA protein promotes invasive behavior of malignant melanoma cells, it is necessary to find a mechanistic explanation for observed MIA effects to develop a novel therapeutic strategy.

3.2 Results

3.2.1 Unidirectional internalization of MIA protein

Integrin heterodimers are known to regulate cell adhesion and migration. The mechanism of integrin recycling by vesicular transport contributes to cell migration by internalizing integrins at the cell rear and thereby facilitates their detachment from surrounding structures.¹⁴

In previous studies it has been shown that MIA protein directly interacts with integrin $\alpha_4\beta_1$ and integrin $\alpha_5\beta_1$. This binding leads to cell detachment by decreasing interactions between melanoma cells and extracellular matrix molecules via inactivation of integrins. We, therefore, hypothesized that MIA protein regulates migratory behavior of melanoma cells by modulating integrin activity. This theory is supported by the fact that MIA expression levels directly correlate with the ability of melanoma cells to form skin cancer metastases.³⁻⁴

As shown in *Figure 1*, Mel Im melanoma cells, seeded in medium confluence and incubated with Cy3-labeled MIA protein, show a strong Cy3-fluorescence intensity in intracellular vesicles asymmetrically distributed at one cell pole. About 40% to 50% of seeded Mel Im cells are migrating; nearly all of them present this characteristic unidirectional MIA-Cy3 staining pattern. Cells treated with Cy3-labeled BSA protein as a negative control under the same experimental conditions did not show any fluorescence signal, indicating that the labeled BSA protein is not endocytosed (*Figure 1 D*).

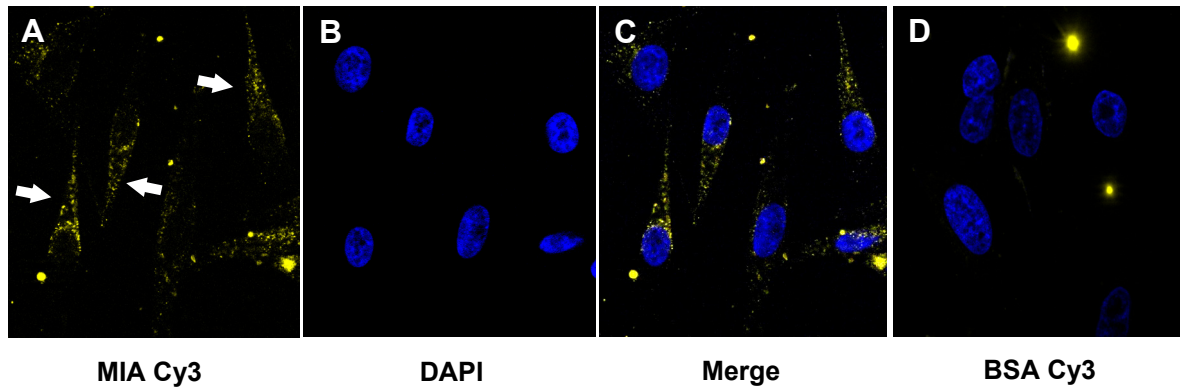


Figure 1: *Internalization of MIA protein at one cell pole*

Mel Im cells were treated with Cy3-labeled MIA protein and, as a negative control, with Cy3-labeled BSA protein. **(A)** Migrating cells internalize MIA protein and show a strong Cy3-fluorescence intensity asymmetrically distributed at one cell pole as indicated by the white arrows. **(B)** DAPI **(C)** Merge **(D)** BSA Cy3 negative control

The same characteristic MIA protein uptake was also found in all other melanoma cell lines tested: Mel Ju, SK Mel 28 and A375 (*Supplementary Figure S2*).

Since MIA protein specifically interferes with attachment of melanoma cells we recently performed a phage display screening experiment to identify potential MIA-inhibitory peptides. These peptides were investigated in attachment analysis in a Boyden Chamber model on their ability to affect MIA function.² AR54, one of these peptides deduced from the FN14 structure, was able to almost completely inhibit MIA function at concentrations of 1 μM without affecting integrin function (*Supplementary Figure S1B*).⁹

After treatment of Mel Im cells with AR54 the endocytosis of Cy3-labeled MIA protein was reduced in a dose dependent manner. AR54 at concentrations of 0.3 μM and 0.5 μM moderately decreases MIA protein endocytosis whereas a concentration of 2 μM almost completely inhibits MIA uptake as shown in *Figure 2*.

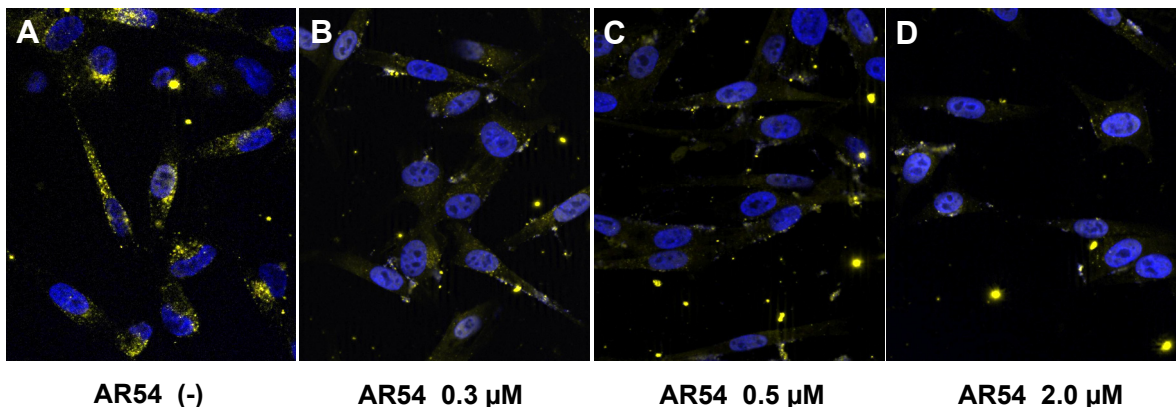


Figure 2: *Dose dependent inhibition of MIA protein internalization by peptide AR54*

Mel Im cells simultaneously were treated with Cy3-labeled MIA protein **(A)** and AR54, a MIA protein binding peptide, which was able to inhibit MIA function. AR54 was added in different concentrations. Final

concentrations of 0.3 μM (**B**) and 0.5 μM (**C**) moderately decrease MIA protein endocytosis whereas concentrations of 2 μM (**D**) almost completely inhibit MIA protein uptake.

For all other melanoma cell lines tested we observed comparable results (*Supplementary Figure S3*).

3.2.2 Internalization of MIA-integrin complexes at the rear of migrating cells

To further elucidate the MIA protein function in migratory behavior of melanoma cells, we determined the direction of cell migration. Illustrated in *Figure 3* are two independent examples (*I and II*) where the observed MIA fluorescence staining pattern argues for a coordinated MIA protein uptake located at one cell pole (*A*). As generally accepted, directed migration begins with cell polarization and it has been shown in previous studies that the microtubule organizing center (MTOC) and the Golgi apparatus are reoriented toward the leading edge of cells in wound-healing migration assays.¹⁵⁻¹⁷ For the determination of the migration direction of Mel Im cells, cells were incubated with Cy3-labeled MIA protein (*A*) and afterwards stained with a Golgi marker (mouse anti-Golgi protein [58K 9] antibody) (*B*). Fluorescence analysis shown in *Figure 3* revealed the uptake of MIA protein containing vesicles at the cell rear, confirming our hypothesis that MIA protein is strongly involved in detachment processes of migrating cells. This mechanism enables tumor cells to migrate in a defined direction. Non-polarized cells and thus non-migrating cells, perceptible by the homogeneous green staining (*II B*), do not show the characteristically distributed Cy3 fluorescence (*II A*). Using the other melanoma cell lines, in migrating cells the same fluorescence staining pattern appears. A375 cells, similar to Mel Im cells, show a strong migratory ability compared to the other cell lines Mel Ju and SK Mel 28 (*Supplementary Figure S4*).

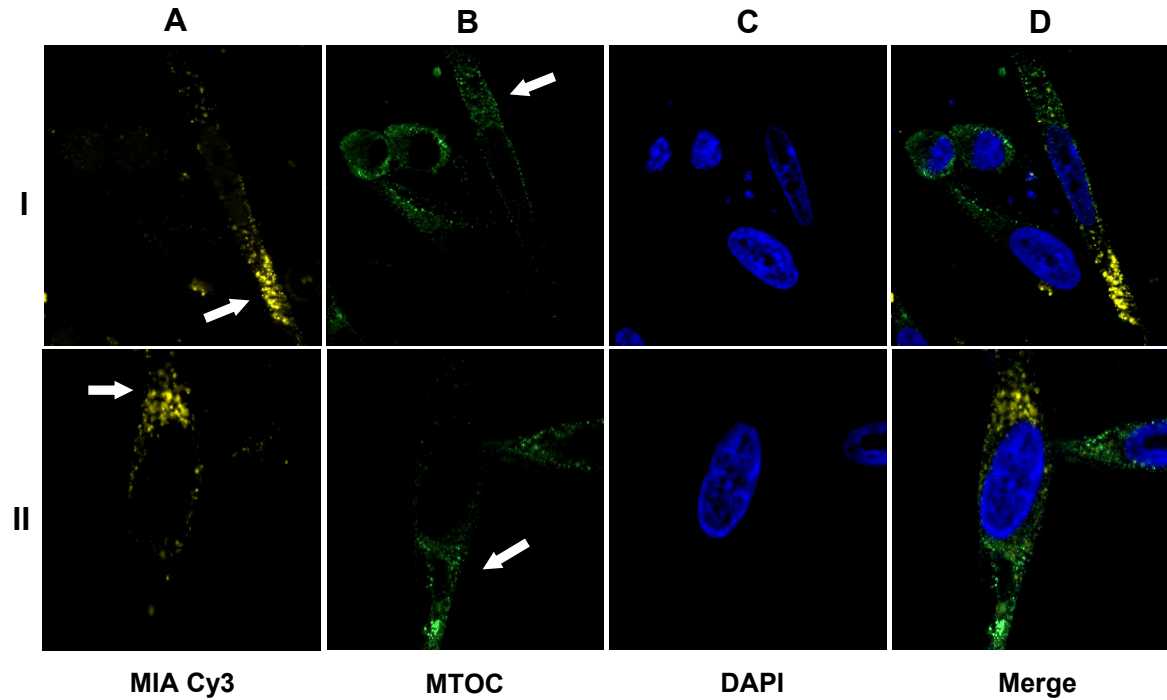


Figure 3: MIA protein is internalized at the rear of migrating cells

For determination of the direction of migration, Cy3-labeled MIA treated Mel Im cells were stained with a Golgi marker mouse anti-Golgi protein [58K 9] antibody. The uptake of Cy3-labeled MIA containing vesicles takes place at the rear part of the cell (A) since the location of the MTOC-Golgi apparatus is toward the leading edge of migrating cells (B). Non-polarized cells and thus non-migrating cells, perceptible by the homogeneous green staining, do not show the characteristic MIA fluorescence located at the cell rear. (C) DAPI. (D) Merge. *I* and *II* are representative examples of two independent experiments.

The observation that the MIA vesicular staining appears at the cell rear and the fact that MIA protein specifically binds to integrin structures $\alpha_4\beta_1$ and $\alpha_5\beta_1$ prompted us to investigate whether MIA protein is internalized together with integrins after binding. Therefore, Mel Im cells were treated with Cy3-labeled MIA protein and stained with anti integrin β_1 [CD29] antibody. As illustrated in *Figure 4*, fluorescence-labeled integrins are distributed all over the cell, whereas in close proximity to the cell membrane integrins appear to accumulate (B). Interestingly, at early stages of the endocytosis process close to the cell membrane, we observed that these integrins are co-localized with Cy3-labeled MIA protein, in particular at the cell rear (C). After staining with an anti-integrin α_5 antibody we observed a similar staining pattern (data not shown). The same results were found for the other melanoma cell lines investigated (*Supplementary Figure S5*). These findings are also supported by data presented in previous studies. Based on far Western blotting and co-immunoprecipitation assays we found a direct interaction of MIA protein with integrin $\alpha_4\beta_1$ and integrin $\alpha_5\beta_1$.¹² Together, these results suggest MIA protein to be internalized into the cell together with integrins $\alpha_5\beta_1$ after binding to these cell adhesion molecules and thereby blocking formation of extracellular matrix contacts.

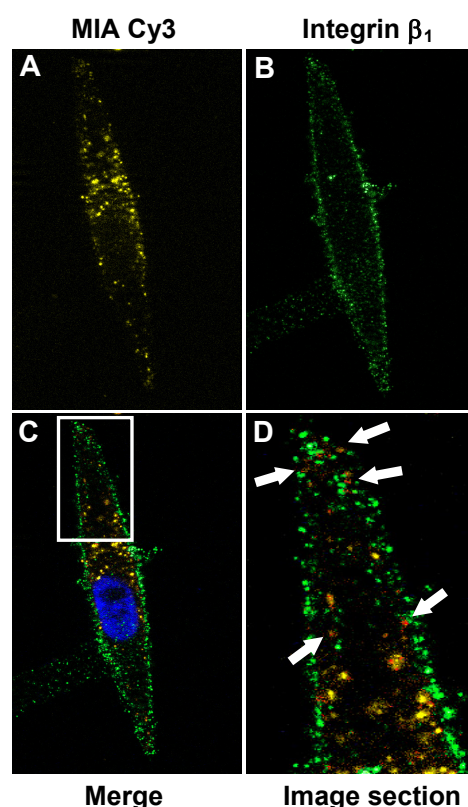


Figure 4: *Internalization of MIA-integrin complexes*

Mel Im cells were treated with Cy3-labeled MIA protein. After fixation cells were stained with anti integrin β_1 [CD29] antibody. **(A)** Cy3-labeled MIA protein is mainly located at one cell pole **(B)** Immunofluorescence-stained integrins are distributed all over the cell and accumulate at or close to the cell membrane. **(C)** Merge. As indicated in the image section by the white arrows, in regions under the cytoplasmic membrane, we observed that integrin β_1 co-localizes with Cy3-labeled MIA protein, here depicted in red. This phenomenon was observed especially at the cell rear.

Nowadays, it is known that integrins are either internalized by clathrin-dependent mechanisms or by non clathrin-dependent mechanisms.¹⁸⁻¹⁹ In terms of the latter, integrins can enter caveolae followed by an internalization route that is regulated by protein kinase C α and dynamin.²⁰ Since we found that MIA protein uptake into cells that were treated with GÖ6976 (*C*), blocking PKC α and β , or BIM1 (*B*), inhibiting PKC α , β and γ , was dramatically decreased (*Figure 5*), our theory of integrin mediated MIA protein uptake was further supported.

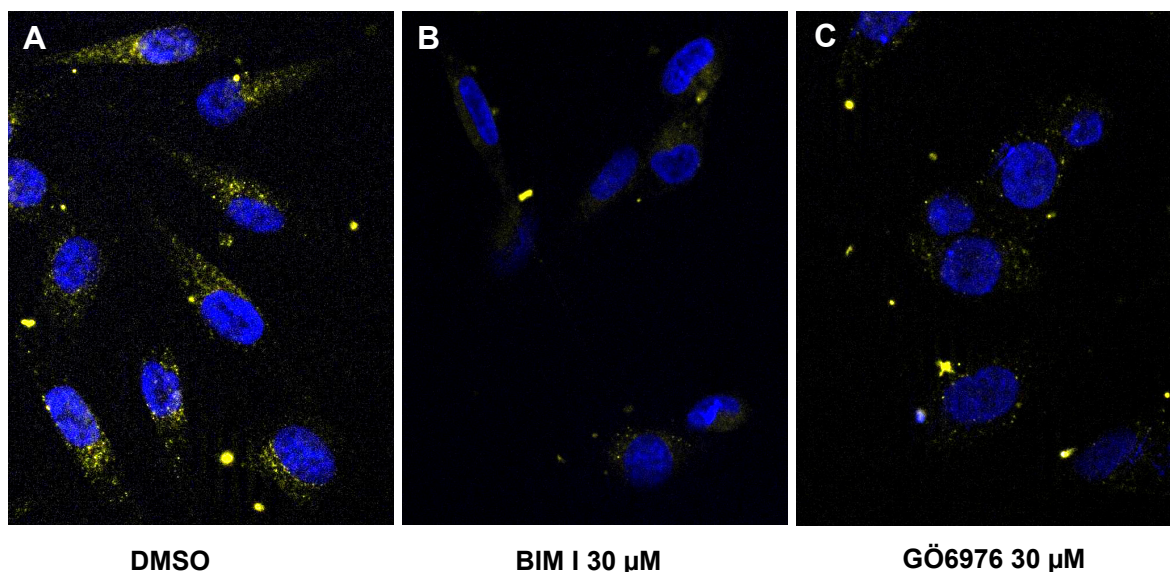


Figure 5: *Inhibition of endocytosis of MIA-integrin complexes by PKC-inhibitors*

Mel Im cells were incubated simultaneously with Cy3-labeled MIA and PKC inhibitors. The DMSO control shows the unidirectional Cy3-labeled MIA protein staining at the cell rear (**A**). Treatment with PKC α , β and γ , inhibitor BIM I (30 μ M) (**B**) and PKC α and β inhibitor GÖ6976 (30 μ M) (**C**), respectively, leads to a dramatical decrease in endocytosis of Cy3-labeled MIA protein.

3.2.3 Intracellular dissociation of MIA-integrin complexes and degradation of MIA protein

In the cytoplasm close to the nucleus, Cy3-labeled MIA protein shows no co-localization with integrins (*Figure 4 C*). Thus, we concluded that MIA-integrin complexes were dissociated after endocytosis and that the two proteins now were transported in different ways. As with other cycling receptors, integrin heterodimers internalize to early endosomes from which they can be either returned directly to the plasma membrane or further trafficked to the perinuclear recycling compartment before recycling through Rab11- and/or Arf6-dependent mechanisms.^{14, 21-23} In *Figure 6* two independent examples (*I and II*) for Mel Im cells treated with Cy3-labeled MIA protein and stained with anti-Rab11 antibody are illustrated. The MIA protein internalization takes place at the rear cell pole (*A*) whereas the Rab11 staining, here depicted in red, is homogeneously distributed all over the cell (*B*). Since Cy3-labeled MIA protein and integrin transporter-protein Rab11 do not co-localize (*D*), our model of intracellular dissociation of endocytosed MIA-integrin complexes further was confirmed. Under the same experimental conditions all other melanoma cell lines show comparable results: Cy3-labeled MIA protein does not co-localize with integrin transporter-protein Rab11 (*Supplementary Figure S6*).

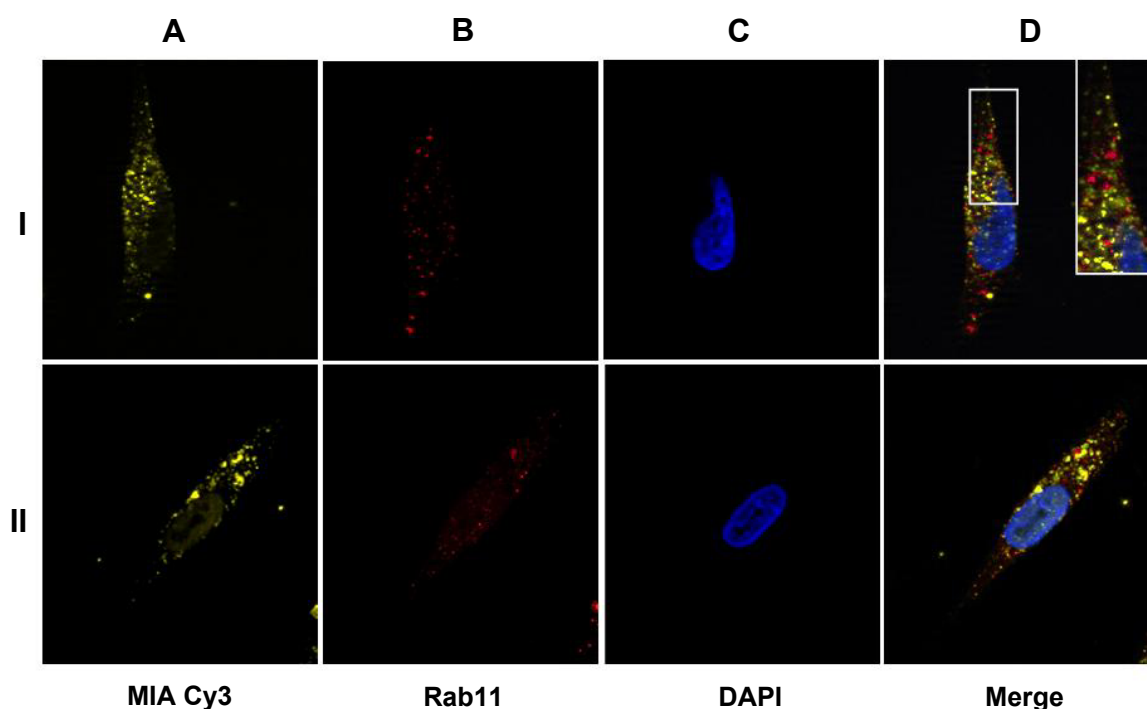


Figure 6: *Dissociation of endocytosed MIA-integrin complexes*

Mel Im cells were treated with Cy3-labeled MIA protein (**A**). After fixation, cells were incubated with anti-Rab11 antibody (**B**). After endocytosis of Cy3-labeled MIA protein it was cleaved from integrins. Thus the integrin transporter-protein Rab11 depicted in red, mediating integrin recycling, does not co-localize with MIA protein. (**C**) DAPI. (**D**) Merge. *I* and *II* are examples of two independent experiments.

To elucidate the fate of internalized MIA protein, we treated cells with Lysotracker red DND99, a chromophore which specifically stains acidic vesicles red in the cytoplasm of cells (*Figure 7 B*). Lysosomes are organelles containing digestive enzymes catalyzing hydrolysis of macromolecules like proteins, polysaccharides, lipids and nucleic acids. The membrane surrounding lysosomes allows the enzymes to work at a pH value of 4 to 5, where these enzymes achieve a high activity. Mel Im melanoma cells were incubated with unlabeled MIA protein. Afterwards, MIA staining was performed using a rabbit anti-MIA antibody. As shown in two independent examples *I* and *II* in *Figure 7 A*, MIA protein distribution depicted in green is similar to that of Cy3-labeled MIA protein shown in previous figures: there is a targeted uptake of MIA protein detectable at the cell rear of migrating cells. As indicated by the white arrows, exactly in regions comprising assemblies of acidic compartments colored in red, there was no MIA-staining detectable, pointing to degradation of MIA protein inside lysosomes. This phenomenon of disappearance of MIA signals strongly contributes to our model of dissociation of MIA protein from integrins after internalization.

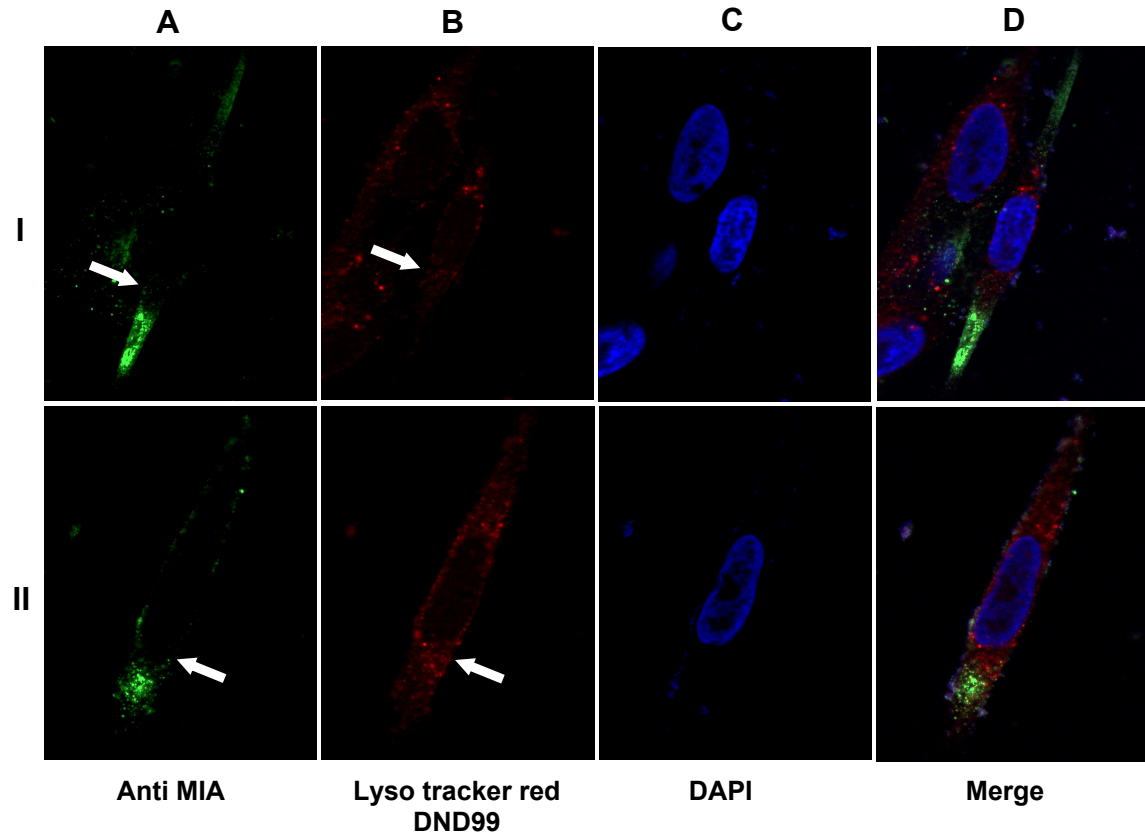


Figure 7: *Degradation of MIA protein after internalization*

Mel Im cells were treated with unlabeled MIA protein and LysoTracker red DND99, a chromophore which specifically stains acidic vesicles red in the cytoplasm of cells. After fixation, MIA protein staining was performed using a rabbit anti-MIA antibody. **(A)** MIA protein distribution depicted in green is similar to that of Cy3-labeled MIA protein: there is a targeted MIA protein uptake detectable at the cell rear of migrating cells. As indicated by the white arrows, exactly in regions comprising assemblies of acidic compartments colored in red **(B)**, there was no MIA-staining detectable. **(C)** DAPI. **(D)** Merge. *I* and *II* represent two independent examples.

To further confirm our hypothesis of MIA protein degradation, cells were also treated with LysoTracker green DND26 together with Cy3-labeled MIA protein. As displayed in *Figure 8 C*, MIA protein co-localizes with acidic cell compartments in close proximity to the nucleus. Unlike detection of MIA protein using an anti-MIA antibody shown in *Figure 7*, this continuous Cy3-fluorescence signal is still detectable inside cytoplasmic acidic vesicles after digestion of the protein at a pH range of pH 4 to 5. In summary, our results demonstrate that MIA protein is internalized into the cell together with integrins and that MIA-integrin binding is dissociated. In the next step, MIA protein is digested in acidic vesicles while integrins are recycled.

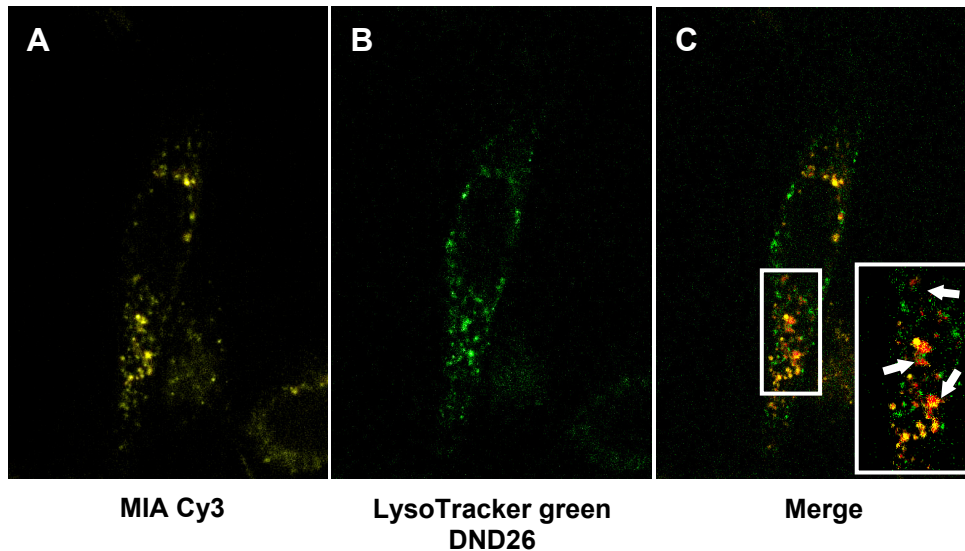


Figure 8: *Degradation of MIA protein in acidic lysosomes*

Mel Im cells simultaneously were treated with Cy3-labeled MIA protein (A) and LysoTracker green DND26 staining acidic lysosomes (B). As illustrated in the merge picture (C), MIA protein co-localizes with acidic cell compartments in the cytoplasm at the centre of the cell close to the nucleus. Co-localization is depicted in red and in the image section it is also indicated by white arrows.

3.3 Discussion

In this study, we analyzed the mechanism by which MIA protein, expressed and secreted by malignant melanoma cells, contributes to alteration of migratory and invasive behavior of these tumor cells. In previous investigations it was shown that MIA protein binds to extracellular matrix molecules including fibronectin, laminin and tenascin.² MIA protein was also described to directly interact with the cell adhesion molecules integrin $\alpha_4\beta_1$ and integrin $\alpha_5\beta_1$.¹² As a result, matrix structures are masked by MIA protein and moreover, neoplastic melanocytes enhance their metastatic capability by specifically changing their attachment to surrounding extracellular matrix molecules and basement membranes.

Experimental data described in this study demonstrate that secreted MIA protein is internalized together with integrin $\alpha_5\beta_1$ after directly binding to this adhesion receptor at the cell surface. We also demonstrate that endocytosis is followed by dissociation of MIA-integrin complexes. Afterwards, MIA protein is degraded in acidic vesicles.

A similar endocytosis mechanism was also described for vitronectin, a plasma protein which was also found in the extracellular matrix. Many functions have been characterized for vitronectin, including regulation of the activity of both thrombin and plasminogen activator, as well as modulating the membrane attack complex of complement. Vitronectin comprises an Arg-Gly-Asp (RGD) sequence that can bind to either the $\alpha_v\beta_3$ or the $\alpha_v\beta_5$ integrin receptor.²⁴⁻²⁶ Similar to MIA protein, vitronectin also mediates cell adhesion by this interaction. As a special feature for internalization of vitronectin together with the cell

adhesion receptor, the interaction of both the $\alpha_v\beta_5$ integrin and a species of heparan sulfate proteoglycan are required. Binding to the extracellular matrix is a prerequisite for endocytosis of vitronectin deduced by the observation that multimeric vitronectin does not appear to be degraded from the fluid phase. Identical to what we observed for MIA protein, receptor-mediated endocytosis is followed by subsequent degradation of vitronectin in lysosomes. Further, it was demonstrated that effectors of protein kinase C, involved in signaling pathways between transmembrane signaling receptors, modulate vitronectin degradation by regulating the internalization.²⁴ The inhibition of receptor mediated endocytosis of MIA protein in cells treated with protein kinase C inhibitors BIM1 and GÖ6976 contributes to our hypothesis that MIA protein internalization may be regulated by a similar mechanism. Unlike vitronectin, MIA protein is bound to the cell surface receptor integrin $\alpha_5\beta_1$ before internalization. In previous studies, it was reported that remodeling of matrix structures occurs via internalization of extracellular matrix proteins and degradation in lysosomes.²⁷⁻³⁰ It was shown that - identical to MIA protein - turnover of extracellular matrix protein fibronectin is processed via integrin $\alpha_5\beta_1$ internalization. This endocytosis mechanism is constitutively regulated by caveolin-1 and can occur in presence or absence of fibronectin and fibronectin matrix.³¹ Not all fibronectin binding integrins can promote fibronectin endocytosis. Of the integrins tested, only $\alpha_5\beta_1$ integrin was shown to participate in fibronectin endocytosis. Identical to our results for MIA protein it was also demonstrated that matrix turnover of fibronectin is followed by lysosomal degradation.³²

Further, the prevention of MIA protein internalization after treatment of cells with peptides deduced from extracellular matrix proteins and integrin structures is consistent with our proposed mechanism. Before initial binding to integrin receptors, MIA protein was captured by these peptides. Next to their canonical role in physical adhesion of cells, interactions between cell surface molecules and matrix components provide pivotal contributions to a broad range of cellular processes in melanocytic cells. Thus, active detachment of melanoma cells induced by MIA protein may also be implicated in regulation of migration, apoptosis, secretion of proteases or matrix proteins, and cell growth.³³⁻³⁸ It is known that such interactions between melanocytic cells and extracellular matrix involve foremost binding of integrins to specific epitopes within fibronectin and depend, to a significant extent, on activation of integrin $\alpha_4\beta_1$ and integrin $\alpha_5\beta_1$.³⁷ Detachment from surrounding matrix structures is a basic requirement for melanoma cells to migrate, invade and finally metastasize in a systemic disease. To impair formation of

metastases and control malignant melanoma metastases at the invasive state it is necessary to anticipate MIA binding to integrins and extracellular matrix molecules. Previously published data provide first evidence for a reduction of tumor size after application of two fibronectin-deduced peptides in a mouse melanoma model.²

In summary, our results demonstrate that MIA protein, binding to integrins and thus promoting detachment of cells from extracellular matrix structures, is internalized into the cell together with these cell adhesion receptors at the cell rear. MIA-integrin binding dissociates and in the next step, MIA protein is digested in acidic vesicles while integrins are recycled. Prevention of MIA protein internalization by capturing the protein by inhibitors *in vivo* may provide a novel therapeutic strategy for therapy of patients suffering from malignant melanoma.

3.4 Materials and Methods

Cell lines and cell culture conditions

The melanoma cell line Mel Im, established from a human metastatic bioptic sample (generous gift from Dr. Johnson, University of Munich, Germany) was used in all experiments. Additionally, main experiments were also conducted using human cell lines Mel Ju, SK Mel 28 and A375, which were all derived from metastasis of malignant melanoma. Cells were maintained in DMEM (PAA Laboratories GmbH, Austria) supplemented with penicillin (400 U/mL), streptomycin (50 µg/mL), l-glutamine (300 µg/mL) and 10% fetal calf serum (Pan Biotech GmbH, Germany) and split in 1:5 ratio every 3 days.

Protein labeling

For the conjugation of the orange fluorescing cyanine dye Cy3, 0.11 mg MIA protein or 0.4 mg BSA, respectively, was dissolved in 1 mL sodium carbonate-sodium bicarbonate buffer (pH 9.3), added to the dye vial (CyTM3 Mono-Reactive Dye Pack, Amersham GE Healthcare, UK) and mixed thoroughly. The reaction was incubated at room temperature for 50 min before separation of protein from free dye by using a SephadexTM G-25 M PD-10 Desalting column (Amersham Pharmacia Biotech, Sweden). During elution two pink bands occurred; the faster moving band represents Cy3-labeled MIA protein and Cy3-labeled BSA, respectively. The procedure was designed to label protein to a final molar dye/protein ratio between 4 and 12.

The fluorescent Cy3 label does not affect binding properties of MIA protein, as deduced from Boyden Chamber invasion experiments, where Mel Im cells were treated with Cy3-labeled MIA protein and, in comparison, with unlabeled MIA protein (*Supplementary Figure S1A*).

Immunofluorescence assays

5 x 10⁵ melanoma cells, Mel Im, Mel Ju, SK Mel28 and A375, respectively, were grown in a 4-well chamber slide in 500 µl DMEM and incubated with 35 µl 4.5 µM Cy3-labeled MIA protein or BSA, respectively, for 90 min at 37°C and 5% CO₂. Afterwards, cells were washed and fixed using 4% paraformaldehyde in 0.1 M phosphate-buffered saline (PBS) for 15 min and permeabilized.³⁹ After rinsing with PBS for 5 times, coverslips were mounted on slides using Hard Set Mounting Medium with DAPI (Vectashield, H-1500) and imaged using an Axio Imager Zeiss Z1 fluorescence microscope (Axiovision Rel. 4.6.3) equipped with an Axio Cam MR camera. Images were taken using 40x or 63x oil immersion lenses. For a better illustration in all pictures Cy3 staining is depicted in yellow. Conspicuous extracellularly located yellow dots perceptible in images comprising MIA Cy3 staining are dye-artifacts.

For Golgi marker experiments cells were seeded and incubated for 24 h before further treatment. During this time span the reorientation of the microtubule organizing center (MTOC), a comparatively slow process that can take several hours after migratory stimuli, is ensured. After fixation of cells with 4% paraformaldehyde in 0.1 M PBS, permeabilizing and blocking of non-specific binding sites with blocking solution (1% BSA/PBS) for 1 h at 4°C and rinsing was performed. Cells were incubated with primary antibody mouse anti-Golgi protein [58K 9] antibody (Abcam, UK) in concentrations of 1 µg/mL at 4°C for 2 h. The amount of migrating cells was determined by counting 50 cells three times. Cells which show the characteristic MTOC staining pattern at the cell front were evaluated as “migrating”, whereas non-polarized cells that show homogenously distributed staining were counted as “non-migrating”.

To illustrate co-localization of MIA protein with integrin $\alpha_5\beta_1$, cells were incubated with a 1:60 dilution of mouse anti human integrin β_1 [CD29] antibody (Chemicon International, USA) or a 1:40 dilution of mouse anti human integrin α_5 antibody (Chemicon International, USA), respectively, at 4°C for 2 h after Cy3-labeled MIA protein treatment, fixation with 4% paraformaldehyde in PBS, permeabilization and blocking of non-specific binding with 1% BSA / PBS. To exclude non-specific binding of target primary antibody

due to Fc-binding or other protein-protein interactions, we also used a mouse IgG isotype control antibody (Chemicon) (data not shown).

To generate MIA / Rab11 co-staining, cells were treated with Cy3-labeled MIA protein, fixed with 4% paraformaldehyde in PBS, permeabilized and non-specific binding sites were blocked using 1% BSA / PBS. Afterwards, cells were incubated with a 1:50 dilution of mouse anti Rab 11 antibody (BD Bioscience Pharmingen, USA) at 4°C for 2 h. After rinsing with PBS for 5 times, cells were covered with a 1:30 dilution of the secondary antibody (FITC-conjugated polyclonal rabbit anti mouse immunoglobulin, DakoCytomation, USA) in PBS at 4°C for 1 h. Afterwards, cells were washed with PBS and mounted with Hard Set Mounting Medium with DAPI (Vectashield, H-1500, USA) or Hard Set Mounting Medium without DAPI (Vectashield, H-1400, USA), respectively.

To selectively stain acidic lysosomes, Mel Im cells, grown on a 4-well chamber slide, were incubated with LysoTracker red DND99 (Molecular Probes, Invitrogen, USA) in a concentration of 60 nM for 90 min at 37°C, 5% CO₂. Afterwards, cells were washed, fixed using 4% paraformaldehyde in 0.1 M PBS for 15 min and permeabilized. After rinsing with PBS for 5 times, cells were covered with blocking solution (1% BSA / PBS) for 1 h at 4°C followed by incubation with an 1:20 dilution of primary antibody rabbit anti MIA antibody (Biogenes, Berlin, Germany) for 2 h at 4°C. After washing with PBS, cells were incubated with a 1:30 dilution of the secondary antibody (FITC conjugated swine anti rabbit immunoglobulin, DakoCytomation). In case of simultaneously staining acidic lysosomes, LysoTracker green DND26 (Molecular Probes, Invitrogen, USA) in a concentration of 600 nM was incubated together with Cy3-labeled MIA protein on Mel Im cells for 90 min at 37°C and 5% CO₂. Without fixation, cells were washed with PBS and mounted using Hard Set Mounting Medium without DAPI (Vectashield, H-1400, USA).

MIA inhibitory peptide and PKC inhibitors

For inhibition of MIA protein uptake, Mel Im, Mel Ju, SK Mel28 and A375 cells, respectively, together with Cy3-labeled MIA protein and the respective inhibitor were incubated for 90 min at 37°C and 5% CO₂. Inhibitors were used in several final concentrations. AR54 (sequence: NSLLVSFQPPRAR), a MIA binding peptide deduced from peptide FN14, which was previously identified in a phage display experiment, was synthesized on solid-phase using HOBt / TBTU / DIEA and Rink Amide MBHA resin and was used at concentrations of 0.3 µM, 0.5 µM, and 2 µM.⁹ Its ability to block MIA function was tested using a Boyden Chamber invasion assay.² AR54 at a final

concentration of 1 μ M was able to almost completely inhibit MIA function without affecting integrin activity, indicating that specific binding of AR54 to MIA protein anticipates MIA interaction to extracellular matrix molecules and integrins (*Supplementary Figure S1B*).

As a negative control cells were also treated with scrambled peptide AR5 (sequence: Gly-Gly-Ser-Gly-NH₂) in concentrations of 1 μ M and 3 μ M. In all cases Cy3-labeled MIA protein uptake was not affected by AR5 (data not shown).

Both PKC α inhibitors 3-(N-[Dimethylamino]propyl-3-indolyl)-4-(3-indolyl)maleimide-3-[1-[3-(Dimethylamino)propyl]1H-indol-3-yl]-4-(1H-indol-3-yl)1H-pyrrole-2,5dione Bisindolyl-maleimide I (BIM I) and 12-(2-Cyanoethyl)-6,7,12,13-tetrahydro-13-methyl-5-oxo-5H-indolo[2,3-a]pyrrolo[3,4-c]carbazole (GÖ6976) were used in a final concentration of 30 μ M. As a control, cells were treated with DMSO.

3.5 Acknowledgements

We thank Dr. Johnson (University of Munich, Germany) for providing melanoma cell lines, Alexander Riechers for synthesis of MIA protein inhibitory peptides, Andrea Sassen and Marietta Bock for technical assistance. This work was supported by the DFG.

3.6 References

1. Bosserhoff, A. K.; Kaufmann, M.; Kaluza, B.; Bartke, I.; Zirngibl, H.; Hein, R.; Stolz, W.; Buettner, R., Melanoma-inhibiting activity, a novel serum marker for progression of malignant melanoma. *Cancer Res* **1997**, 57, (15), 3149-53.
2. Bosserhoff, A. K.; Stoll, R.; Sleeman, J. P.; Bataille, F.; Buettner, R.; Holak, T. A., Active detachment involves inhibition of cell-matrix contacts of malignant melanoma cells by secretion of melanoma inhibitory activity. *Lab Invest* **2003**, 83, (11), 1583-94.
3. Guba, M.; Bosserhoff, A. K.; Steinbauer, M.; Abels, C.; Anthuber, M.; Buettner, R.; Jauch, K. W., Overexpression of melanoma inhibitory activity (MIA) enhances extravasation and metastasis of A-mel 3 melanoma cells in vivo. *Br J Cancer* **2000**, 83, (9), 1216-22.
4. Bosserhoff, A. K.; Echtenacher, B.; Hein, R.; Buettner, R., Functional role of melanoma inhibitory activity in regulating invasion and metastasis of malignant melanoma cells in vivo. *Melanoma Res* **2001**, 11, (4), 417-21.

5. Dreau, D.; Bosserhoff, A. K.; White, R. L.; Buettner, R.; Holder, W. D., Melanoma-inhibitory activity protein concentrations in blood of melanoma patients treated with immunotherapy. *Oncol Res* **1999**, 11, (1), 55-61.
6. Stahlecker, J.; Gauger, A.; Bosserhoff, A.; Buttner, R.; Ring, J.; Hein, R., MIA as a reliable tumor marker in the serum of patients with malignant melanoma. *Anticancer Res* **2000**, 20, (6D), 5041-4.
7. Stoll, R.; Renner, C.; Ambrosius, D.; Golob, M.; Voelter, W.; Buettner, R.; Bosserhoff, A. K.; Holak, T. A., Sequence-specific ^1H , ^{13}C , and ^{15}N assignment of the human melanoma inhibitory activity (MIA) protein. *J Biomol NMR* **2000**, 17, (1), 87-8.
8. Stoll, R.; Renner, C.; Buettner, R.; Voelter, W.; Bosserhoff, A. K.; Holak, T. A., Backbone dynamics of the human MIA protein studied by ^{15}N NMR relaxation: implications for extended interactions of SH3 domains. *Protein Sci* **2003**, 12, (3), 510-9.
9. Stoll, R.; Renner, C.; Zweckstetter, M.; Bruggert, M.; Ambrosius, D.; Palme, S.; Engh, R. A.; Golob, M.; Breibach, I.; Buettner, R.; Voelter, W.; Holak, T. A.; Bosserhoff, A. K., The extracellular human melanoma inhibitory activity (MIA) protein adopts an SH3 domain-like fold. *EMBO J* **2001**, 20, (3), 340-9.
10. Loughheed, J. C.; Holton, J. M.; Alber, T.; Bazan, J. F.; Handel, T. M., Structure of melanoma inhibitory activity protein, a member of a recently identified family of secreted proteins. *Proc Natl Acad Sci U S A* **2001**, 98, (10), 5515-20.
11. Stoll, R.; Bosserhoff, A., Extracellular SH3 domain containing proteins - features of a new protein family. *Curr Protein Pept Sci* **2008**, 9, (3), 221-6.
12. Bauer, R.; Humphries, M.; Fassler, R.; Winklmeier, A.; Craig, S. E.; Bosserhoff, A. K., Regulation of integrin activity by MIA. *J Biol Chem* **2006**, 281, (17), 11669-77.
13. Bretscher, M. S., Circulating integrins: alpha 5 beta 1, alpha 6 beta 4 and Mac-1, but not alpha 3 beta 1, alpha 4 beta 1 or LFA-1. *EMBO J* **1992**, 11, (2), 405-10.
14. Caswell, P. T.; Norman, J. C., Integrin trafficking and the control of cell migration. *Traffic* **2006**, 7, (1), 14-21.
15. Kupfer, A.; Louvard, D.; Singer, S. J., Polarization of the Golgi apparatus and the microtubule-organizing center in cultured fibroblasts at the edge of an experimental wound. *Proc Natl Acad Sci U S A* **1982**, 79, (8), 2603-7.
16. Magdalena, J.; Millard, T. H.; Machesky, L. M., Microtubule involvement in NIH 3T3 Golgi and MTOC polarity establishment. *J Cell Sci* **2003**, 116, (Pt 4), 743-56.

17. Prigozhina, N. L.; Waterman-Storer, C. M., Protein kinase D-mediated anterograde membrane trafficking is required for fibroblast motility. *Curr Biol* **2004**, 14, (2), 88-98.
18. Altankov, G.; Grinnell, F., Fibronectin receptor internalization and AP-2 complex reorganization in potassium-depleted fibroblasts. *Exp Cell Res* **1995**, 216, (2), 299-309.
19. Liu, L.; He, B.; Liu, W. M.; Zhou, D.; Cox, J. V.; Zhang, X. A., Tetraspanin CD151 promotes cell migration by regulating integrin trafficking. *J Biol Chem* **2007**, 282, (43), 31631-42.
20. Nishimura, T.; Kaibuchi, K., Numb controls integrin endocytosis for directional cell migration with aPKC and PAR-3. *Dev Cell* **2007**, 13, (1), 15-28.
21. Jones, M. C.; Caswell, P. T.; Norman, J. C., Endocytic recycling pathways: emerging regulators of cell migration. *Curr Opin Cell Biol* **2006**, 18, (5), 549-57.
22. Pellinen, T.; Ivaska, J., Integrin traffic. *J Cell Sci* **2006**, 119, (Pt 18), 3723-31.
23. Ramsay, A. G.; Marshall, J. F.; Hart, I. R., Integrin trafficking and its role in cancer metastasis. *Cancer Metastasis Rev* **2007**, 26, (3-4), 567-78.
24. Panetti, T. S.; Wilcox, S. A.; Horzempa, C.; McKeown-Longo, P. J., Alpha v beta 5 integrin receptor-mediated endocytosis of vitronectin is protein kinase C-dependent. *J Biol Chem* **1995**, 270, (31), 18593-7.
25. Pijuan-Thompson, V.; Gladson, C. L., Ligation of integrin alpha5beta1 is required for internalization of vitronectin by integrin alphavbeta3. *J Biol Chem* **1997**, 272, (5), 2736-43.
26. Tomasini, B. R.; Mosher, D. F., Vitronectin. *Prog Hemost Thromb* **1991**, 10, 269-305.
27. Godyna, S.; Liau, G.; Popa, I.; Stefansson, S.; Argraves, W. S., Identification of the low density lipoprotein receptor-related protein (LRP) as an endocytic receptor for thrombospondin-1. *J Cell Biol* **1995**, 129, (5), 1403-10.
28. Memmo, L. M.; McKeown-Longo, P., The alphavbeta5 integrin functions as an endocytic receptor for vitronectin. *J Cell Sci* **1998**, 111 (Pt 4), 425-33.
29. Murphy-Ullrich, J. E.; Mosher, D. F., Interactions of thrombospondin with endothelial cells: receptor-mediated binding and degradation. *J Cell Biol* **1987**, 105, (4), 1603-11.

30. Wienke, D.; MacFadyen, J. R.; Isacke, C. M., Identification and characterization of the endocytic transmembrane glycoprotein Endo180 as a novel collagen receptor. *Mol Biol Cell* **2003**, 14, (9), 3592-604.
31. Sottile, J.; Chandler, J., Fibronectin matrix turnover occurs through a caveolin-1-dependent process. *Mol Biol Cell* **2005**, 16, (2), 757-68.
32. Shi, F.; Sottile, J., Caveolin-1-dependent beta1 integrin endocytosis is a critical regulator of fibronectin turnover. *J Cell Sci* **2008**, 121, (Pt 14), 2360-71.
33. Bates, R. C.; Lincz, L. F.; Burns, G. F., Involvement of integrins in cell survival. *Cancer Metastasis Rev* **1995**, 14, (3), 191-203.
34. Boudreau, N.; Sympton, C. J.; Werb, Z.; Bissell, M. J., Suppression of ICE and apoptosis in mammary epithelial cells by extracellular matrix. *Science* **1995**, 267, (5199), 891-3.
35. Clarke, A. S.; Lotz, M. M.; Chao, C.; Mercurio, A. M., Activation of the p21 pathway of growth arrest and apoptosis by the beta 4 integrin cytoplasmic domain. *J Biol Chem* **1995**, 270, (39), 22673-6.
36. Langholz, O.; Rockel, D.; Mauch, C.; Kozłowska, E.; Bank, I.; Krieg, T.; Eckes, B., Collagen and collagenase gene expression in three-dimensional collagen lattices are differentially regulated by alpha 1 beta 1 and alpha 2 beta 1 integrins. *J Cell Biol* **1995**, 131, (6 Pt 2), 1903-15.
37. Scott, G.; Ryan, D. H.; McCarthy, J. B., Molecular mechanisms of human melanocyte attachment to fibronectin. *J Invest Dermatol* **1992**, 99, (6), 787-94.
38. Varner, J. A.; Emerson, D. A.; Juliano, R. L., Integrin alpha 5 beta 1 expression negatively regulates cell growth: reversal by attachment to fibronectin. *Mol Biol Cell* **1995**, 6, (6), 725-40.
39. Arndt, S.; Poser, I.; Moser, M.; Bosserhoff, A. K., Fussel-15, a novel Ski/Sno homolog protein, antagonizes BMP signaling. *Mol Cell Neurosci* **2007**, 34, (4), 603-11.

3.7 Supplementary Information

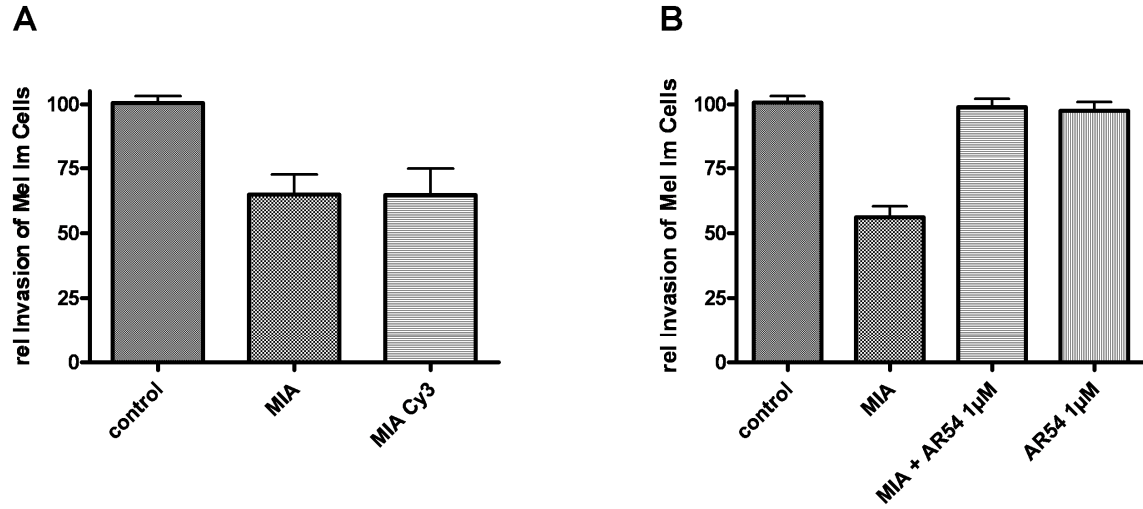


Figure S1: Invasion of Mel Im cells (indicated in %, control set as 100%) was measured in Boyden Chambers. Polycarbonate filters with 8 μm pore size were coated with matrigel. Fibroblast-conditioned medium was placed as a chemoattractant into the lower compartment. After incubation at 37°C for 4 hours, cells adhering to the lower filter surface were fixed, stained and counted. All data were observed in at least three independent experiments. **(A)** Mel Im cells were treated with Cy3-labeled MIA protein and unlabeled MIA protein (50 ng/ml), respectively. The fluorescent Cy3 label does not affect binding properties of MIA protein. **(B)** Mel Im cells were treated with MIA protein, MIA inhibitory peptide AR54 together with MIA protein and AR54 alone. AR54 at a final concentration of 1 μM was able to almost completely inhibit MIA function without affecting integrin activity, indicating that specific binding of AR54 to MIA protein anticipates MIA interaction to extracellular matrix molecules and integrins.

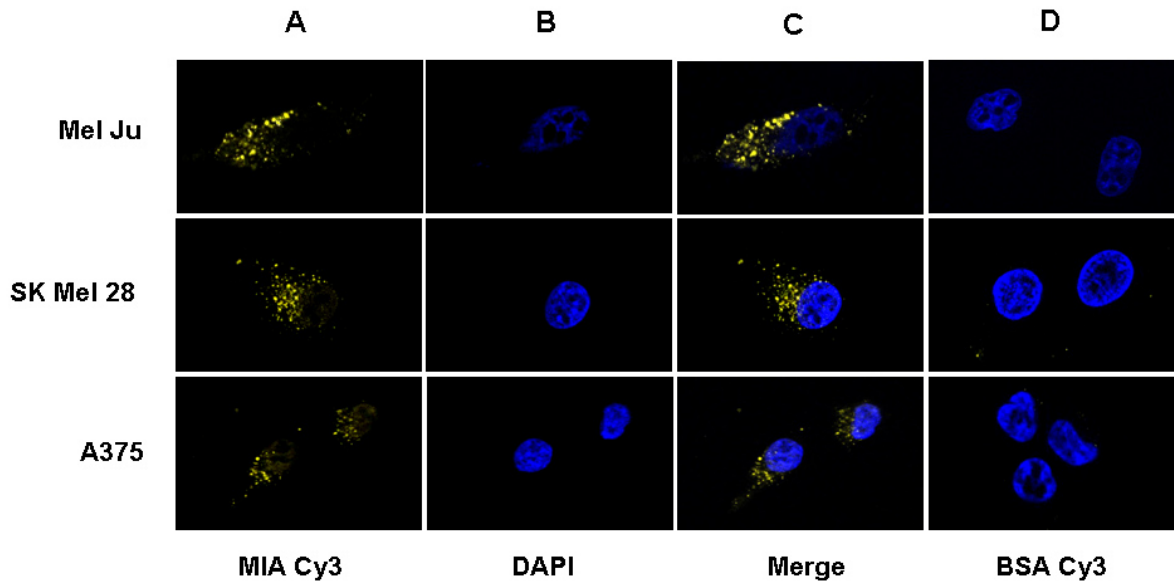


Figure S2: The melanoma cell lines Mel Ju, SK Mel 28 and A375 were treated with Cy3-labeled MIA protein and as a negative control with Cy3-labeled BSA. **(A)** Migrating cells internalize MIA protein and show a strong Cy3-fluorescence intensity asymmetrically distributed at one cell pole. **(B)** DAPI **(C)** Merge **(D)** BSA Cy3 negative control.

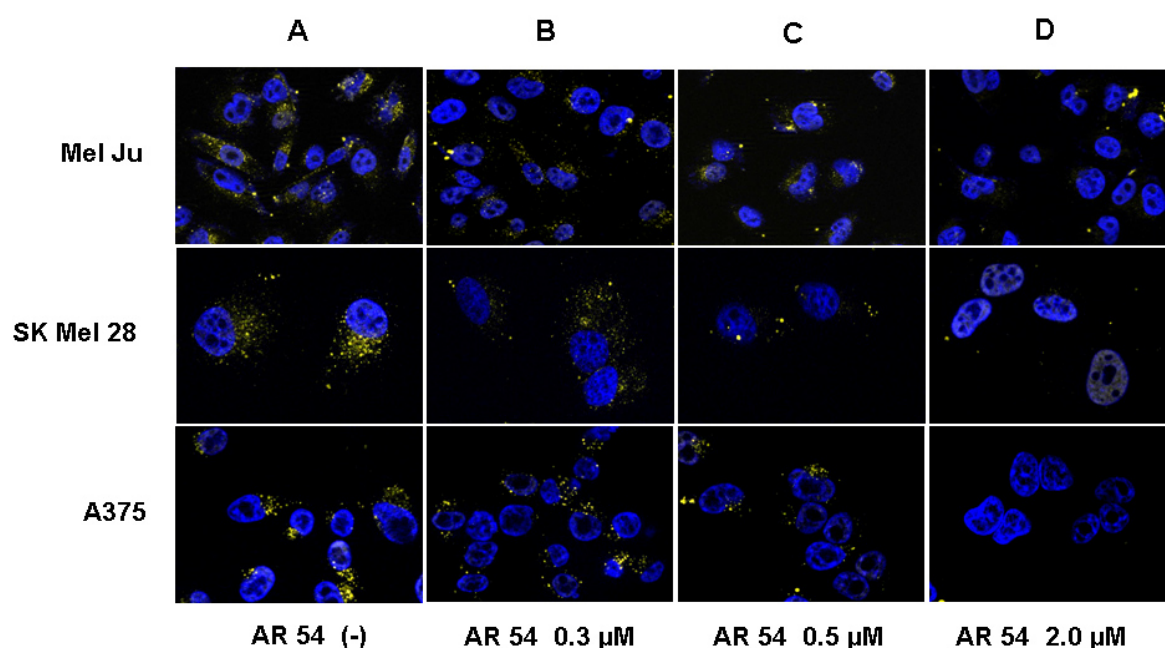


Figure S3: Mel Ju, SK Mel 28 and A375 cells simultaneously were treated with Cy3-labeled MIA protein (A) and AR54, a MIA protein binding peptide, which was able to inhibit MIA function. AR54 was added in different concentrations. Final concentrations of 0.3 μM (B) and 0.5 μM (C) moderately decrease MIA protein endocytosis whereas concentrations of 2 μM (D) almost completely inhibit MIA protein uptake.

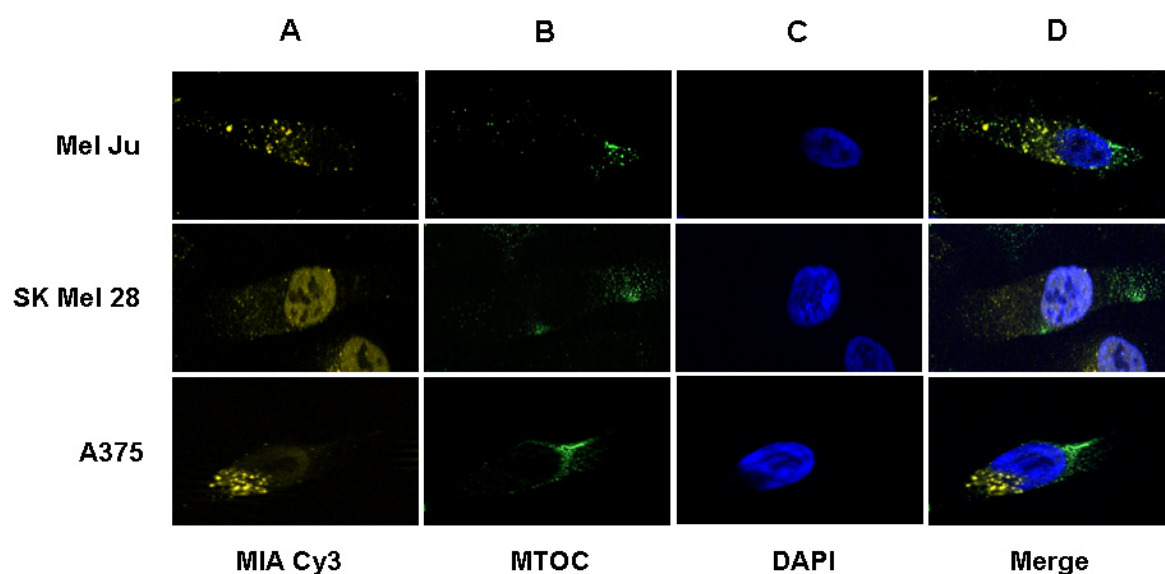


Figure S4: For determination of the direction of migration, Cy3-labeled MIA treated Mel Ju, SK Mel 28 and A375 cells, respectively, were stained with a Golgi marker mouse anti-Golgi protein [58K 9] antibody. The uptake of Cy3-labeled MIA containing vesicles takes place at the rear part of the cell (A) since the location of the MTOC-Golgi apparatus is toward the leading edge of migrating cells (B). (C) DAPI. (D) Merge.

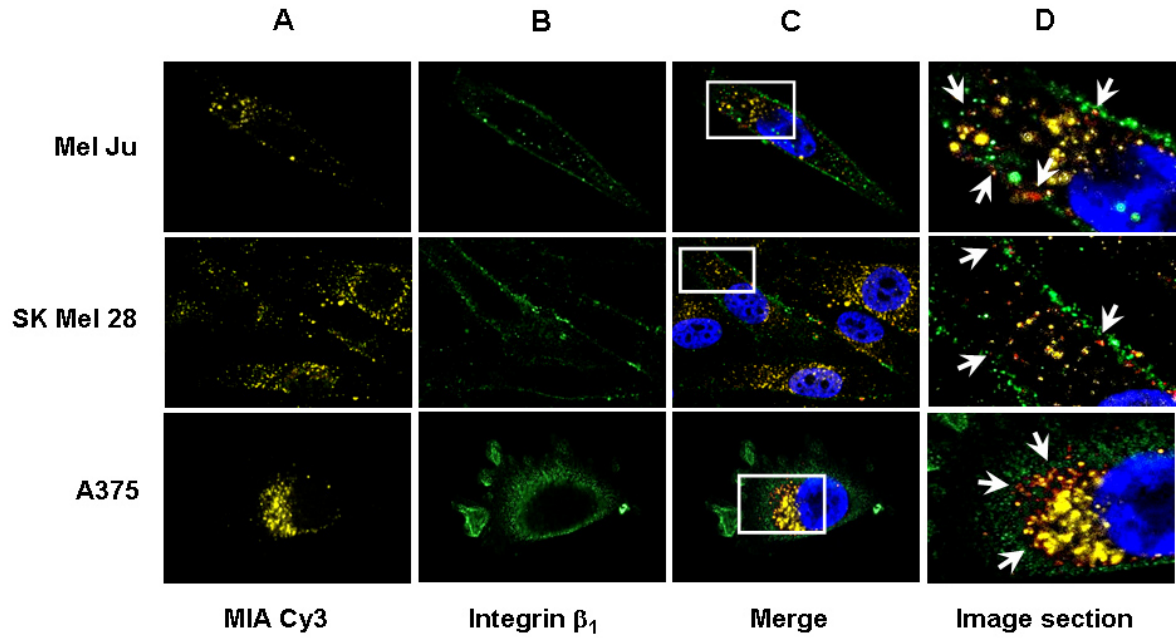


Figure S5: Melanoma cell lines Mel Ju, SK Mel 28 and A375 were treated with Cy3-labeled MIA protein. After fixation cells were stained with anti integrin β_1 [CD29] antibody. (A) Cy3-labeled MIA protein is mainly located at one cell pole (B) Immunofluorescence-labeled integrins are distributed all over the cell and accumulate at or close to the cell membrane. (C) Merge. As indicated by the white arrows, in regions under the cytoplasmic membrane, we observed that integrin β_1 co-localizes with Cy3-labeled MIA protein. This phenomenon was observed especially at the cell rear.

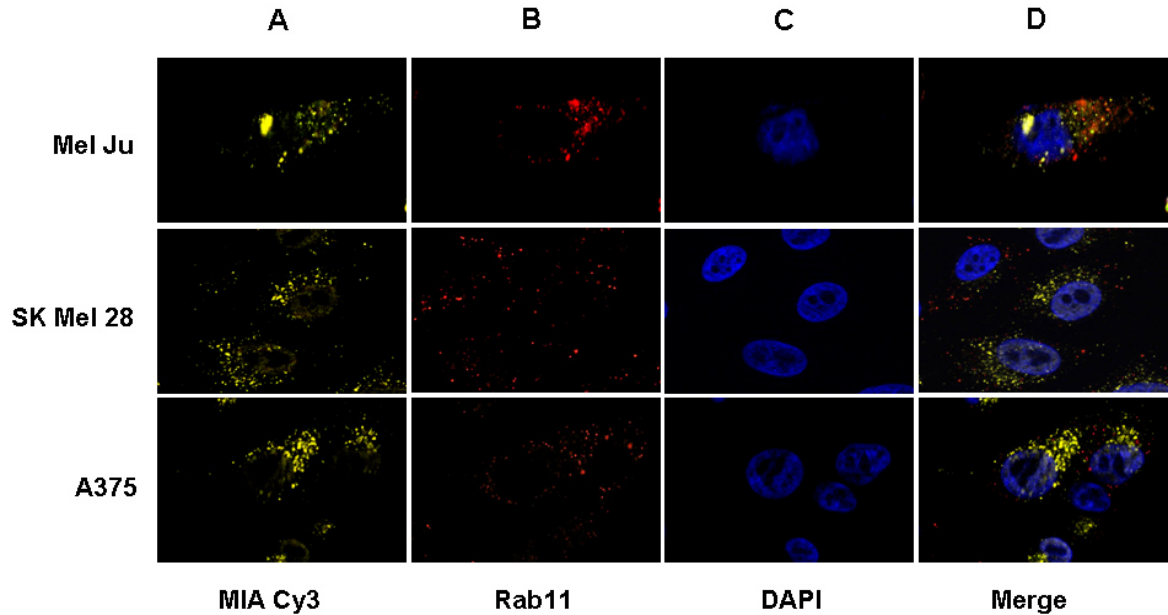


Figure S6: Mel Ju, Sk Mel 28 and A375 cells, respectively, were treated with Cy3-labeled MIA protein (A). After fixation, cells were incubated with anti-Rab11 antibody (B). After endocytosis of Cy3-labeled MIA protein was cleaved from integrins. The integrin transporter-protein Rab11, mediating integrin recycling, is here depicted in red. (C) DAPI. (D) Merge. MIA protein, shown in yellow, and Rab11, depicted in red, do not co-localize.

4 Heterogeneous Transition Metal-based Fluorescence Polarization (HTFP) Assay for Probing Protein Interactions

Abstract

Analyses of protein interactions are fundamental for the investigation of molecular mechanisms responsible for cellular processes and diseases as well as for drug discovery in the pharmaceutical industry. The present study details the development of a fluorescence polarization (FP) assay using the example of Melanoma Inhibitory Activity (MIA)-binding compounds and studies of the binding properties of this protein. Already existing FP assays can, dependent on the lifetime of the fluorescent label, only determine interactions with either high or low molecular weight interaction partners. Our new concept eliminates this limitation by immobilizing a known binding partner of MIA protein to a well plate and by labeling the target protein using luminescent transition metal labels such as Ru(bpy)₃ for binding studies with both high and low molecular weight interaction partners. Due to the use of a functionalized surface, we termed our concept Heterogeneous Transition metal based FP assay (HTFP). The independency of the assay from molecular weight of potential binding partners allows investigations on subjects as diverse as multimerization, interactions with pharmacophores or determination of binding affinities.

The results of this chapter have been published:

Riechers, A., Schmidt, J., König, B., Bosserhoff, A. K.; Heterogeneous Transition Metal-based Fluorescence Polarization (HTFP) Assay for Probing Protein Interactions. *Biotechniques* **2009**; 47, 837-844.

Author Contributions:

I focused on protein labeling and in vitro analysis, cell culture experiments and the design of the HTFP assay. A. Riechers has established the HTFP assay and performed most of the measurements. B. König and A. K. Bosserhoff have been supervising this project.

4.1 Introduction

Protein interactions play a fundamental role in many biochemical processes like signal transduction, immune reaction, cell cycle control, differentiation and protein folding. They are also responsible for a number of diseases including cancer due to loss of protein function as a consequence of mutations. The search for potent and selective inhibitors for specific proteins is essential in pharmaceutical drug design and various techniques have been established for probing protein interactions. However, the applicability of the techniques is often restricted by the molecular weight of the binding partners. We describe here a screening assay based on fluorescence polarization measurements enabling high throughput screening and addressing this limitation by using the example of MIA-inhibitory compounds. MIA protein has previously been identified as an 11 kDa molecule physiologically produced by cartilage, strongly expressed and secreted by malignant melanoma cells but not expressed in melanocytes.¹⁻² Since MIA protein expression levels *in vivo* directly correlate with progressive malignancy of melanocytic tumors it serves as a reliable clinical tumor marker to detect and monitor metastatic diseases.^{1, 3-4} Recent data describe a direct interaction of MIA protein with cell adhesion receptors integrin $\alpha_4\beta_1$ and integrin $\alpha_5\beta_1$ and extra cellular matrix molecules including fibronectin.⁵⁻⁶ By modulating integrin activity and masking matrix structures MIA protein mediates detachment of melanoma cells resulting in enhanced invasive and migratory potential that finally strongly contributes to the formation of metastasis.⁷ In previous studies, the MIA binding peptide FN14, matching a fibronectin domain, was identified in a phage display experiment.⁷⁻⁸ AR54, a MIA binding peptide deduced from peptide FN14 was able to functionally inhibit MIA protein *in vitro*. Using this peptide we aimed to establish an assay which allows detection of potential MIA-inhibitory compounds.

To investigate interactions of MIA protein, commonly used methods like fluorescence emission titration and FRET-based experiments were found to be inappropriate due to inherent tendency of MIA protein to form aggregates.⁸ Since Dynamic Light Scattering (DLS), NMR and isothermal calorimetry (ITC) were not sensitive enough to detect binding events at physiologically relevant concentrations, we decided to employ fluorescence polarization for elucidating the interaction of MIA protein with AR54. However, traditional FP assays are limited by the molecular weight of the interaction partner. For the evaluation of binding of low molecular weight compounds to proteins, assays are performed entirely in solution and are thus limited to the use of organic fluorophores due to the short fluorescence lifetime required. Typically, the displacement of an already

known and labeled inhibitory compound from the target protein by a low molecular weight drug candidate is determined in these FP assays. Although luminescent transition metal complexes have been used in FP immunoassays⁹⁻²¹ this assay concept in solution is not feasible for binding investigations of low molecular weight compounds, for example in drug candidate screening due to the dependence of fluorescence polarization on molecular weight and fluorescence lifetime. Luminescent transition metal complexes have a number of advantages compared to organic fluorophores such as a large Stokes shift, high photostability and the option to be used in time-gated measurements. These time-gated measurements offer the possibility of multiple labeling using transition metals with different lifetimes despite possible spectral overlap and the elimination of autofluorescence of biological material. By using a well plate functionalized with a MIA protein binding compound, we created a binding partner of significantly higher molecular weight than any peptide or protein. As described here, we have developed a fluorescence polarization assay capable of handling both high and low molecular weight interaction partners and termed our experimental setup Heterogeneous Transition metal based Fluorescence Polarization (HTFP) assay.

4.2 Results

In malignant melanoma, MIA protein facilitates cell detachment by mediating integrin activity and further by masking binding sites for cell adhesion molecules at extracellular matrix structures. To prevent formation of metastasis it is desirable to find substances that specifically bind to MIA protein and thereby functionally reduce MIA-induced effects. Here, MIA and known binding partners were used to develop an assay format capable of high throughput analysis based on fluorescence polarization measurements to identify and characterize protein interactions. The use of a multi-well plate makes it possible to assay more samples in significantly less time using few reagents.

4.2.1 *Heterogeneous Transition metal based Fluorescence Polarization (HTFP) assay development*

Peptide AR54, deduced from the peptide FN14, which was previously identified in a phage display experiment,⁷⁻⁸ was tested for its ability to functionally inhibit MIA protein *in vitro* using a Boyden Chamber invasion assay. The peptide was able to almost completely inhibit MIA protein function by preventing interactions of MIA protein with extracellular matrix molecules and integrins without affecting cell migration itself.²² This prompted us

to investigate this interaction of the inhibitory peptide with MIA in fluorescence emission titration experiments, a method that is generally used to obtain information about stoichiometry and binding constants. While a FRET experiment with an N-methylanthraniloyl labeled AR54 derivative failed due to spectral overlap, FP experiments with a carboxyfluorescein labeled derivative were compromised by nonspecific interactions of MIA protein and the respective control protein with the fluorophore. We, therefore, reevaluated the choice of our assay format and decided to establish a new fluorescence polarization based assay.

By labeling the protein rather than the inhibitor AR54, we envisioned that a large change in molecular weight should be observable if the labeled protein of interest was bound by an inhibitory compound immobilized to a well plate (*Figure 1*). As a label, we chose the luminescent $\text{Ru}(\text{bpy})_3$ complex due to its sufficiently long lifetime. The FP signal should decrease after competitive displacement of labeled MIA protein from immobilized AR54 by an inhibitory compound.

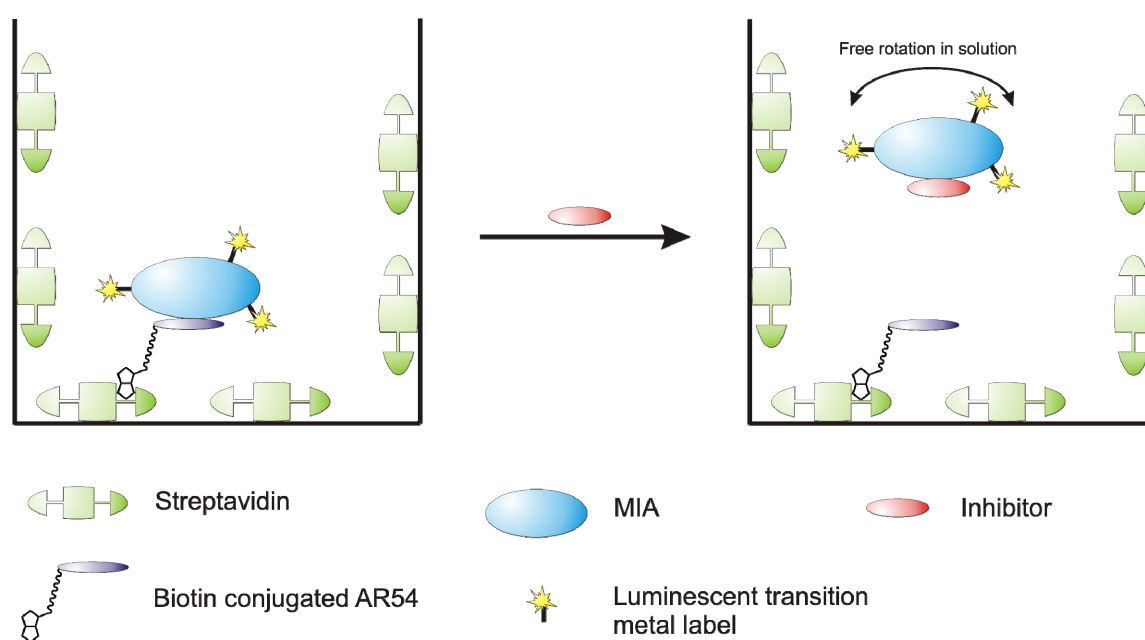


Figure 1: Concept of the FP assay using a luminescent transition metal complex as label

Binding of $\text{Ru}(\text{bpy})_3$ -labeled MIA protein to the immobilized inhibitory peptide AR54 leads to a large change in molecular weight resulting in a dramatic increase of the fluorescence polarization signal (left). After competitive displacement of labeled MIA protein from immobilized AR54 by an inhibitory compound (right) the FP signal decreases. The HTFP assay enables the performance of a high throughput screening of large substance libraries in search for a potent MIA protein inhibitor.

4.2.2 Functional activity of Ru(bpy)₃-labeled MIA protein

To ensure that the luminescent Ru(bpy)₃-label does not affect binding properties of MIA protein we performed Boyden Chamber invasion experiments, where Mel Im cells were treated with Ru(bpy)₃-labeled MIA protein and, in comparison, with unlabeled MIA protein. Non-modified MIA protein reduces cell invasion by about 40% to 50% in this *in vitro* model since MIA protein specifically interferes with attachment of melanoma cells to matrigel.⁷ Both MIA proteins, the unlabeled and the Ru(bpy)₃ labeled one behave identically revealing that Ru(bpy)₃-labeled MIA is functionally active (data not shown).

4.2.3 Heterogeneous Transition metal based Fluorescence Polarization (HTFP) assay results

4.2.3.1 Binding of MIA-Ru(bpy)₃ to AR54, 30 kDa and 70 kDa fibronectin fragments

First, we measured the FP signal of MIA-Ru(bpy)₃ in a well coated with AR54-Biotin compared to an uncoated well. The significant increase in FP in the well coated with AR54-Biotin was attributed to the severely restricted rotational mobility of MIA-Ru(bpy)₃ bound to the immobilized AR54-Biotin (*Figure 2*). In order to assess whether we could displace MIA-Ru(bpy)₃ from the immobilized AR54-Biotin, we treated this complex with 7.8 μM AR54 in solution. In this case, the fluorescence polarization of MIA-Ru(bpy)₃ was almost identical to the MIA-Ru(bpy)₃ free in solution in a well not coated with AR54-Biotin. This demonstrates that the molecular mobility is unhindered and that the binding is reversible.

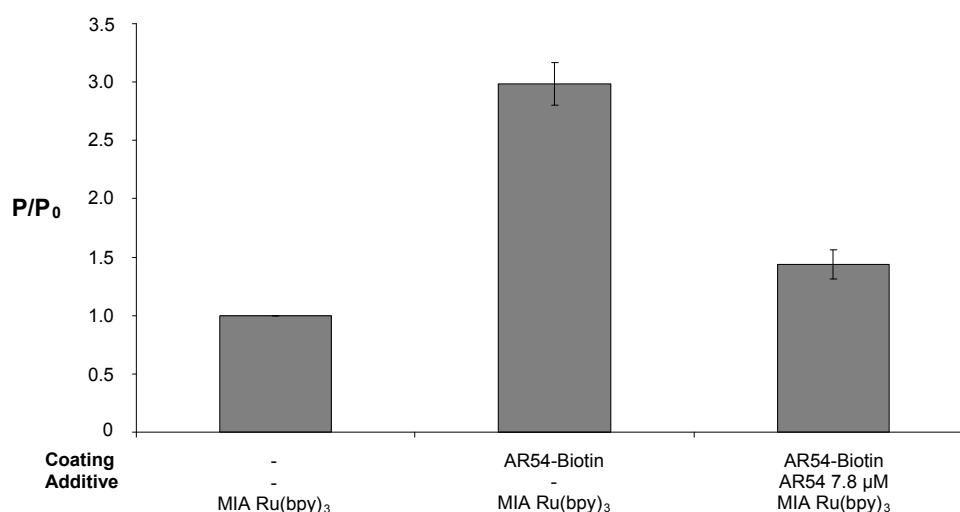


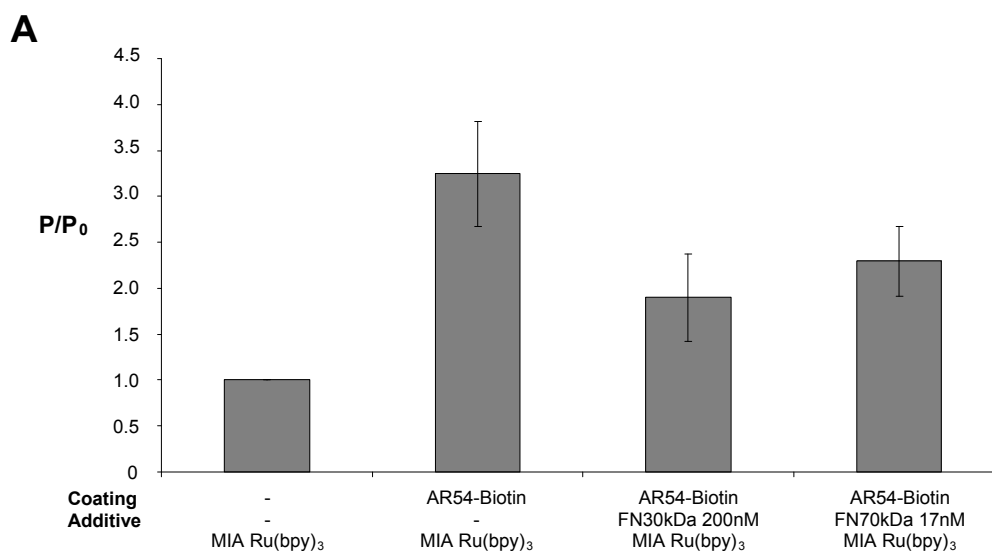
Figure 2: HTFP assay investigation of interaction of AR54 with MIA-Ru(bpy)₃

In the AR54-Biotin treated well, fluorescence polarization signal increases due to binding of Ru(bpy)₃-labeled MIA protein to immobilized AR54 peptide. After addition of AR54 at a final concentration of 7.8 μM

the detected fluorescence polarization of MIA-Ru(bpy)₃ is almost identical to the MIA-Ru(bpy)₃ free in solution in a well not coated with AR54-Biotin, demonstrating that after displacement from immobilized AR54-Biotin the molecular mobility is unhindered.

The interaction of MIA with fibronectin has been described.⁶ In order to test our assay concept with this known interaction partner, we applied 30 kDa and 70 kDa proteolytic fragments of human fibronectin shown in *Figure 3A*. As expected, the fluorescence polarization decreased upon addition of the fibronectin fragments. Hence, we have validated our HTFP assay with the known interactions of MIA protein with AR54 and fibronectin and demonstrate that this assay concept is capable of detecting protein interactions with a small peptide as well as a 70 kDa protein.

Additionally, we have performed a titration of MIA-Ru(bpy)₃ with 30 kDa fibronectin fragment to demonstrate that our assay is also capable of determining binding constants. As presented in *Figure 3B*, we determined a K_d value of 33 nM. The failure of all the alternatives as described before led us to conclude that our assay should be beneficial for investigating proteins prone to multimerization. Obviously aggregation can lead to artifacts in other binding experiments while our assay format circumvents this problem due to the long lifetime of the luminescent label.



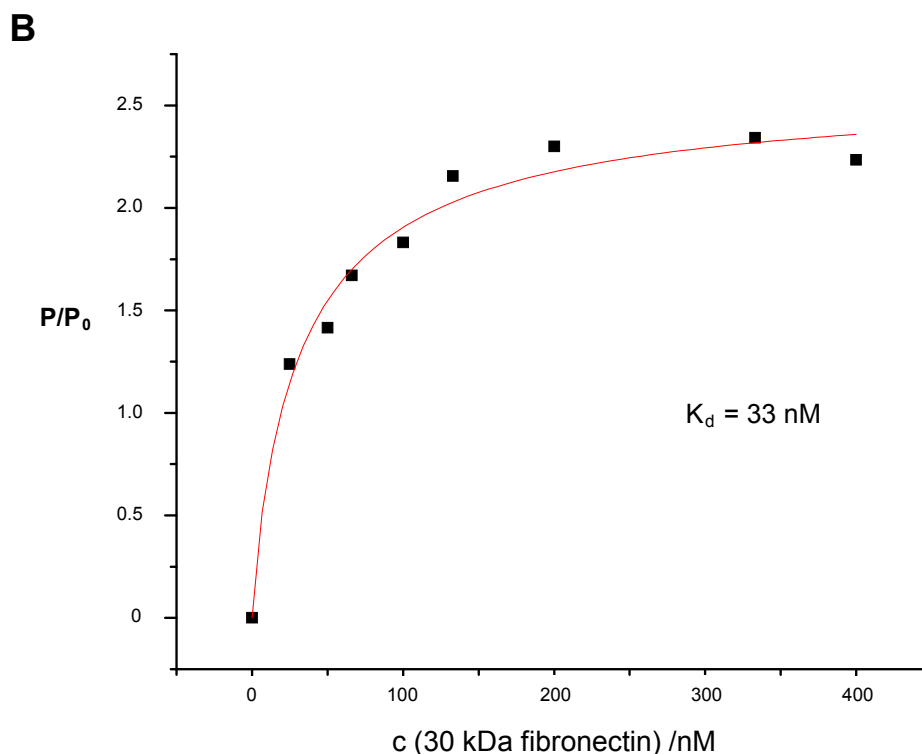


Figure 3: HTFP assay investigation of interaction of 30 kDa and 70 kDa fibronectin fragments with MIA-Ru-(bpy)₃ (A) 30 kDa and 70 kDa proteolytic fragments of human fibronectin, known to interact with MIA protein, were applied in the HTFP assay. The fluorescence polarization signal decreases, indicating a displacement of MIA protein from AR54-Biotin. (B) Titration of MIA-Ru(bpy)₃ with 30 kDa human proteolytic fibronectin fragment. The observed K_d is 33 nM. All experiments were performed in triplicates.

4.2.3.2 Buffer additives and detergent controls

We envisioned this system to act as a screening platform for the identification of potential MIA protein inhibitors and further applications. Accordingly, we investigated the influence of various buffer additives and detergents commonly used in molecular biology. As expected, the addition of 0.1% Triton X-100 or 0.1% 2-mercaptoethanol disrupted the interaction of MIA-Ru(bpy)₃ and AR54-Biotin (data not shown). While DMSO, which is often used in inhibitor screening for dissolving compound libraries, could be tolerated for concentrations of up to 2.5%, the addition of 50 mM EDTA induced to a significant decrease in FP signal (data not shown). This can be explained by a photoinduced redox reaction involving the luminescent label Ru(bpy)₃ and EDTA.²³ A similar decrease was also observed in the absence of AR54-Biotin, further indicating such an interaction.

4.3.2.3 Multimerization studies

Considering the aggregation of MIA protein, we explored the capabilities of the HTFP assay to investigate this phenomenon (Figure 4A). The addition of an excess of unlabeled MIA protein to MIA-Ru(bpy)₃ proves that the size of the multimers does not change and

that there are no aggregates consisting of about ten or more molecules. We estimate this from the lifetime of the label and the molecular weight of the protein by the Perrin equation.²⁴ To prove the existence of smaller aggregates, we coated wells with a MIA-Biotin conjugate. Indeed, a large increase in fluorescence polarization was detected, indicating the presence of direct MIA-MIA interactions. The formation of multimeric structures of MIA protein was also confirmed by Western blot analysis as shown in *Figure 4B*. These aggregates appear to be extraordinarily stable since they can even be observed after treatment with denaturing and reducing Laemmli buffer at 70°C.

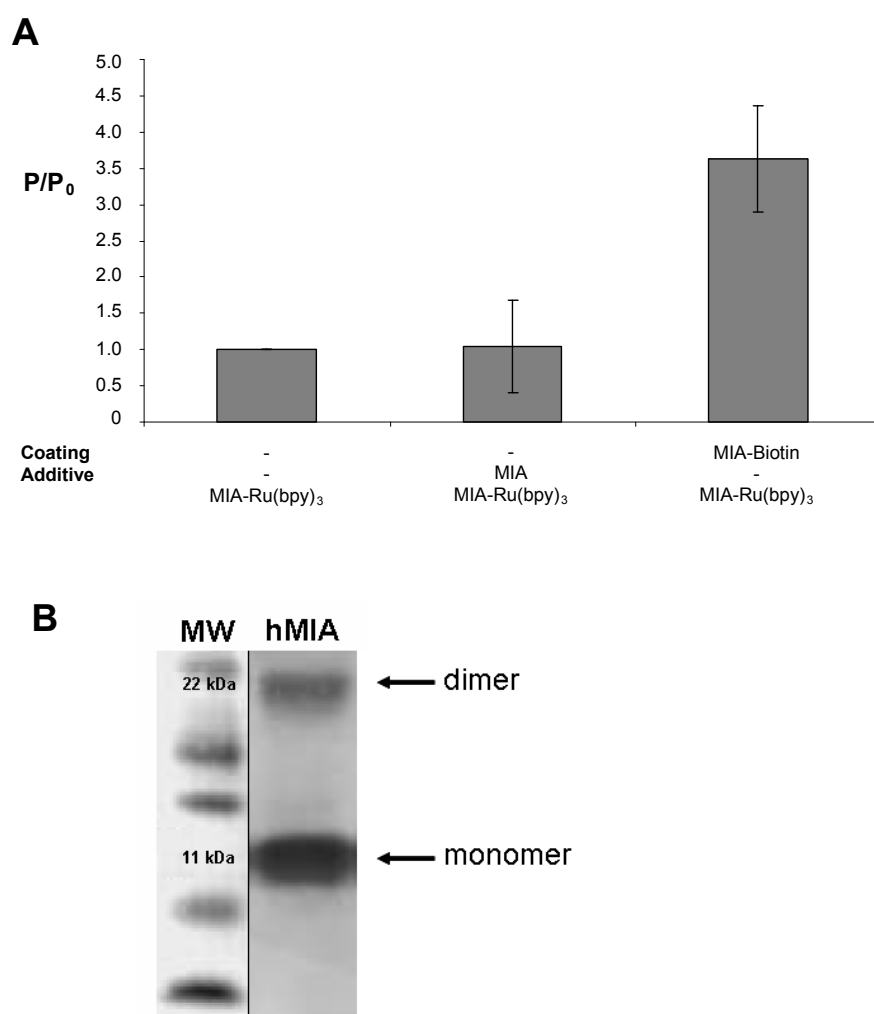


Figure 4: HTFP assay investigation of MIA protein aggregation

(A) Analysis of MIA aggregation was performed under physiological conditions using DPBS buffer in an AR54-uncoated well. The addition of an excess of unlabeled MIA protein proves that there are no aggregates formed consisting of about ten or more molecules, as estimated from the lifetime of the label and the molecular weight of the protein. We then coated wells with a MIA-Biotin conjugate to prove the existence of smaller aggregates and observed a large increase in fluorescence polarization, indicating the formation of such smaller aggregates. **(B)** As also demonstrated by Western blot analysis, 11 kDa MIA protein forms multimeric structures that seem to be extraordinarily stable since they can not be degraded after treatment with denaturing and reducing Laemmli buffer at 70°C for 10 min. All experiments were performed in triplicates.

4.3 Discussion

Several methods have been developed for the investigation of protein interactions. While surface plasmon resonance (SPR)²⁵ can also be used for small molecule interactions with the help of antibodies, it is still costly due to the usually proprietary chips. Far-Western blotting is time consuming and also not suitable for high throughput applications.²⁶ Furthermore, this method relies on the refolding of the protein to the native conformation on the membrane, which may not always be successful. Immunoprecipitation and pull-down experiments are equally far more time-consuming than fluorescence based investigations.²⁷ Binding experiments using the 1-anilino-8-naphthalene sulfonate (ANS) probe,²⁸ while well-plate compatible, suffer from the short excitation and emission wavelengths. Automated isothermal calorimetry (ITC) measurements offer the advantage of label-free detection, but still require relatively large amounts of substance.

Methods capable of handling high throughput screenings include various types of microarrays using enzymes, isotopes or fluorescent labels. However, these techniques require special safety precautions, antibodies and washing steps which may lead to cross-contamination and other artifacts.

Fluorescence polarization detection is both high throughput capable and self-referenced, meaning that no washing steps are required. This is clearly an advantage over the traditional ELISA concept. However, traditional homogeneous FP assays are limited by the molecular weight of the interaction partner to be investigated due to the short lifetime of the required organic fluorophores. We extend this range by immobilizing a known interaction partner of MIA protein and labeling of MIA protein with a luminescent transition metal chelate. This would not be possible in an assay conducted entirely in solution due to the long lifetime. The maximum acceptable molecular weight of the interaction partner obviously depends on the decay time of the label on the target. Given the decay time of Ru(bpy)₃, we estimate from the Perrin equation²⁴ that interactions with binding partners of up to 500 kDa should still be observable, however, that limit could be raised by using a transition metal with a longer decay time. A further limitation of our assay is the fact that it will be difficult to estimate aggregate sizes from the polarization values due to the long decay time.

The results show that our HTFP assay allows the investigation of protein/small molecule as well as protein/protein interactions. As presented for the interaction of MIA protein with AR54, this FP assay should also be amenable for the screening of libraries of potential drug candidates. Furthermore, the long lifetime of the luminescent transition metal

complex label also allows the identification of proteins interacting with other proteins. Additionally, our HTFP assay is also suitable for the investigation of protein aggregation and compounds cleaving these aggregates. In contrast to traditional homogeneous FP assays, interactions with both high and low molecular weight compounds can be investigated. This makes it especially useful for proteins prone to forming multimeric structures. This tolerance of the HTFP assay for aggregation makes it unique and should allow the investigation of proteins which show aggregation-related artifacts in other assays. Since our assay format is variously applicable it is conceivable that it also might be used for many different analytical or diagnostic applications. It enables the investigation of protein complexes for example for cell signaling molecules, transport proteins or transcription factors. It could also be used for the identification of an initiator or regulator of polymerization reactions for instance for actin or tubulin subunits as existing in dynamic processes of the cytoskeleton. This assay may also serve for the identification of activators or co-activators for enzymatic reactions as well as for the design of immunoassays in the field of serology and diagnostic. Since the HTFP assay is based on a luminescent transition metal complex label our assay benefits from all the associated advantages over organic fluorophores. While the inherent photostability is obviously convenient, the large Stokes shift increases the signal to noise ratio and allows a broader selection of suitable emission filters for the spectrometer. Furthermore, the long lifetime of transition metal complex labels also opens the possibility of time-gated measurements. This may be employed for multi-label experiments with different transition metal complexes with different lifetimes which may be resolved regardless of spectral overlap. Complex biological matrices in the samples are also tolerable since the autofluorescence of biological material has a very short lifetime and can thus be eliminated.

4.4 Materials and Methods

Cell lines and cell culture conditions

The melanoma cell line Mel Im, established from a human metastatic tumor sample (generous gift from Dr. Johnson, University of Munich, Germany), was used in Boyden Chamber invasion experiments. Cells were maintained in DMEM (PAA Laboratories GmbH, Austria) supplemented with penicillin (400 U/mL), streptomycin (50 µg/mL), l-glutamine (300 µg/mL) and 10% fetal calf serum (Pan Biotech GmbH, Germany) and split in 1:5 ratio every three days.

Boyden Chamber Invasion Assay

Invasion assays were performed in Boyden Chambers containing polycarbonate filters with 8 μm pore size (Neuro Probe, Gaithersburg, MD, USA) essentially as described previously.²⁹ Filters were coated with matrigel, a commercially available reconstituted basement membrane (diluted 1:3 in H_2O ; BD Bioscience, Bradford, MA, USA). The lower compartment was filled with fibroblast-conditioned medium used as a chemo attractant. Mel Im melanoma cells were harvested by trypsinization for 2 min, resuspended in DMEM without FCS at a density 2.5×10^4 cells/mL, and placed in the upper compartment of the chamber. Except for the control experiment with untreated cells and experiments where cells were only treated with the peptide, MIA protein or $\text{Ru}(\text{bpy})_3$ -labelled MIA protein, respectively, was added to the cell suspension at a final concentration of 200 ng/mL. Peptide AR54 (sequence: NSLLVSFQPPRAR) was used at a final concentration of 1 μM . After incubation at 37°C for 4 h filters were removed. Cells adhering to the lower surface of the filter were fixed, stained, and counted. Experiments were carried out in triplicates and repeated at least three times.

Protein analysis in vitro (Western blotting)

MIA protein was denaturated at 70°C for 10 min after addition of reducing and denaturing Roti-Load buffer (Roth, Karlsruhe, Germany) and subsequently separated on sodium dodecyl sulfate 12.75% polyacrylamid gels (SDS-PAGE) (Invitrogen, Groningen, The Netherlands). After transferring the proteins onto a polyvinylidene fluoride (PVDF) membrane (BioRad, Richmond, VA, USA), the membrane was blocked using 3% BSA/PBS for 1 h at RT and incubated with a 1:150 dilution of primary polyclonal rabbit anti MIA antibody (Biogenes, Berlin, Germany) in 3% BSA/PBS overnight at 4°C. After washing in PBS the membrane was incubated with a 1:2000 dilution of an alkaline-phosphate coupled secondary antibody (Chemikon, Hofheim, Germany) for 2 h at RT. Finally, after washing steps, immunoreactions were visualized by nitro blue tetrazolium/5-bromo-4-chloro-3-indolyl phosphate (NBT/BCIP) (Invitrogen, CA, USA) staining.

Luminescent labeling of human MIA protein

Human MIA protein (100 μg) was labeled with $\text{Ru}(\text{bpy})_3$ -isothiocyanate (1 mg) (Active Motif Chromeon, Germany) in 640 μL bicarbonate buffer pH 9.3 supplemented with 200 μL DMSO required for dissolving the dye. After 50 min, the reaction mixture was

purified on a size exclusion column (SephadexTM G-25 M PD-10 Desalting column, Amersham Pharmacia Biotech, Sweden) and samples of the collected fractions as well as a dilution series of unlabeled MIA protein were analyzed by Western blotting as described above.

Biotin conjugation of peptide AR54

0.25 mg of AR54 was dissolved in 30 μ L of bicarbonate buffer pH 9.3. After addition of 0.38 mg Biotin-NHS (Calbiochem, USA) in 10 μ L DMSO the reaction mixture was incubated overnight at 4°C. As the NHS-ester was expected to be completely reacted or hydrolyzed, no purification was carried out.

Coating of well plates with AR54-Biotin and MIA-Biotin

Black streptavidin coated 96 well plates (Greiner Bio-one, Germany) with a loading of 20 pmol streptavidin per well were treated with 20 equivalents AR54-Biotin per mol of (tetrameric) streptavidin in PBS pH 7.4. An uncoated control lane was sealed with adhesive film to prevent contamination with AR54-Biotin. After addition of AR54-Biotin, the entire plate was sealed with adhesive film and incubated for 3 h under agitation. The coated lanes were washed five times with PBS pH 7.4 before being air-dried and sealed with adhesive film which was removed only immediately before use of each lane.

MIA-Biotin was prepared as previously reported ⁶ and used for treating a well plate as described above, except that the plate was not dried and used for measurements immediately.

Polarization assay setup

All measurements were performed at room temperature on a Polarstar Optima microplate reader (BMG Labtech, Germany). A 390-10 nm bandpass filter was used for excitation while a 520 nm longpass filter was used for the emission light. Even though the extinction coefficient is higher at longer wavelengths, we chose a shorter excitation wavelength as this led to higher polarization values. A MIA-Ru(bpy)₃ concentration of 55 fM was used in all experiments. A solution volume of 250 μ L per well was found to give a low standard deviation with high signal intensity. Unless otherwise indicated, all measurements were performed in DPBS without calcium or magnesium (PAN Biotech GmbH, Germany). Addition of components to the wells was done in the following order: interaction partner, buffer, MIA-Ru(bpy)₃. Owing to different reaction kinetics, measurements were performed

every 5 min over a 30 min period. Polarization values are reported relative (P/P_0) to the value of free MIA-Ru(bpy)₃ in solution in a well not treated with AR54-Biotin. All reported values are an average of three independent measurements.

4.5 Acknowledgement

We thank Peter Oefner and the Center of Excellence for Fluorescent Bioanalytics for providing access to the Polarstar microplate reader and Jörg Plümpe (Active Motif Chromeon) for the generous gift of the Ru(bpy)₃-isothiocyanate dye. This work was supported by the University of Regensburg and a grant from the DFG (Deutsche Forschungsgemeinschaft).

4.6 References

1. Bosserhoff, A. K.; Kaufmann, M.; Kaluza, B.; Bartke, I.; Zirngibl, H.; Hein, R.; Stolz, W.; Buettner, R., Melanoma-inhibiting activity, a novel serum marker for progression of malignant melanoma. *Cancer Res* **1997**, 57, (15), 3149-53.
2. Bosserhoff, A. K.; Buettner, R., Establishing the protein MIA (melanoma inhibitory activity) as a marker for chondrocyte differentiation. *Biomaterials* **2003**, 24, (19), 3229-34.
3. Dreau, D.; Bosserhoff, A. K.; White, R. L.; Buettner, R.; Holder, W. D., Melanoma-inhibitory activity protein concentrations in blood of melanoma patients treated with immunotherapy. *Oncol Res* **1999**, 11, (1), 55-61.
4. Stahlecker, J.; Gauger, A.; Bosserhoff, A.; Buettner, R.; Ring, J.; Hein, R., MIA as a reliable tumor marker in the serum of patients with malignant melanoma. *Anticancer Res* **2000**, 20, (6D), 5041-4.
5. Bosserhoff, A. K.; Buettner, R., Expression, function and clinical relevance of MIA (melanoma inhibitory activity). *Histol Histopathol* **2002**, 17, (1), 289-300.
6. Bauer, R.; Humphries, M.; Fassler, R.; Winklmeier, A.; Craig, S. E.; Bosserhoff, A. K., Regulation of integrin activity by MIA. *J Biol Chem* **2006**, 281, (17), 11669-77.
7. Bosserhoff, A. K.; Stoll, R.; Sleeman, J. P.; Bataille, F.; Buettner, R.; Holak, T. A., Active detachment involves inhibition of cell-matrix contacts of malignant melanoma cells by secretion of melanoma inhibitory activity. *Lab Invest* **2003**, 83, (11), 1583-94.
8. Stoll, R.; Renner, C.; Zweckstetter, M.; Bruggert, M.; Ambrosius, D.; Palme, S.; Engh, R. A.; Golob, M.; Breibach, I.; Buettner, R.; Voelter, W.; Holak, T. A.;

- Bosserhoff, A. K., The extracellular human melanoma inhibitory activity (MIA) protein adopts an SH3 domain-like fold. *EMBO J* **2001**, 20, (3), 340-9.
9. Durkop, A.; Lehmann, F.; Wolfbeis, O. S., Polarization immunoassays using reactive ruthenium metal-ligand complexes as luminescent labels. *Anal Bioanal Chem* **2002**, 372, (5-6), 688-94.
 10. Guo, X. Q.; Castellano, F. N.; Li, L.; Lakowicz, J. R., A long-lifetime Ru(II) metal-ligand complex as a membrane probe. *Biophys Chem* **1998**, 71, (1), 51-62.
 11. Szmecinski, H.; Castellano, F. N.; Terpetschnig, E.; Dattelbaum, J. D.; Lakowicz, J. R.; Meyer, G. J., Long-lifetime Ru(II) complexes for the measurement of high molecular weight protein hydrodynamics. *Biochim Biophys Acta* **1998**, 1383, (1), 151-9.
 12. Guo, X. Q.; Castellano, F. N.; Li, L.; Lakowicz, J. R., Use of a long-lifetime Re(I) complex in fluorescence polarization immunoassays of high-molecular-weight analytes. *Anal Chem* **1998**, 70, (3), 632-7.
 13. Terpetschnig, E.; Dattelbaum, J. D.; Szmecinski, H.; Lakowicz, J. R., Synthesis and spectral characterization of a thiol-reactive long-lifetime Ru(II) complex. *Anal Biochem* **1997**, 251, (2), 241-5.
 14. Terpetschnig, E.; Szmecinski, H.; Lakowicz, J. R., Fluorescence polarization immunoassay of a high-molecular-weight antigen using a long wavelength-absorbing and laser diode-excitable metal-ligand complex. *Anal Biochem* **1996**, 240, (1), 54-9.
 15. Szmecinski, H.; Terpetschnig, E.; Lakowicz, J. R., Synthesis and evaluation of Ru-complexes as anisotropy probes for protein hydrodynamics and immunoassays of high-molecular-weight antigens. *Biophys Chem* **1996**, 62, (1-3), 109-20.
 16. Terpetschnig, E.; Szmecinski, H.; Malak, H.; Lakowicz, J. R., Metal-ligand complexes as a new class of long-lived fluorophores for protein hydrodynamics. *Biophys J* **1995**, 68, (1), 342-50.
 17. Terpetschnig, E.; Szmecinski, H.; Lakowicz, J. R., Fluorescence polarization immunoassay of a high-molecular-weight antigen based on a long-lifetime Ru-ligand complex. *Anal Biochem* **1995**, 227, (1), 140-7.
 18. Nasir, M. S.; Jolley, M. E., Fluorescence polarization: an analytical tool for immunoassay and drug discovery. *Comb Chem High Throughput Screen* **1999**, 2, (4), 177-90.

19. Hun, X.; Zhang, Z., Fluoroimmunoassay for tumor necrosis factor- α in human serum using Ru(bpy)₃Cl₂-doped fluorescent silica nanoparticles as labels. *Talanta* **2007**, 73, (2), 366-71.
20. Sanchez-Martinez, M. L.; Aguilar-Caballos, M. P.; Gomez-Hens, A., Long-wavelength fluorescence polarization immunoassay: determination of amikacin on solid surface and gliadins in solution. *Anal Chem* **2007**, 79, (19), 7424-30.
21. Sanchez-Martinez, M. L.; Aguilar-Caballos, M. P.; Eremin, S. A.; Gomez-Hens, A., Long-wavelength fluorescence polarization immunoassay for surfactant determination. *Talanta* **2007**, 72, (1), 243-8.
22. Schmidt, J.; Bosserhoff, A. K., Processing of MIA protein during melanoma cell migration. *Int J Cancer* **2009**, 125, (7), 1587-94.
23. Ismail, K. Z.; Weber, S. G., Tris(2,2'-bipyridine)ruthenium (II) as a peroxide-producing replacement for enzymes as chemical labels. *Biosens Bioelectron* **1991**, 6, (8), 699-705.
24. Lakowicz, J. R., *Principles of fluorescence spectroscopy*. Springer Science + Business Media LLC: New York, 2006.
25. Myszka, D. G., Analysis of small-molecule interactions using Biacore S51 technology. *Anal Biochem* **2004**, 329, (2), 316-23.
26. Wu, Y.; Li, Q.; Chen, X. Z., Detecting protein-protein interactions by Far western blotting. *Nat Protoc* **2007**, 2, (12), 3278-84.
27. Arany, I.; Faisal, A.; Nagamine, Y.; Safirstein, R. L., p66shc inhibits pro-survival epidermal growth factor receptor/ERK signaling during severe oxidative stress in mouse renal proximal tubule cells. *J Biol Chem* **2008**, 283, (10), 6110-7.
28. Gasymov, O. K.; Glasgow, B. J., ANS fluorescence: potential to augment the identification of the external binding sites of proteins. *Biochim Biophys Acta* **2007**, 1774, (3), 403-11.
29. Stoll, R.; Lodermeier, S.; Bosserhoff, A. K., Detailed analysis of MIA protein by mutagenesis. *Biol Chem* **2006**, 387, (12), 1601-6.

5 Dissociation of Functionally Active MIA Dimers by Dodecapeptide AR71 Strongly Reduces Formation of Metastases in Malignant Melanoma

Abstract

Melanoma inhibitory activity (MIA) protein, secreted by malignant melanoma cells, strongly supports formation of metastases through inhibiting cell-matrix interactions. Here, we present the molecular mechanism of MIA action and a way of inhibiting its activity. In contrast to previous hypotheses, our results revealed that MIA acts as a dimer to reach functional activity. Based on this new finding, we screened peptides for their ability to inhibit MIA-MIA interaction, resulting in the identification of dodecapeptide AR71. NMR spectroscopy confirmed its binding to the dimerization domain while functional analysis *in vitro* revealed complete inhibition of MIA function. Crucially, injecting AR71 *i.v.* into a mouse model of melanoma metastases led to strong reduction of the formation of metastases *in vivo*. These findings provide an excellent basis for rationally designing a novel pharmacophore which inhibits MIA dimerization and activity, strongly reduces formation of metastases and thus could provide an effective therapy for malignant melanoma.

The results of this chapter have been submitted for publication:

Schmidt, J., Riechers, A., Stoll, R., Amann, T., Fink, F., Hellerbrand, C., Gronwald, W., König, B., Bosserhoff, A. K.; Dissociation of Functionally Active MIA Dimers by Dodecapeptide AR71 Strongly Reduces Formation of Metastases in Malignant Melanoma. *Nat Med* **2010**

Author Contributions:

I focused on protein analysis, immune fluorescence studies, evaluation of histological sections as well as cell culture experiments and cloning. A. Riechers has performed Western blot analysis and all HTFP assay measurements. R. Stoll has conducted the NMR protein binding studies. T. Amann and C. Hellerbrand have helped conducting the animal experiments. F. Fink and W. Gronwald have designed the dimer model. B. König and A. K. Bosserhoff have been supervising this project.

5.1 Introduction

Malignant melanoma is characterized by aggressive local growth and early formation of metastasis. In order to identify autocrine growth-regulatory factors secreted by melanoma cells, melanoma inhibitory activity (MIA), an 11 kDa protein, strongly expressed and secreted by melanocytic tumor cells was purified from tissue culture supernatant of the human melanoma cell line HTZ-19.¹⁻² Today it serves as a reliable clinical serum tumor marker for detection of metastatic diseases and monitoring therapy responses of patients suffering from malignant melanoma. In addition, MIA plays an important functional role in melanoma development and cell invasion as its expression levels directly correlate with the capability of melanoma cells to form metastases in syngeneic animals.³⁻⁵

After transcription, MIA mRNA is translated into a 131 amino acid precursor molecule and processed into a mature protein consisting of 107 amino acids after cleavage of the secretion signal sequence.² The transport of MIA protein to the cell rear is induced after migratory stimuli.⁶ Following secretion, MIA subsequently binds to cell adhesion receptors integrin $\alpha_4\beta_1$ and integrin $\alpha_5\beta_1$. In addition, MIA masks their binding sites at ECM molecules including fibronectin, laminin and tenascin.^{3, 7} Consequently, cell adhesion contacts are reduced, enabling tumor cells to migrate and invade into healthy tissue, resulting in enhanced metastatic potential.

Previously, the three-dimensional structure of MIA protein was solved by multidimensional nuclear magnetic resonance (NMR) spectroscopy and X-ray crystallography techniques.⁸⁻¹² Corresponding data indicated that MIA defines a novel type of secreted protein comprising an SH3 domain like fold.

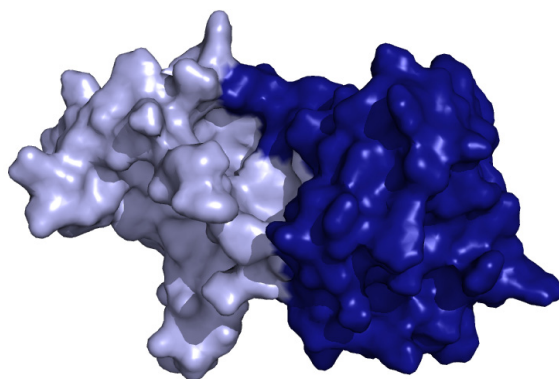
In the present study we aimed to determine the so far unknown molecular mechanism of MIA. By functionally analyzing MIA mutants we demonstrate for the first time that MIA achieves functional activity by self assembly. Peptidic dimerization inhibitors were identified and analyzed in *in vitro* and *in vivo* studies, thus providing an excellent starting point for the development of a new inhibitory strategy. Based on these new data presented here, the rational design and development of a novel pharmacophore which inhibits MIA and thus strongly reduces tumor cell invasion and formation of metastases could provide a key element in malignant melanoma therapy.

5.2 Results

5.2.1 MIA protein is functionally active as a dimer

Although MIA was thought to act as a monomer, recent data suggests that, as detailed below, the active form of the protein consists of a dimer. Using the PreBI modeling software (<http://pre-s.protein.osaka-u.ac.jp/prebi/>) for the prediction of the putative dimer interface together with the HADDOCK protein-protein docking program, we obtained a model of the MIA dimer comprising a head to tail linkage (*Figure 1A*).¹³ The dimerization interfaces are located around Y30 and at the region K53-L58 in the n-Src loop and the cleft next to Q65-A73 in the distal loop. Further supporting our results, the regions determined to form the interface have been described as crucial for functional activity in a previous mutagenesis study.¹⁴ In addition, Western blot analysis of MIA also demonstrates that apart from the monomeric species dimers exist.¹⁵ We, therefore, aimed to investigate the physiological relevance of MIA dimers and the possible correlation between dimerization and functional activity. Having identified the most likely positions of the dimerization interfaces, mutants of MIA were tested for their capability to form dimers by Western blot analysis (*Figure 1B*). MIA mutants were expressed in an *in vitro* transcription/translation system. All mutants showed correct folding as evidenced by a MIA-ELISA and were selected as not carrying a mutation in the dimerization regions, apart from G61R.¹⁴ Recombinant wt MIA and all mutants clearly show a dimer band except for G61R. Interestingly, all mutants but G61R are functionally active in Boyden chamber invasion assays, as presented in *Figure 1C*. MIA wt (RTS) and mutants D29G/Y69H, V46F/S81P, T89P and K91N can exhibit this effect to the same extent while MIA mutant G61R completely loses activity. The sites of mutations not affecting functional activity (*Figure 1D*, depicted in grey) are located outside the dimerization regions, whereas G61R (*Figure 1D*, depicted in magenta) is buried in the dimerization cleft (depicted in red) in close proximity to the distal loop.

A



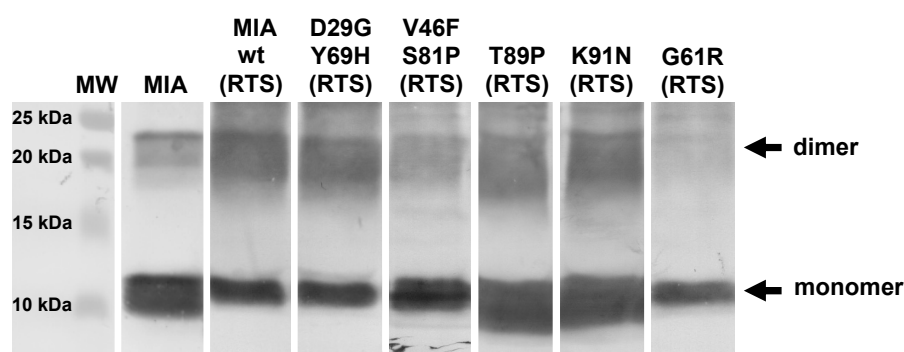
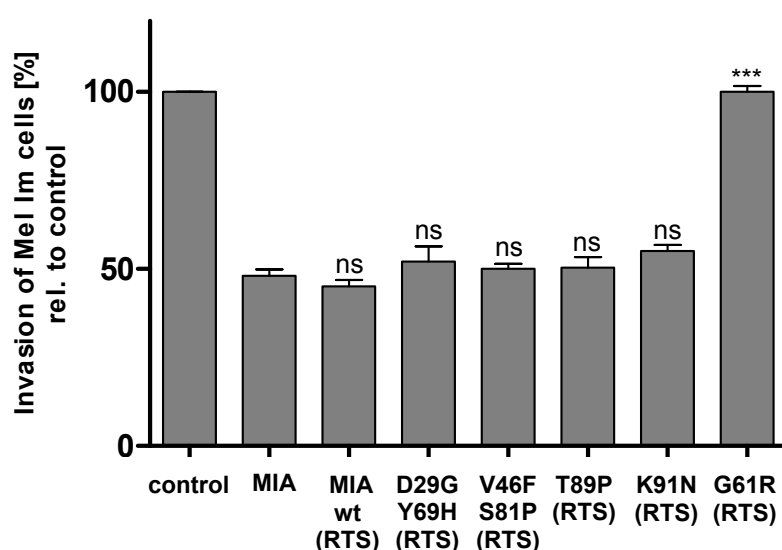
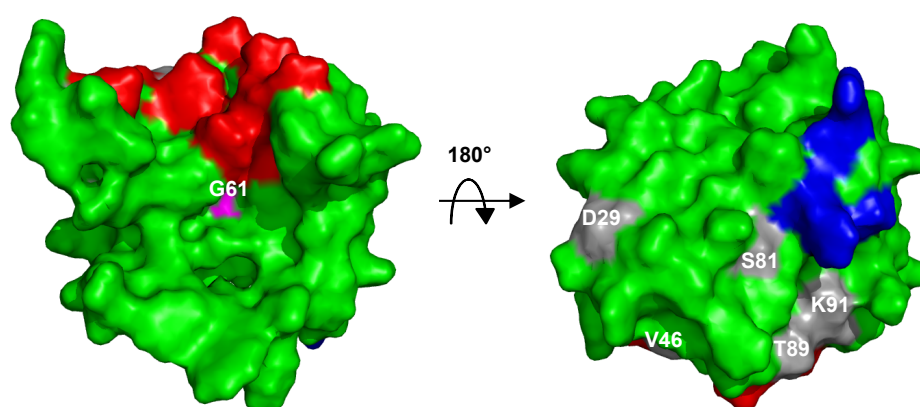
B**C****D**

Figure 1: MIA protein is functionally inactive as a monomer

(A) Structure of the MIA dimer according to shape complementarity analyses. The MIA dimer is characterized by a head-to-tail orientation, with the dimerization domains consisting of the n-Src loop and the cleft next to the distal loop. (B) Western blot analysis of MIA assessing their ability to form dimers. The first lane shows recombinant wt MIA, followed by the same protein in an unpurified RTS expression system (wt) and mutants D29G/Y69H, V46F/S81P, T89P, K91N and G61R. All homologues, except for G61R, clearly show a dimer band. (C) Correlation between dimerization and functional activity revealed that all MIA

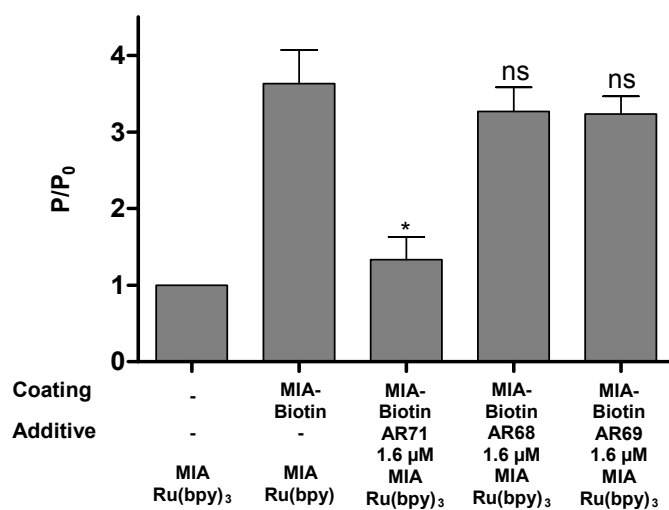
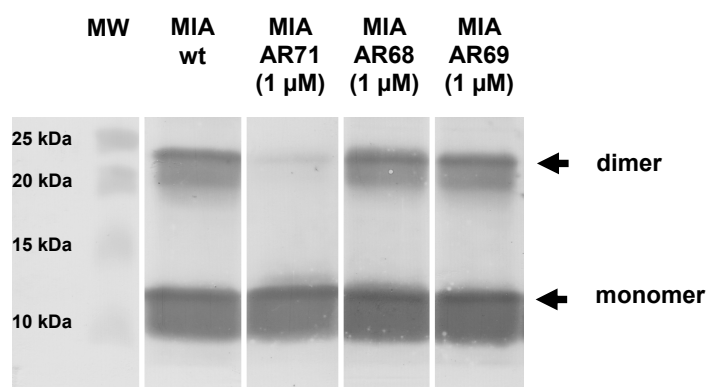
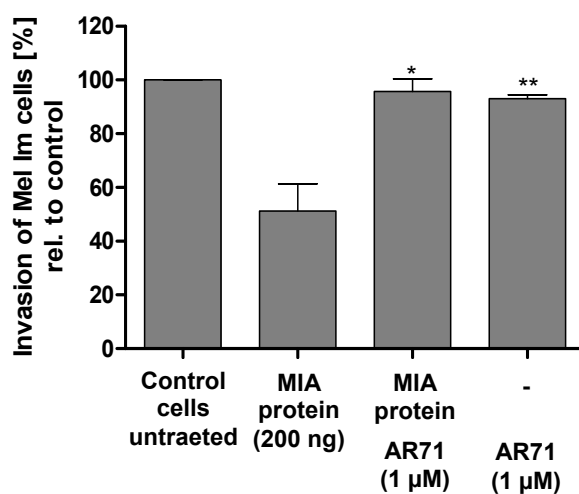
mutants capable to dimerize are functionally active in Boyden chamber invasion assays as reflected by a reduction in the number of invaded cells due to interference with cell adhesion. Mutant G61R, which does not form protein dimers does not show any MIA induced effect. **(D)** NMR structure of MIA showing the dimerization domains and the mutation sites. The dimerization domains in the n-Src loop and next to the distal loop are depicted in blue and red, respectively. Mutation sites which do not influence dimerization and functional activity are shown in grey and obviously lie outside the dimerization domains. The site of mutation G61R, which is in direct contact with the dimerization domain next to the distal loop, is shown in magenta. This figure was generated using PyMol (Delano, W. L., The PyMol Molecular Graphics System (2002) Delano Scientific, Palo Alto, CA, USA).

5.2.2 Peptide AR71 prevents MIA protein dimerization

We then aimed to identify peptides inhibiting MIA dimerization in a newly developed heterogeneous transition-metal based fluorescence polarization (HTFP) assay.¹⁵ First, MIA-MIA interaction was confirmed using this assay. Here, we immobilized a MIA-biotin conjugate in a streptavidin-coated well plate and added MIA labelled with the luminescent transition-metal complex Ru(bpy)₃. As depicted in *Figure 2A*, a significant increase in FP signal in the wells coated with MIA-biotin was observed compared to control wells not functionalized with MIA-biotin. This was attributed to the severely restricted rotational mobility of MIA-Ru(bpy)₃ bound to the immobilized MIA-biotin.

We then screened peptides, previously identified by phage display and known to generally bind to MIA¹¹, for their potential to prevent MIA dimerization and induce dissociation of already existing protein dimers using the HTFP assay. As shown in *Figure 2A*, peptide AR71 (sequence: Ac-FHWRYPLPLPGQ-NH₂) was found to be particularly potent in dissociating MIA dimers which led to a decrease in FP signal due to increased rotational diffusion of the dissociated monomeric MIA-Ru(bpy)₃. This effect of AR71 was confirmed by Western Blot analysis (*Figure 2B*). Preincubation of MIA with 1 µM peptide AR71 leads to a strong reduction of the dimer bands compared to the control lane or other MIA-binding peptides used (AR68, AR69).

To prove that AR71 functionally inhibits MIA, Boyden chamber invasion assays were performed (*Figure 2C*). In these *in vitro* experiments, MIA interferes with the attachment of cells to matrigel, as reflected by a decrease in cell invasion. After external treatment with MIA, invasion of Mel Im cells is significantly reduced about 40% to 50% compared to untreated control cells. Pre-incubation of MIA with the inhibitory peptide AR71 results in a complete neutralization of the effect caused by MIA, as reflected in the number of invaded cells. Treatment of cells with peptide AR71 alone does not influence the migratory behaviour of melanoma cells.

A**B****C****Figure 2: Peptide AR71 prevents MIA dimerization**

(A) Heterogeneous transition-metal based fluorescence polarization (HTFP) assay for probing AR71 for its ability to directly interfere with MIA-MIA interaction. In the control lanes the FP signal of MIA- Ru(bpy)_3

was measured in a well coated with MIA-biotin compared to an uncoated well. The significant increase in FP in the well coated with MIA-biotin indicates binding of MIA-Ru(bpy)₃ to the immobilized MIA-biotin. The binding of MIA-inhibitory compound AR71 promotes dissociation of MIA dimers and displaces the surface-bound MIA-Ru(bpy)₃, as reflected by a decrease in fluorescence polarization signal. Peptides AR68 and AR69, also derived from phage display, do not interfere with MIA-MIA interaction. **(B)** Western Blot analysis of MIA incubated with 1 μ M AR71 demonstrates peptide-induced dissociation of the dimer, as deduced by a strong reduction of the dimer bands compared to the control lane. MIA-binding peptides AR68 and AR69 do not lead to reduced dimer formation. **(C)** Boyden chamber invasion assays using the human melanoma cell line Mel Im indicate that AR71 almost completely inhibits MIA activity. Interference of MIA with cell attachment to matrigel results in a decrease in cell invasion; after external treatment with MIA invasion of Mel Im cells is significantly reduced about 40% to 50% compared to untreated control cells. Pre-incubation of MIA with the respective inhibitory peptide results in a complete neutralization of the MIA effect. The two control lanes confirm that AR71 alone does not influence the migratory behaviour since exposure of cells to the peptide in absence of MIA does not alter the quantity of migrated cells.

5.2.3 MIA interacts with AR71

After demonstrating the potential of AR71 to inhibit MIA function in *in vitro* models, we could show by multidimensional NMR spectroscopy that MIA binds to this peptide ligand. In addition, the potential binding site of AR71 was identified using ¹⁵N labeled MIA and unlabeled peptide. By using increasing amounts of AR71 peptide, the induced chemical shift changes of the MIA ¹H^N and ¹⁵N^H resonances were classified according to the degree of the combined chemical shift perturbations. Further analysis of the solvent accessibility (with a threshold of 20 %) and cluster analysis of the residues effected by peptide binding reveals that the binding interface potentially comprises residues C17, S18, Y47, G66, D67, L76, W102, D103 and C106 of MIA (*Figure 3A*) It can therefore be assumed that the peptide predominantly binds to the binding site depicted on the left side of *Figure 3A*, whereas the opposite side of the molecule most probably does not participate in binding.

After stably transfecting B16 mouse melanoma cells with a secretion-signal containing AR71-HisTag construct (Sig-AR71-HisTag), we first analysed expression and localization of endogenous AR71-HisTag peptide. Co-staining of MIA protein and AR71-HisTag revealed a colocalization in close proximity to the nucleus. Immunofluorescence studies show the localization of MIA (*green, Figure 3Ba*) and AR71-HisTag (*for demonstrating colocalization with MIA, the red TRITC emission has been changed to yellow in this false-color illustration, Figure 3Bb*). The colocalization, depicted in red, is indicated by white arrows in *Figure 3Bc*. The excess of MIA not colocalized with AR71 is due to internalization of exogenous MIA protein by the melanoma cells.¹⁶ *Figure 3Bd* shows the corresponding mock control.

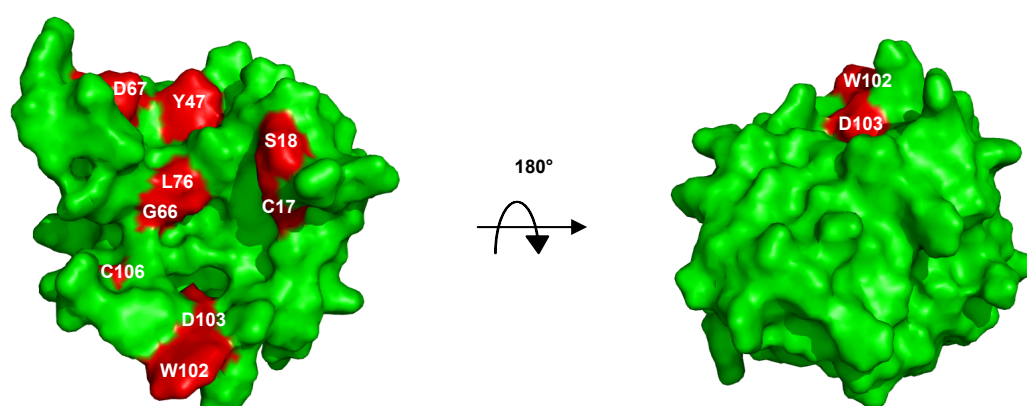
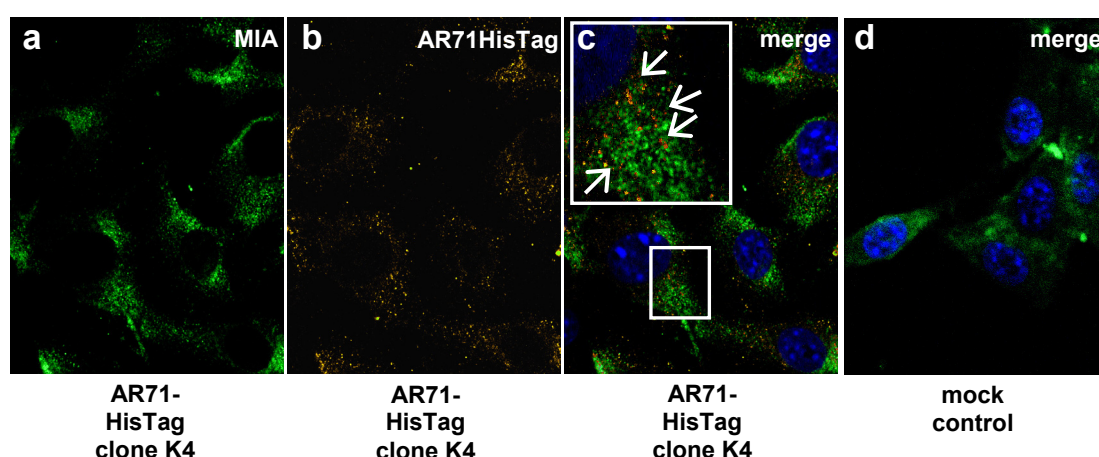
A**B**

Figure 3: Chemical shift differences of MIA upon titration with the dodecapeptide AR71

(A) Most significant chemical shift differences projected onto the van der Waals surface of MIA upon titration with the peptide AR71 are shown in red. The binding site is located in the dimerization domain next to the distal loop (compare Figure 1D). This figure was generated using PyMol (Delano, W. L., The PyMol Molecular Graphics System (2002) Delano Scientific, Palo Alto, CA, USA). (B) Immunofluorescence studies of murine B16 melanoma cells stably transfected with a (Sig)-AR71-HisTag construct. While a) shows MIA (FITC) and b) displays AR71-HisTag (TRITC with color changed from red to yellow for better visualization of colocalization), colocalization shown in red is indicated by white arrows in c). d) Corresponding mock control without AR71-HisTag.

5.2.4 Effect of MIA inhibitory peptide AR71 on formation of metastases *in vivo*

MIA expression levels of malignant melanoma cells strictly correlate with a highly invasive phenotype *in vitro* and *in vivo*.¹⁷⁻¹⁹ Further, *in vivo* studies have demonstrated the strong contribution of MIA for melanoma cell invasion and migration.⁴⁻⁵

In order to assess the ability of peptide AR71 to inhibit the formation of metastases by generating inactive MIA monomers *in vivo*, a previously developed metastasis assay was employed.²⁰ In this assay, melanoma cells metastasize from the primary tumor in the

spleen via the portal vein into the liver. Nine days after injection of the cells into the spleen, the mice were sacrificed, the livers were resected and tissue sections were prepared. Here, we used the stably transfected murine B16 melanoma cells with a Sig-AR71-HisTag containing construct. *In vitro* analysis by Boyden chamber assay confirmed that migration is drastically reduced in Sig-AR71-HisTag expressing cell clones compared to mock control cells (*Figure 4A*). The interference of AR71-HisTag with MIA-MIA interaction was also confirmed in the HTFP assay using wells coated with MIA-biotin (data not shown). Subsequently, a Sig-AR71-HisTag clone as well as a corresponding mock control was injected into the spleen of C57Bl6 mice, respectively. Histological analysis of haematoxylin and eosin stained liver sections revealed that mice being injected with Sig-AR71-HisTag clones comprised significantly fewer metastases than the mock control (*Figure 4B*). Four representative histological liver sections (hematoxylin and eosin stained) of mice injected with the B16 mock control or mice injected with the Sig-AR71-HisTag expressing cell clone, respectively, are shown in *Figure 4C*. Black arrows indicate the small metastases in the mock control which are exceedingly reduced in the liver of mice injected with the Sig-AR71-HisTag expressing cell clone. No adverse effects of AR71 on other organs and tissues were observed.

These results prompted us to investigate whether AR71 peptide could also reduce the formation of metastases when given as an *i.v.* administration treatment. Therefore, wild type murine B16 melanoma cells were injected into the spleen of C57Bl6 mice with the mice being subsequently treated with *i.v.* injections of AR71 (50 µg every 24 h). After nine days, the mice were sacrificed, the livers were resected and again tissue sections were prepared. Histological analyses revealed a significant reduction of the average number of metastases in the liver of mice treated with AR71 compared to the liver of untreated control mice, as shown in figure *Figure 4D*. Four representative histological liver sections (hematoxylin and eosin stained) of untreated and treated mice, respectively, are shown in *Figure 4E*. Again no adverse effects on other organs and tissues were observed.

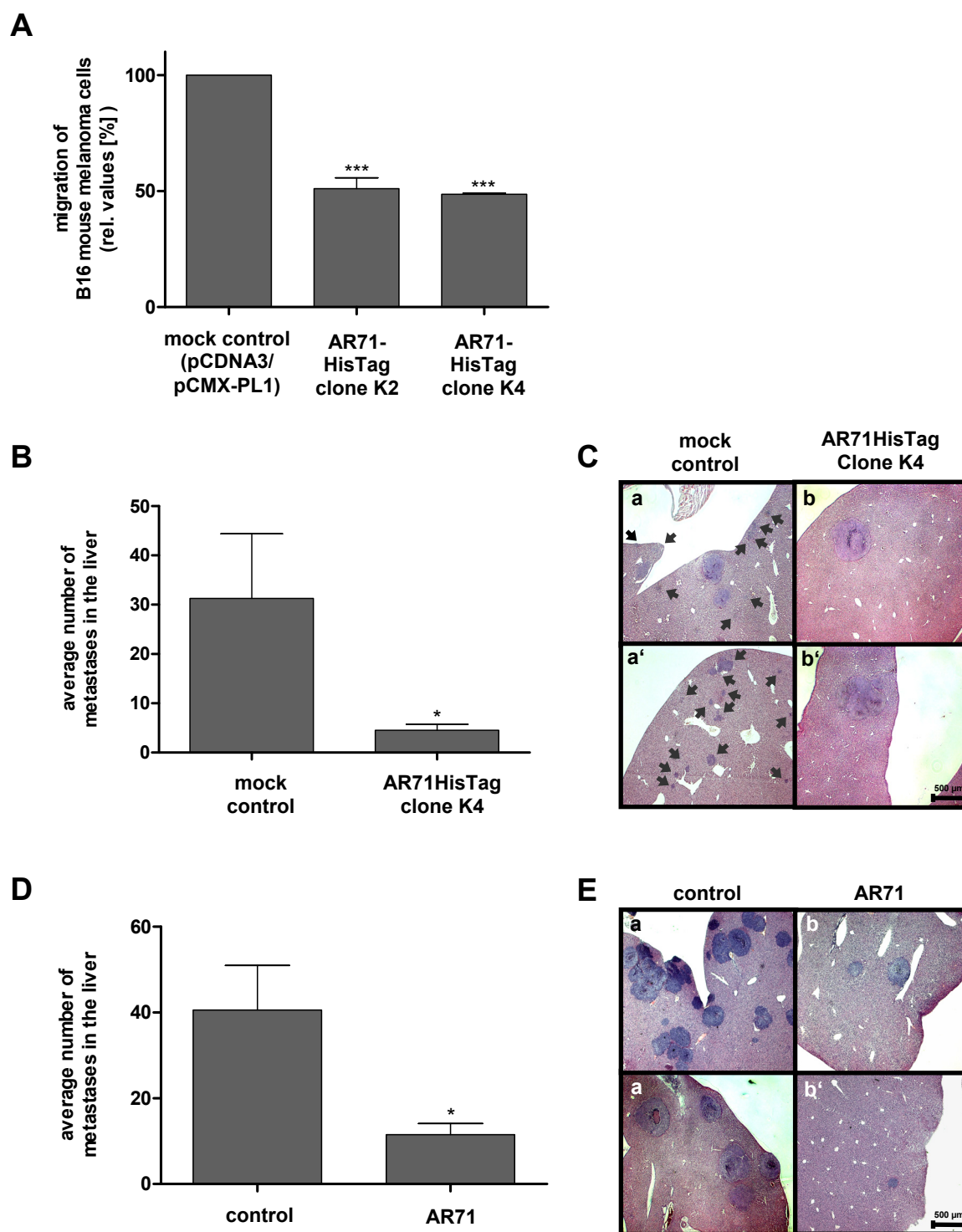


Figure 4: Effect of MIA inhibitory peptide AR71 on formation of metastases *in vivo*

(A) Murine B16 melanoma cells stably transfected with a (secretion-signal)-AR71-HisTag containing construct were analyzed for their migratory activity in a Boyden chamber assay. Compared to the mock control, migration is drastically reduced in the two Sig-AR71-HisTag expressing cell clones clone K2 and clone K4. (B) Sig-AR71-HisTag clone K4 as well as a corresponding mock control were injected into the spleen of B1/6N mice, respectively. Histological analysis of haematoxylin and eosin stained liver sections revealed that mice being injected with Sig-AR71-HisTag clones comprised significantly fewer metastases than the mock control. (C) Representative histological liver sections (hematoxylin and eosin stained), two of mice injected with the B16 mock control (a and a') and two of mice injected with the Sig-AR71-HisTag expressing cell clone K4 (b and b'). Black arrows indicate small metastases. (D) Wild type murine B16

melanoma cells were injected into the spleen of Bl/6N mice with the mice being subsequently treated with *i.v.* injections of AR71 (50 µg every 24 h). Histological analyses revealed a significant reduction of the average number of metastases in the liver of mice treated with AR71 compared to the liver of untreated control mice. **(E)** Representative histological liver sections (hematoxylin and eosin stained), two of untreated (a and a') and two of treated mice (b and b').

5.3 Discussion

Primary melanomas often reach a high proliferation rate and acquire competence for metastasis in early stages of the disease. As already presented in previous studies, MIA plays a fundamental role in this process.³⁻⁴ However, hitherto the molecular mechanism by which MIA enables tumor cell release from the primary tumor and promotes formation of metastases elsewhere in the body was poorly understood.

Here, we newly describe that MIA is active as a dimer. MIA dimerization is supported by *in silico* studies as well as Western blot analysis, mutagenesis studies and HTFP assay measurements.¹⁵ We identified the probable dimerization domains as being located in the n-Src loop and in the cleft next to the distal loop. Additionally, this tendency of MIA to form homomeric linkages was also indicated by previous NMR spectroscopy experiments revealing a transversal relaxation time (T_2) shorter than expected for an 11 kDa protein.^{10, 21}

However, until now, dimerization of MIA has not been correlated with functional activity. Our studies revealed that MIA is functionally inactive as a monomeric species and only wt MIA and MIA mutants still forming dimers were found to be functionally active in Boyden chamber invasion assays. The mutants D29G/Y69H, V46F/S81P, T89P and K91N are still able to dimerize. Replacement of these amino acids outside the dimerization domains in the n-Src loop and next to the distal loop does not hinder dimerization and consequently does not influence functional activity. In contrast, the mutation G61R is located at the dimerization interface next to the distal loop of MIA. In this mutant, glycine, an uncharged amino acid residue with minimum sterical demand is replaced by arginine, a positively charged and very large residue. As expected, this exchange strongly impacts formation of MIA dimers due to sterical demand and charge repulsion between the two respective MIA-MIA binding sites. The fact that monomeric MIA is functionally completely inactive suggests that the active site for integrin and ECM binding could potentially be generated by self assembly of two identical MIA subunits.

The concept of proteins that require dimerization in order to reach functional activity has been described for example for lipoprotein lipase which is converted into inactive monomers by angiopoietin-like protein 4. Concomitant with dissociation of functionally

active dimers into monomers, an irreversible loss of catalytic activity was found.²² Furthermore, this functional coupling between oligomerization and activity of proteins has also been reported for herpesvirus protease, which is also inactivated after dimer disruption.²³⁻²⁴

The feasibility of inhibiting protein activity via preventing dimerization was discussed in a study by *Wlodawer et al.* describing a similar mechanism for inhibiting HIV-1 protease, a homodimeric protein. requiring dimerization for activation.²⁵ The inhibition is achieved by targeting the dimerization interface using peptides promoting dissociation.²⁶ The design of small molecules intended to disrupt the dimer and /or bind to an inactive protein monomer, therefore, offers an alternative to the strategy of targeting of the active site.

In our search for MIA inhibitory compounds, we employed the HTFP assay as a rapid screening platform to identify peptides that prevent the assembly of inactive monomers to functionally active MIA dimers. The dodecapeptide AR71 was found to exhibit significant MIA inhibitory effect in *in vitro* experiments. As reflected by the HTFP assay and Western Blot analysis, inhibitory peptide AR71 promotes dissociation of MIA aggregates, while our NMR investigations revealed it to directly bind to the dimerization domain next to the distal loop.

Having demonstrated the inhibitory effect of AR71 in the *in vitro* models, we employed an established *in vivo* metastasis assay to evaluate the capability of peptide AR71 to prevent the formation of metastasis of malignant melanoma by inhibiting MIA.²⁰ In our first model, Sig-AR71-HisTag expressing B16 cell clones and the respective mock control cells were analyzed for their metastatic potential. With the addition of an N-terminal secretion sequence ensuring peptide processing into the endoplasmic reticulum, we expected subsequent binding and thus inactivation of MIA by preventing formation of functionally active protein dimers directly at the location of protein biosynthesis. In immunofluorescence studies we could observe this colocalization of MIA and AR71-HisTag in the cells. In an *in vivo* mouse model, the expression of AR71 by the stably transfected B16 cells led to a dramatic reduction in the formation of metastases compared to mock control, again reflecting the need for MIA to form dimers to reach functional activity.

Even though peptides are generally quickly degraded *in vivo* by proteases and renally cleared, we also observed a significant reduction in the formation of metastases in an *in vivo* injection model of AR71. Again, the particularly strong reduction in the number of

metastases proves the potency of AR71 to suppress the metastatic spread of melanoma cells *in vivo*.

To conclude, we have contributed to the understanding of the molecular function of MIA by *in vitro* studies which included multidimensional NMR spectroscopy. These investigations revealed that MIA is functionally active as a dimer. By specifically screening MIA-binding peptide ligands for their ability to prevent MIA dimerization, we identified dodecapeptide AR71 and demonstrate the potency of this peptide to significantly reduce the formation of metastases of murine B16 malignant melanoma cells *in vivo*. This study details the mechanism by which peptide AR71 inhibits MIA mediated metastatic spread of tumor cells and provides a novel leading structure for the design of potent therapeutics for the treatment of malignant melanoma. To overcome the drug resistance observed with current treatments, this new strategy of dimerization inhibitors may be useful for prevention or at least reduction of metastatic spread in early stages of the disease. Specifically inhibiting the formation of metastases should provide a very effective therapy since malignant melanoma is not fatal because of the primary tumor but because of organ failure due to formation of metastases. In addition, most conventional treatments still affect cancer cells as well as other fast-dividing cell types, resulting in the desire for a more targeted therapy. By targeting MIA, which is only expressed in malignant melanoma and in early-phase differentiating chondrocytes, the adverse reactions of treatment with MIA inhibitory compounds should be minimal. Side effects on cartilage are not expected since MIA-deficient mice show no phenotype changes, as previously demonstrated.²⁷

We feel that this study provides an excellent starting point for the development of a new strategy in malignant melanoma therapy. Targeting MIA leads to strongly reduced tumor cell invasion and formation of metastases and thus provides a new concept of therapeutic intervention.

5.4 Materials and methods

Cell lines and cell culture conditions

The melanoma cell line Mel Im, established from a human metastatic biptic sample (generous gift from Dr. Johnson, University of Munich, Germany) was used in all experiments. Additionally, main experiments were also conducted using the human cell line Mel Ju and the murine cell line B16, which were derived from metastases of malignant melanoma. All cells were maintained in DMEM (PAA Laboratories GmbH, Cölbe, Germany) supplemented with penicillin (400 U/mL), streptomycin (50 µg/mL),

l-glutamine (300 µg/mL) and 10% fetal calf serum (Pan Biotech GmbH, Aidenbach, Germany) and split in 1:6 ratio every 3 days.

Protein analysis in vitro (Western blotting)

Protein samples were denaturated at 70°C for 10 min after addition of reducing and denaturing Roti-Load buffer (Roth, Karlsruhe, Germany) and subsequently separated on sodium dodecyl sulfate 12.75% polyacrylamid gels (SDS-PAGE) (Invitrogen, Groningen, The Netherlands). In the multimerization studies, MIA protein (1 µg) was incubated with AR71 (2.5 µg) overnight at RT before being treated as described above. After transferring the proteins onto a polyvinylidene fluoride (PVDF) membrane (BioRad, Richmond, VA, USA), the membrane was blocked using 3% BSA/PBS for 1 h at RT and incubated with a 1:150 dilution of primary polyclonal rabbit anti MIA antibody (Biogenes, Berlin, Germany) in 3% BSA/PBS overnight at 4°C. After washing in PBS the membrane was incubated with a 1:2000 dilution of an alkaline-phosphate coupled secondary antibody (Chemikon, Hofheim, Germany) for 2 h at RT. Finally, after washing steps, immunoreactions were visualized by nitro blue tetrazolium/5-bromo-4-chloro-3-indolyl phosphate (NBT/BCIP) (Invitrogen, Karlsruhe, Germany) staining.

Boyden Chamber Invasion Assay

Invasion assays were performed in Boyden Chambers containing polycarbonate filters with 8-µm pore size (Neuro Probe, Gaithersburg, MD, USA) essentially as described previously.¹⁴ Filters were coated with matrigel, a commercially available reconstituted basement membrane (diluted 1:3 in H₂O; BD Bioscience, Bradford, MA, USA). The lower compartment was filled with fibroblast-conditioned medium used as a chemo attractant. Mel Im melanoma cells were harvested by trypsinization for 2 min at RT, resuspended in DMEM without FCS at a density 2.5×10^4 cells/mL, and placed in the upper compartment of the chamber. Except for the control experiment with untreated cells and experiments where cells were only treated with the respective peptide, MIA was added to the cell suspension at a final concentration of 200 ng/mL. Peptide AR71 (sequence: Ac-FHWRYPPLPGQ-NH₂) was used at a final concentration of 1 µM. MIA expressing murine B16 melanoma cells stably co-transfected with Sig-AR71-HisTag containing pCMX-PL1 vector and an antibiotic resistance comprising plasmid (pCDNA3), and the respective mock control were also investigated for their ability to migrate.²⁸ Therefore, cells were harvested by trypsinization for 2 min at RT, resuspended in DMEM without

FCS at a density 2.5×10^4 cells/mL, and placed in the upper compartment of the chamber. After incubation at 37°C for 4 h filters were removed. Cells adhering to the lower surface of the filter were fixed, stained, and counted. Experiments were carried out in triplicates and repeated at least three times.

Coating of well plates with MIA-Biotin

Black, streptavidin coated 96 well plates (from Greiner Bio-one, Frickenhausen, Germany) were coated with MIA-Biotin as described previously.^{7, 15} An uncoated control lane was sealed with adhesive film to prevent contamination. The MIA-Biotin coated plate was used for measurements immediately.

Polarization assay setup

All measurements were performed at RT on a Polarstar Optima microplate reader (BMG Labtech, Offenburg, Germany). A 390-10 nm bandpass filter was used for excitation while a 520 nm longpass filter was used for the emission light. Even though the extinction coefficient is higher at longer wavelengths, we chose a shorter excitation wavelength as this led to higher polarization values. MIA-Ru(bpy)₃ was prepared and tested for functional activity as described previously.¹⁵ A MIA-Ru(bpy)₃ concentration of 55 fM was used in all experiments. A solution volume of 250 µL per well was found to give a low standard deviation with high signal intensity. All measurements were performed in DPBS without calcium or magnesium (PAN Biotech GmbH, Aidenbach, Germany). Addition of components to the wells was done in the following order: inhibitory peptide, buffer, MIA-Ru(bpy)₃. Owing to different reaction kinetics, measurements were performed every 5 min over a 30 min period. Polarization values are reported relative (P/P_0) to the value of free MIA-Ru(bpy)₃ in solution in a well not treated with MIA-biotin. All reported values are an average of three independent measurements.

Cloning Strategy

Signal-AR71-HisTag pCMX-PL1-plasmid construction: The Signal-AR71-HisTag pCMX-PL1 expression plasmid was created by PCR amplification of the human hydrophobic signal-peptide sequence, responsible for transport into the endoplasmic reticulum, from a Signal-MIA containing expression plasmid using the MJ Research PTC-200 Peltier Thermo Cycler (BioRad, Munich, Germany). The HisTag sequence was inserted at the C-terminal end of the AR71 peptide using the primers 5'- GAC GAA TTC

ATG GCC CGG TCC CTG GTG - 3' and 5'- GAC AAG CTT TCA GTG ATG GTG ATG GTG ATG CTG GCC GGG CAA GGG CAA GGG GTA TCT CCA GTG GAA CCT GAC ACC AGG TCC GGA GAA -3'. After amplification of the Signal-AR71-HisTag fragment, the PCR product was digested with EcoRI and HindIII (NEB, Frankfurt, Germany) The insert was purified by gel extraction (Qiagen, Hilden, Germany) and cloned into the EcoRI and HindIII sites of the eukaryotic expression vector pCMX-PL1 which was previously purified and prepared for ligation using T4-Ligase (NEB, Frankfurt, Germany).²⁸ After transformation in DH10 β cells (NEB, Frankfurt, Germany) according to the manufacturer's instructions, the plasmid was isolated using the MIDI Kit (Qiagen, Hilden, Germany) and quantified by a gene quant II RNA/DNA Calculator (Pharmacia Biotech, Nümbrecht, Germany). The sequence of the PCR-generated clone was confirmed by DNA sequencing.

Stable transfection of murine B16 melanoma cells

For transfection, 1.5×10^5 cells/mL were seeded in 6-well plates (Corning Omnilab, Munich, Germany) and cultured in 2 mL of Dulbecco's modified Eagle's medium (PAA, Cölbe, Germany) with 10% fetal calf serum (Pan, Aidenbach, Germany). Cells were transfected with 0.8 μ g of the respective control or His-tagged AR71 containing pCMX-PL1 vector and 0.2 μ g pcDNA3 providing geneticin (Invitrogen, Karlsruhe, Germany) resistance using the LipofectaminPlus (Invitrogen, Karlsruhe, Germany) method according to the manufacturer's instructions. After selection of cells comprising antibiotic resistance we confirmed expression and localization of AR71 peptide on mRNA and protein level by PCR and immunofluorescence, respectively.

Recombinant expression of MIA and mutant forms

In vitro protein expression reactions of recombinant human MIA and its mutants were performed with the Rapid Translation System RTS 500 E. coli HY Disulfite Kit (Roche, Mannheim, Germany) according to the manufacturer's instructions. All reactions were carried out over night at 30°C or 25°C with efficient stirring in the RTS 500 instrument. MIA mutants were checked for correct folding and function as previously described.¹⁴

NMR Spectroscopy

All spectra were recorded at 300 K and pH 7 on a Bruker DRX600 spectrometer equipped with a pulsed field gradient triple resonance probe. Water suppression in experiments

recorded on samples in H₂O was achieved by incorporation of a Watergate sequence into the various pulse sequences.²⁹⁻³¹ 2D ¹H-¹⁵N HSQC spectra with reduced signal loss due to fast exchanging protons were recorded using procedures described previously.³² All spectra were processed with NMRPipe and analyzed with NMRView.³³⁻³⁴ Data handling was performed with NMRView. Structure visualisation and superimpositions were done with PyMol (Delano, W. L., The PyMol Molecular Graphics System (2002) Delano Scientific, Palo Alto, CA, USA).

Dimer model

The PreBI modeling software (<http://pre-s.protein.osaka-u.ac.jp/prebi/>) was used together with the published X-ray structure of MIA (PDBid: 1I1J) for the prediction of the putative dimer interface. Employing the monomeric NMR structure of MIA (PDBid: 1HJD) together with the interface information obtained in the previous step a three-dimensional model of the dimeric complex was calculated. Computations were performed using the data driven protein-protein docking program HADDOCK.¹³

Protein binding studies

The NMR titration of MIA with AR71 consisted of monitoring changes in chemical shifts and line widths of the backbone amide resonances of uniformly ¹⁵N-enriched MIA samples as a function of ligand concentration.³⁵⁻³⁸

In vivo metastasis assay

To determine the effect of peptide AR71 on the metastatic potential of murine B16 melanoma cells *in vivo*, a previously developed mouse metastases model was used.²⁰ 1 x 10⁵ cells of the AR71-HisTag expressing B16 cell clone AR71-His K4 as well as the corresponding mock control cells were injected into the spleen of mice (n = 8 for mock control cells as well as for AR71-HisTag K4 cells, respectively). After nine days, mice were sacrificed, the livers were resected and the number and size of visible black tumor nodules on the surface of the livers was noticed. Tissues were fixed in formalin and afterwards paraffin embedded sections were hematoxylin and eosin stained for histological analysis.

Additionally, 1 x 10⁵ wt mouse melanoma B16 cells suspended in a solution containing AR71 (1 mg/mL) and 0.9% NaCl, or NaCl alone for the control mice, respectively, were injected into the spleen of each animal (n = 8 for treated mice, as well as for control

without AR71). Peptide AR71 was injected *i.v.* (50 µg every 24 h). After nine days, the mice were sacrificed and the livers were excised. Following formalin fixation, tissues were embedded in paraffin. Afterwards, sections were prepared and stained using hematoxylin and eosin before being subjected to histological analysis.

Immunofluorescence assays

5 x 10⁵ murine B16 melanoma cells were grown in a 4-well chamber slide (Falcon, BD Bioscience, Heidelberg, Germany). After stable transfection with a Sig-AR71-HisTag containing expression plasmid and the respective pCMX-PL1 mock control, cells were incubated for 48 h at 37°C and 8% CO₂. Afterwards, cells were washed and fixed using 4% paraformaldehyde in 0.1 M phosphate-buffered saline (PBS) for 15 min. After permeabilization of cells, blocking of non-specific binding sites with blocking solution (1% BSA/PBS) for 1 h at 4°C was performed. Cells were incubated with primary antibodies rabbit anti-MIA (Biogenes, Berlin, Germany) and mouse anti-HisTag (BD Bioscience, Pharmingen, Germany) at a concentration of 1 µg/mL at 4°C for 2 h. After rinsing with PBS 5 times, cells were first covered with a 1:200 dilution of the secondary antibody TRITC anti-mouse (TRITC-conjugated donkey anti-mouse antibody, Jackson Immuno Research Laboratories, West Grove, PA, USA) and FITC anti-rabbit (FITC-conjugated polyclonal swine anti rabbit immunoglobulin, DakoCytomation, Glostrup, Denmark) in PBS at 4°C for 1 h, respectively. Following incubation with primary antibodies, cells were washed with PBS and coverslips were mounted on slides using Hard Set Mounting Medium with DAPI (Vectashield, H-1500, Linearis, Wertheim Germany) and imaged using an Axio Imager Zeiss Z1 fluorescence microscope (Axiovision Rel. 4.6.3) equipped with an Axio Cam MR camera. Images were taken using 63x oil immersion lenses.

Statistical analysis

In the bar graphs, results are expressed as mean ± S.D. (range) or percent. Comparison between groups was made using the Student's unpaired t-test. A p-value <0.05 was considered as statistically significant (ns: not significant, *: p<0.05, **: p<0.01, ***: p<0.001). All calculations were made using the GraphPad Prism Software (GraphPad Software, Inc., San Diego, USA).

5.5 Acknowledgement

We thank Susanne Wallner, Sibylla Lodermeier and Simone Kaufmann for technical assistance, the Center of Excellence for Fluorescent Bioanalytics (KFB) for providing access to the BMG Polarstar microplatereader, Judy Johnson for providing us with the Mel Im cell line and Thomas Schubert for histological evaluation. This work was supported by a DFG grant (SFB 642, A6). Furthermore, R. S. gratefully recognizes generous support from the BMBF, FCI, Proteincenter (NRW Center of Excellence), and RUBiospek. We are grateful to Prof. Dr. von Kiedrowski for providing generous access to the DRX600 spectrometer.

5.6 References

1. Bosserhoff, A. K.; Kaufmann, M.; Kaluza, B.; Bartke, I.; Zirngibl, H.; Hein, R.; Stolz, W.; Buettner, R., Melanoma-inhibiting activity, a novel serum marker for progression of malignant melanoma. *Cancer Res* **1997**, 57, (15), 3149-53.
2. Blesch, A.; Bosserhoff, A. K.; Apfel, R.; Behl, C.; Hessdoerfer, B.; Schmitt, A.; Jachimczak, P.; Lottspeich, F.; Buettner, R.; Bogdahn, U., Cloning of a novel malignant melanoma-derived growth-regulatory protein, MIA. *Cancer Res* **1994**, 54, (21), 5695-701.
3. Bosserhoff, A. K.; Stoll, R.; Sleeman, J. P.; Bataille, F.; Buettner, R.; Holak, T. A., Active detachment involves inhibition of cell-matrix contacts of malignant melanoma cells by secretion of melanoma inhibitory activity. *Lab Invest* **2003**, 83, (11), 1583-94.
4. Bosserhoff, A. K.; Echtenacher, B.; Hein, R.; Buettner, R., Functional role of melanoma inhibitory activity in regulating invasion and metastasis of malignant melanoma cells in vivo. *Melanoma Res* **2001**, 11, (4), 417-21.
5. Guba, M.; Bosserhoff, A. K.; Steinbauer, M.; Abels, C.; Anthuber, M.; Buettner, R.; Jauch, K. W., Overexpression of melanoma inhibitory activity (MIA) enhances extravasation and metastasis of A-mel 3 melanoma cells in vivo. *Br J Cancer* **2000**, 83, (9), 1216-22.
6. Schmidt, J.; Friebe, K.; Schönherr, R.; Coppolino, M. G.; Bosserhoff, A. K., Directed, Migration-associated Secretion of Melanoma Inhibitory Activity (MIA) at the Cell Rear is supported by KCNN4 Potassium Channels. *Cell Res* **2010**, (submitted).

7. Bauer, R.; Humphries, M.; Fassler, R.; Winklmeier, A.; Craig, S. E.; Bosserhoff, A. K., Regulation of integrin activity by MIA. *J Biol Chem* **2006**, 281, (17), 11669-77.
8. Stoll, R.; Bosserhoff, A., Extracellular SH3 domain containing proteins - features of a new protein family. *Curr Protein Pept Sci* **2008**, 9, (3), 221-6.
9. Stoll, R.; Renner, C.; Ambrosius, D.; Golob, M.; Voelter, W.; Buettner, R.; Bosserhoff, A. K.; Holak, T. A., Sequence-specific ^1H , ^{13}C , and ^{15}N assignment of the human melanoma inhibitory activity (MIA) protein. *J Biomol NMR* **2000**, 17, (1), 87-8.
10. Stoll, R.; Renner, C.; Buettner, R.; Voelter, W.; Bosserhoff, A. K.; Holak, T. A., Backbone dynamics of the human MIA protein studied by ^{15}N NMR relaxation: implications for extended interactions of SH3 domains. *Protein Sci* **2003**, 12, (3), 510-9.
11. Stoll, R.; Renner, C.; Zweckstetter, M.; Bruggert, M.; Ambrosius, D.; Palme, S.; Engh, R. A.; Golob, M.; Breibach, I.; Buettner, R.; Voelter, W.; Holak, T. A.; Bosserhoff, A. K., The extracellular human melanoma inhibitory activity (MIA) protein adopts an SH3 domain-like fold. *EMBO J* **2001**, 20, (3), 340-9.
12. Loughheed, J. C.; Holton, J. M.; Alber, T.; Bazan, J. F.; Handel, T. M., Structure of melanoma inhibitory activity protein, a member of a recently identified family of secreted proteins. *Proc Natl Acad Sci U S A* **2001**, 98, (10), 5515-20.
13. Dominguez, C.; Boelens, R.; Bonvin, A. M., HADDOCK: a protein-protein docking approach based on biochemical or biophysical information. *J Am Chem Soc* **2003**, 125, (7), 1731-7.
14. Stoll, R.; Lodermeier, S.; Bosserhoff, A. K., Detailed analysis of MIA protein by mutagenesis. *Biol Chem* **2006**, 387, (12), 1601-6.
15. Riechers, A.; Schmidt, J.; König, B.; Bosserhoff, A. K., Heterogeneous transition metal-based fluorescence polarization (HTFP) assay for probing protein interactions. *Biotechniques* **2009**, 47, (4), 837-44.
16. Schmidt, J.; Bosserhoff, A. K., Processing of MIA protein during melanoma cell migration. *Int J Cancer* **2009**, 125, (7), 1587-94.
17. Bosserhoff, A. K.; Hein, R.; Bogdahn, U.; Buettner, R., Structure and promoter analysis of the gene encoding the human melanoma-inhibiting protein MIA. *J Biol Chem* **1996**, 271, (1), 490-5.

18. Bosserhoff, A. K.; Lederer, M.; Kaufmann, M.; Hein, R.; Stolz, W.; Apfel, R.; Bogdahn, U.; Buettner, R., MIA, a novel serum marker for progression of malignant melanoma. *Anticancer Res* **1999**, 19, (4A), 2691-3.
19. Stahlecker, J.; Gauger, A.; Bosserhoff, A.; Buttner, R.; Ring, J.; Hein, R., MIA as a reliable tumor marker in the serum of patients with malignant melanoma. *Anticancer Res* **2000**, 20, (6D), 5041-4.
20. Carrascal, M. T.; Mendoza, L.; Valcarcel, M.; Salado, C.; Egilegor, E.; Telleria, N.; Vidal-Vanaclocha, F.; Dinarello, C. A., Interleukin-18 binding protein reduces b16 melanoma hepatic metastasis by neutralizing adhesiveness and growth factors of sinusoidal endothelium. *Cancer Res* **2003**, 63, (2), 491-7.
21. Loughheed, J. C.; Domaille, P. J.; Handel, T. M., Solution structure and dynamics of melanoma inhibitory activity protein. *J Biomol NMR* **2002**, 22, (3), 211-23.
22. Osborne, J. C., Jr.; Bengtsson-Olivecrona, G.; Lee, N. S.; Olivecrona, T., Studies on inactivation of lipoprotein lipase: role of the dimer to monomer dissociation. *Biochemistry* **1985**, 24, (20), 5606-11.
23. Nomura, A. M.; Marnett, A. B.; Shimba, N.; Dotsch, V.; Craik, C. S., One functional switch mediates reversible and irreversible inactivation of a herpesvirus protease. *Biochemistry* **2006**, 45, (11), 3572-9.
24. Pray, T. R.; Nomura, A. M.; Pennington, M. W.; Craik, C. S., Auto-inactivation by cleavage within the dimer interface of Kaposi's sarcoma-associated herpesvirus protease. *J Mol Biol* **1999**, 289, (2), 197-203.
25. Wlodawer, A.; Miller, M.; Jaskolski, M.; Sathyanarayana, B. K.; Baldwin, E.; Weber, I. T.; Selk, L. M.; Clawson, L.; Schneider, J.; Kent, S. B., Conserved folding in retroviral proteases: crystal structure of a synthetic HIV-1 protease. *Science* **1989**, 245, (4918), 616-21.
26. Boggetto, N.; Reboud-Ravaux, M., Dimerization inhibitors of HIV-1 protease. *Biol Chem* **2002**, 383, (9), 1321-4.
27. Moser, M.; Bosserhoff, A. K.; Hunziker, E. B.; Sandell, L.; Fassler, R.; Buettner, R., Ultrastructural cartilage abnormalities in MIA/CD-RAP-deficient mice. *Mol Cell Biol* **2002**, 22, (5), 1438-45.
28. Tatzel, J.; Poser, I.; Schroeder, J.; Bosserhoff, A. K., Inhibition of melanoma inhibitory activity (MIA) expression in melanoma cells leads to molecular and phenotypic changes. *Pigment Cell Res* **2005**, 18, (2), 92-101.

29. Braunschweiler, L.; Ernst, R. R., Coherence Transfer by Isotropic Mixing - Application to Proton Correlation Spectroscopy. *Journal of Magnetic Resonance* **1983**, 53, 521-528.
30. Davis, D. G.; Bax, A., Simplification of H-1-NMR Spectra by Selective Excitation of Experimental Subspectra. *J Am Chem Soc* **1985**, 107, 7197-7198.
31. Shaka, A. J.; Lee, C. J.; Pines, A., Iterative Schemes for Bilinear Operators - Application to Spin Decoupling. *Journal of Magnetic Resonance* **1988**, 77, 274-293.
32. Mori, S.; Abeygunawardana, C.; Johnson, M. O.; van Zijl, P. C., Improved sensitivity of HSQC spectra of exchanging protons at short interscan delays using a new fast HSQC (FHSQC) detection scheme that avoids water saturation. *J Magn Reson B* **1995**, 108, (1), 94-8.
33. Johnson, R. D.; Bluemler, P.; Rafey, R.; Brodbeck, D., Visualization of Multidimensional NMR Data. *Abstr Pap Am Chem S* **1994**, 207, (138-COMP).
34. Delaglio, F.; Grzesiek, S.; Vuister, G. W.; Zhu, G.; Pfeifer, J.; Bax, A., NMRPipe: a multidimensional spectral processing system based on UNIX pipes. *J Biomol NMR* **1995**, 6, (3), 277-93.
35. Berghaus, C.; Schwarten, M.; Heumann, R.; Stoll, R., Sequence-specific ¹H, ¹³C, and ¹⁵N backbone assignment of the GTPase rRheb in its GDP-bound form. *Biomol NMR Assign* **2007**, 1, (1), 45-7.
36. Schwarten, M.; Berghaus, C.; Heumann, R.; Stoll, R., Sequence-specific ¹H, ¹³C, and ¹⁵N backbone assignment of the activated 21 kDa GTPase rRheb. *Biomol NMR Assign* **2007**, 1, (1), 105-8.
37. Song, J.; Markley, J. L., NMR chemical shift mapping of the binding site of a protein proteinase inhibitor: changes in the ¹H, ¹³C and ¹⁵N NMR chemical shifts of turkey ovomucoid third domain upon binding to bovine chymotrypsin A(alpha). *J Mol Recognit* **2001**, 14, (3), 166-71.
38. Stoll, R.; Renner, C.; Hansen, S.; Palme, S.; Klein, C.; Belling, A.; Zeslawski, W.; Kamionka, M.; Rehm, T.; Muhlhahn, P.; Schumacher, R.; Hesse, F.; Kaluza, B.; Voelter, W.; Engh, R. A.; Holak, T. A., Chalcone derivatives antagonize interactions between the human oncoprotein MDM2 and p53. *Biochemistry* **2001**, 40, (2), 336-44.

6 Summary

Melanoma inhibitory activity (MIA), an 11 kDa protein expressed and secreted by malignant melanoma cells, plays a key role in development and progression of malignant melanoma. It facilitates the release of tumor cells from the primary tumor and thus strongly promotes formation of metastases. However, the processing of MIA protein during cell migration and the characterization of protein activity on a molecular level has not been elucidated so far.

These studies detail the mechanism by which MIA protein contributes to the aggressive and invasive behaviour of malignant melanoma cells. After migratory stimuli of tumor cells a directed, microtubule based protein transport to the rear cell pole is induced. MIA protein secretion is a Ca^{2+} -dependent process regulated by the calcium activated potassium channel KCNN4 (IKCa1). This channel type has previously been reported to be in the active state at the rear pole of migrating cells. Following secretion, MIA protein directly interacts with cell adhesion receptors, including integrin $\alpha_4\beta_1$ and $\alpha_5\beta_1$, and extracellular matrix molecules. MIA-integrin-complexes are subsequently internalized into the cell. After dissociation of these complexes, MIA protein is degraded in acidic vesicles while integrins are transported to the cell front to form new adhesion contacts. Since MIA protein secretion is restricted to the cell rear, it mediates localized tumor cell detachment from surrounding structures of the primary tumor and enables invasion into healthy tissues.

At the molecular level, NMR spectroscopy revealed that MIA protein forms homodimers with head to tail linkages. As indicated by mutant analysis in Boyden Chamber invasion assays and further *in vitro* protein analyses, MIA protein reaches functional activity via self assembly. To inhibit MIA protein function by preventing protein dimerization, MIA-binding peptides, which were previously identified in a page display experiment, were specifically screened for their ability to dissociate MIA protein dimers. In order to conduct this screening, a heterogeneous transition-metal based fluorescence polarization assay (HTFP assay) was developed. In this assay format, MIA protein was immobilized in a well plate and MIA protein interactions were detected when the addition of Ru(bpy)₃-labeled MIA protein led to an increase in the fluorescence polarization signal. Dodecapeptide AR71 dissociated MIA protein assemblies, as evidenced by a strong decrease in the fluorescence polarization signal. In addition, Western blot analysis also confirmed monomerization of MIA protein after treatment with AR71, while NMR-spectroscopy revealed that AR71 directly binds to the dimerization domain.

By performing Boyden chamber invasion assays functional inhibition of MIA protein by peptide AR71 was also demonstrated *in vitro*. Therefore, the MIA inhibitory effect of AR71 was analyzed in a murine melanoma metastases *in vivo* model. It was clearly demonstrated that treatment with dodecapeptide AR71 strongly reduces the number of metastases *in vivo*. These studies may constitute a foundation for the development of a MIA protein inhibitor which could represent a new therapeutic strategy as an antimetastatic treatment for malignant melanoma.

7 Zusammenfassung

Melanoma inhibitory activity (MIA), ein 11 kDa großes Protein, wird von malignen Melanomzellen exprimiert und sekretiert. MIA Protein spielt eine wichtige Rolle bei der Entwicklung und Progression des malignen Melanoms. Durch direkte Interaktion mit Zelladhäsionsmolekülen und Strukturen der extrazellulären Matrix erleichtert MIA Protein das Ablösen von entarteten Zellen aus dem Primärtumorverband und fördert somit die Metastasenbildung. Der detaillierte Mechanismus des Proteintransportes während der Zellmigration und die Charakterisierung der Proteinaktivität auf molekularer Ebene sind jedoch bis heute noch nicht vollständig aufgeklärt.

Die in dieser Studie erstellten Daten zeigen, auf welchem Mechanismus basierend MIA Protein zum aggressiven Verhalten und invasiven Phänotyp der malignen Melanomzellen beiträgt. Nach migratorischem Stimulus der Tumorzellen wird MIA Protein, eingeschlossen in sekretorischen Vesikeln, entlang von Mikrotubulisträngen gerichtet zum hinteren Zellpol transportiert. Die anschließende Proteinsekretion ist ein Ca^{2+} abhängiger Prozess, der vom Calcium-aktivierten Kaliumkanal KCNN4 (IKCa1) reguliert wird. In einer bereits veröffentlichten Studie ist beschrieben worden, dass dieser Kanal nur am hinteren Zellpol migrierender Zellen im aktiven Zustand ist. Nach der Sekretion bindet MIA direkt an Zelladhäsionsrezeptoren wie Integrin $\alpha_4\beta_1$ und $\alpha_5\beta_1$, und an extrazelluläre Matrixstrukturen. MIA-Integrin-Komplexe werden sofort nach ihrer Bildung internalisiert. Nach ihrer Aufnahme dissoziieren die Komplexe, MIA Protein wird in Lysosomen abgebaut während Integrine wieder zur Zellfront transportiert werden um dort neue Zelladhäsionskontakte bilden zu können. Da sich die MIA Proteinsekretion in migrierenden Zellen auf den hinteren Zellpol beschränkt, unterstützt MIA fokales Ablösen der Tumorzelle von umgebenden Strukturen und ermöglicht so eine gerichtete Invasion in umliegendes gesundes Gewebe.

Molekulare Protein Analysen mittels NMR-Spektroskopie zeigen, dass MIA ein Homodimer mit sogenanntem „head to tail“ Bindungsmotiv bildet. In Western Blot Analysen und *in vitro* Invasions Experimenten mit MIA Mutanten wurde gezeigt, dass MIA Protein durch Dimerisierung funktionelle Aktivität erlangt. Um MIA Protein funktionell zu hemmen, wurde gezielt nach MIA Protein bindenden Peptiden gescreent, die in der Lage sind Dimerisierung zu verhindern bzw. bereits bestehende Dimere aufzubrechen und damit das Protein zu inaktivieren.

Zur Durchführung eines solchen Screening Experiments wurde ein heterogener Übergangsmetall-basierter Fluoreszenz Polarisations Assay (HTFP assay) entwickelt. Für diese Untersuchungsmethode wird biotinyliertes MIA Protein in einer Streptavidin beschichteten Wellplate immobilisiert. Nach Zugabe von Ru(bpy)₃ markiertem MIA Protein kommt es zur Protein-Protein Interaktion und damit auch zum Anstiegs des Fluoreszenzpolarisationssignals. Das Dodekapeptid AR71 dissoziiert MIA-MIA Bindungen und führt zu einer starken Abnahme des Fluoreszenzpolarisationssignals. Auch in Western Blot Analysen bestätigt sich, dass MIA Dimere nach Behandlung mit Peptid AR71 aufgebrochen werden. Die Binding-Site dieses Peptids wurde mittels NMR-Spektroskopie identifiziert. Sie befindet sich genau in der Dimerisierungsdomäne des MIA Proteins. Da Peptid AR71 MIA Protein Aktivität *in vitro* hemmt, wurde der inhibitorische Effekt des Peptids auch *in vivo* in einem murinen Melanom Metastasen Modell analysiert. Die Behandlung der Tiere mit Dodekapeptid AR71 führt zu einer stark reduzierten Anzahl der Metastasen. Diese Studien bestätigen, dass MIA Protein ein neues Target Molekül für die Behandlung des malignen Melanoms darstellt. Ein MIA Protein Inhibitor könnte einen neuen, antimetastatischen Therapieansatz liefern.

8 Abbreviations

ANS	1-anilino-8-naphthalene sulfonate
Arf6	ADP-ribosylation factor 6
BCIP	5-bromo-4-chloro-3-indolyl phosphate
BIMI	bisindolylmaleimide I
BSA	bovine serum albumin
COP I	coat protein complex I
COP II	coat protein complex II
DAPI	4',6-diamidino-2-phenylindole
DIEA	N,N-diisopropylethylamine
DLS	dynamic light scattering
DMEM	Dulbecco's modified Eagle's medium
DMSO	dimethylsulfoxide
ECM	extracellular matrix
EDTA	ethylenediamine tetraacetic acid
ELISA	enzyme-linked immunosorbent assay
FCS	fetal calf serum
FITC	fluorescence-isothiocyanat
FP	fluorescence polarization
FRET	fluorescence resonance energy transfer
HOBt	hydroxybenzotriazole
HTFP assay	heterogeneous transition metal based fluorescence polarization assay
ITC	isothermal calorimetry
kDa	kilo Dalton
KCNN4	Ca ²⁺ -activated K ⁺ -channel, subfamily N, member 4
MBHA	4-methylbenzhydramine hydrochloride
MIA	melanoma inhibitory activity
MTOC	microtubule organizing center
MW	molecular weight
NBT	nitro blue tetrazolium
NHS	N-hydroxy succinimide
NMR	nuclear magnetic resonance
PBS	phosphate buffered saline

PCR	polymerase chain reaction
PKC	protein kinase C
PVDF	polyvinylidene fluoride
Rab11	Rab-protein 11, member of the Ras superfamily of GTPases
RT	room temperature
Ru(bpy)₃	tris(2,2'-bipyridine)ruthenium (II)
SDS-PAGE	sodium dodecyl sulphate polyacrylamide gel electrophoresis
SNARE	soluble N-ethylmaleimide-sensitive-factor attachment receptor
SPR	surface plasmon resonance
TBTU	O-(benzotriazol-1-yl)-N,N,N',N'-tetramethyluronium tetrafluoroborate
WT	wild type

9 Appendix

Publications

Schmidt J., Bosserhoff A. K.; MIA - a New Target Protein for Malignant Melanoma Therapy. **2010**; (manuscript in preparation)

Schmidt J., Riechers A., Stoll R., Amann T., König B., Bosserhoff A. K.; Dissociation of functionally active MIA protein dimers by dodecapeptide AR71 strongly reduces formation of metastases in malignant melanoma. *Nat Med* **2010**; (submitted)

Schmidt F., Schmidt J., Riechers A., König B.; Zn²⁺-cyclen-pyrene as non-intercalating DNA staining reagent. **2010**; (manuscript in preparation)

Schmidt J., Friebel K., Schönherr R., Coppolino M. G., Bosserhoff A. K.; Directed, Migration-associated Secretion of Melanoma Inhibitory Activity (MIA) at the Cell Rear is supported by KCNN4 Potassium Channels. *Cell Res* **2009**; (submitted)

Riechers A., Schmidt J., König B., Bosserhoff A. K.; Heterogeneous Transition Metal-based Fluorescence Polarization (HTFP) Assay for Probing Protein Interactions. *Biotechniques* **2009**; 47, 837-844

Schmidt J., Bosserhoff A. K.; Processing of MIA protein during cell migration. *Int J Cancer* **2009**; 125(7):1587-94

Taha H. M., Schmidt J., Göttle M., Suryanarayana S., Shen Y., Tang W. J., Gille A., Geduhn J., König B., Dove S., Seifert R.; Molecular analysis of the interaction of anthrax adenyl cyclase toxin, edema factor, with 2'(3')-O-(N-(methyl)anthraniloyl)-substituted purine and pyrimidine nucleotides. *Mol Pharmacol.* **2009**; 75(3): 693-703

Curriculum Vitae

Personal Information

Name: Jennifer Schmidt, maiden name Meier
Gender: Female
Date of birth: 01. January 1979
Place of birth: Holzminden
Nationality: German

Education / Training

03/2007 – present PhD-Thesis in the research group of Prof. Dr. Anja Katrin Bosserhoff, Institute of Pathology, University Hospital of Regensburg, Germany, under supervision of Prof. Dr. Burkhard König, Institute of Organic Chemistry, University of Regensburg, Germany.
Title: “Molecular Relevance and Structural Characterization of Melanoma Inhibitory Activity (MIA) Protein”

01/2007 Diploma

02/2006 – 01/2007 Diploma Thesis in the research group of Prof. Dr. Roland Seifert, Institute for Pharmacology and Toxicology, University of Regensburg, Germany. The experimental work was conducted at the Department of Pharmacology and Toxicology, University of Kansas, USA.
Title: “Molecular Analysis of Anthrax Edema Factor with Fluorescent Nucleotides”

10/2004 – 11/2005 Graduate Studies in the field of Medicinal Chemistry, University of Regensburg, Germany

10/2004 Bachelor in Chemistry, University of Regensburg, Germany

11/2003 – 09/2004 Graduate Studies in the field of Chemistry, University of Regensburg, Germany

10/2003 Pre-degree in Chemistry, University of Heidelberg, Germany

10/2001 – 09/2003	Undergraduate Studies in the field of Chemistry, University of Heidelberg, Germany
09/2003	State Examination as assistant medical technician (MTLA), Lemgo, Germany
09/1998 – 09/2001	Training as assistant medical technician (MTLA), MTLA-School Klinikum Lippe-Lemgo GmbH, Lemgo, Germany
06/1998	Abitur (A-Level) Georg von Langen Gymnasium, Holzminden, Germany

Internships / Professional Experience

04/2006 – 08/2006	Employment as assistant medical technician (hourly job), Department of Medicinal Chemistry, University of Kansas, USA
10/2004	Practical Course „Chemical Engineering I“, Karl-Winnacker-Institut der DECHEMA e.V.“, Frankfurt am Main, Germany
03/2004	Practical Course „Chemical Engineering II“, Karl-Winnacker-Institut der DECHEMA e.V.“, Frankfurt am Main, Germany

Additional Qualifications

03/2009	Vocational training “Gentechnikfortbildungsveranstaltung für Projektleiter und Beauftragte für Biologische Sicherheit (BBS)”, University of Regensburg, Germany
02/2006	Continuing education “Sicherer Umgang mit Radionukliden”, University of Regensburg, Germany

Awards

2009	German Society of Cell Biology (DGZ) Poster Award
2004	Götz / Durand Award

Conferences / Seminars

- | | |
|---------|---|
| 09/2009 | 11 th Young Scientist Meeting “Imaging Cell Migration” of the German Society of Cell Biology (DGZ), Martinsried, Germany |
| 06/2008 | Retreat of the Institute of Pathology, Parsberg, Germany |
| 02/2008 | XXXV. Jahrestagung der Arbeitsgemeinschaft Dermatologische Forschung (ADF), Erlangen, Germany |
| 09/2006 | 3 rd Summer School Medicinal Chemistry, University of Regensburg, Germany |
| 04/2006 | 44 th annual Medicinal Chemistry MIKI Meeting, University of Illinois at Chicago, Chicago, USA |